

การสังเคราะห์อนุพันธ์ของสารฟurocoumarin ที่มีฤทธิ์ต้านมะเร็ง

Synthesis of Furocoumarin Derivatives as Anti-cancer Agents

โดย

นางสาวจิภาดา เอกรุ่งเรืองกิจ

รายงานนี้เป็นส่วนหนึ่งของการศึกษาตามหลักสูตร ปริญญาวิทยาศาสตรบัณฑิต ภาควิชาเคมี

คณะวิทยาศาสตร์ จุฬาลงกรณ์มหาวิทยาลัย ปีการศึกษา 2562

Project Title: Synthesis of Furocoumarin Derivatives as Anti-cancer Agents

Student Name: Miss Chiphada Aekrungrueangkit

Accepted by the Department of Chemistry, Faculty of Science, Chulalongkorn University in
Partial Fulfillment of the Requirements for the Degree of Bachelor of Science

SENIOR PROJECT COMMITTEES

- | | |
|---|-----------------|
| 1. Assistant Professor Warinthorn Chavasiri | Chair Committee |
| 2. Dr. Junjuda Unruangsri, Ph.D. | Committee |
| 3. Dr. Tanatorn Khotavivattana, Ph.D. | Project Advisor |

This report was approved by head of Department of Chemistry



(Dr. Tanatorn Khotavivattana, Ph.D.)

Project Advisor



(Associate Professor Vudhichai Parasuk, Ph.D.)

Head of Department Chemistry

Date 25... Month May Year 2020

Project Title: Synthesis of Furocoumarin Derivatives as Anti-cancer Agents

Student Name: Miss Chiphada Aekrungrueangkit

Project Advisor: Tanatorn Khotavivattana, Ph.D.

Department of Chemistry, Faculty of Science, Chulalongkorn University, Academic Year 2019

ABSTRACT

Furocoumarin derivatives such as bergamottin, 8-hydroxypsoralen, and methoxsalen are one of the interesting compounds which showed potential as a core structure for further development in the areas of anti-cancer agents. Literature shows that the anticancer activity especially the amide group at the C-5 position of methoxsalen. On the other hand, furocoumarin derivatives have been reported to cause DNA crosslink when stimulated by light, leading to high cytotoxicity towards normal cells. Therefore, in this work, we have synthesized various functional groups of furocoumarin derivatives especially the amide group to further enhance the anticancer activity. We also aim to reduce the side effects by synthesising the tetracyclic furocoumarin derivatives. Twenty-two novel of furocoumarin derivatives were successfully synthesized. All final products were characterized by nuclear magnetic resonance spectroscopy (NMR), high-resolution mass spectrometry (HRMS), and fourier-transform infrared spectroscopy (FTIR). The synthesized novel products (**1**, **2**, **3a-3k** and **3m**) and methoxsalen were evaluated for anticancer activity; breast cancer (MDA-MB-231 cell and T47-D cell), liver cancer (HepG2 cell and S102), leukemia (HL-60 and MOLT-3), lung cancer (A549 and H69AR), cholangiocarcinoma (HuCCA-1), HeLA cell and normal embryonic lung cell (MRC-5) by MTT assay and XTT assay at Chulabhorn Research Institute. According to the results, bromophenyl containing compound **3d** has significantly greater anticancer activity. For the structure-activity relationship (SAR), the compounds containing electron withdrawing group had better anticancer activity than electron donating group in most cancer cells. This information could become valuable for the drug discovery and the development of anticancer drug in the future.

Keywords: furocoumarin, methoxsalen, anticancer, SAR

ACKNOWLEDGEMENTS

Throughout the entire period of senior project, I had gained memorable experiences and practical laboratory skills. I not only learned more chemistry knowledge but also had a chance to implement the knowledge I learned. I would like to thank and acknowledge everyone who was involved in creating this great opportunity for us to successfully achieve this project.

First and foremost, I sincerely thank my senior project advisor, Tanatorn Kohtavivattana Ph.D., for enthusiastically great support, advice, about teaching, and living throughout the project. The project would not be smoothly accomplished without his remarkable assist. I truly appreciate the effort he put into this project and I deeply thank you for giving me the opportunity to do a research on this exciting topic.

Moreover, I am extremely grateful to express Dr. Jutatip Boonsombat and Dr. Sanit Thongnest from Chulabhorn Research Institute for allowing me to gain memorable experiences and practical laboratory skills, use the facility needed for this experiment and especially for anticancer evaluation from Chulabhorn Research Institute.

Finally, I would like to take this opportunity to thank my family who were continuously supporting me throughout my life and leaving me free in all my decisions. Furthermore, I am very much indebted and grateful to all my friends, every member of CU chem-85, all who involved in the project, and especially TK-lab members for their moral support, helpfulness, and willingness to listen to all the problems during this project.

Chiphada Aekrungrueangkit

TABLE OF CONTENTS

	Page
ABSTRACT (THAI)	III
ABSTRACT (ENGLISH)	IV
ACKNOWLEDGEMENTS	V
TABLE OF CONTENTS	VI
LIST OF TABLES	IX
LIST OF FIGURES	X
CHAPTER I INTRODUCTION	1
1.1. Background and significance of research	1
1.2. Literature review	2
1.2.1. Cancer.....	2
1.2.2. SAR in drug discovery.....	2
1.2.3. Furocoumarin derivatives.....	3
1.2.3.1. Furocoumarin derivatives as anticancer.....	3
1.2.3.1.1. Modification of the methoxy groups at the C-8 position	3
1.2.3.1.2. Modification of the functional groups at the C-5 position	5
1.2.3. Current medications for the treatment of leishmaniasis	5
1.2.3.2. SAR of furocoumarin derivatives	8
1.2.4. Cytotoxic of furocoumarin derivatives	9
1.3. Objectives and Scope of research	10
1.3.1. Objective	10
1.3.2. Scope of research	10
CHAPTER II EXPERIMENTS	12
2.1. Chemical synthesis	12
2.1.1. Materials and instrument for chemical synthetic section	12
2.1.2. Experimental procedure for the synthesis	13
2.1.2.1. General procedure A	13
2.1.2.2. Synthesis of compound 1 and compound 2	13
2.1.2.2.1. 9-methoxy-4-nitro-7H-furo[3,2-g]chromen-7-one (1)	13

2.1.2.2.2. 4-amino-9-methoxy-7H-furo[3,2-g]chromen-7-one (2)	14
2.1.2.3. Synthesis of 3a-3m	14
2.1.2.3.1. N-(9-methoxy-7-oxo-7H-furo[3,2-g]chromen-4-yl)benzamide (3a) ...	14
2.1.2.3.2. 4-fluoro-N-(9-methoxy-7-oxo-7H-furo[3,2-g]chromen-4-yl)benzamide (3b)	15
2.1.2.3.3. N-(9-methoxy-7-oxo-7H-furo[3,2-g]chromen-4-yl)-4- (trifluoromethyl)benzamide (3c)	16
2.1.2.3.4. 4-bromo-N-(9-methoxy-7-oxo-7H-furo[3,2-g]chromen-4-yl)benzamide (3d)	16
2.1.2.3.5. N-(9-methoxy-7-oxo-7H-furo[3,2-g]chromen-4-yl)furan-2-carboxamide (3e)	17
2.1.2.3.6. N-(9-methoxy-7-oxo-7H-furo[3,2-g]chromen-4-yl) thiophene-2- carboxamide (3f)	17
2.1.2.3.7. N-(9-methoxy-7-oxo-7H-furo[3,2-g]chromen-4-yl)propionamide (3g)	18
2.1.2.3.8. N-(9-methoxy-7-oxo-7H-furo[3,2-g]chromen-4-yl)isobutyramide (3h)	19
2.1.2.3.9. N-(9-methoxy-7-oxo-7H-furo[3,2-g]chromen-4-yl)pivalamide (3i)	19
2.1.2.3.10. 4-methoxy-N-(9-methoxy-7-oxo-7H-furo[3,2-g]chromen-4-yl) benzamide (3j)	20
2.1.2.3.11. N-hexanoyl-N-(9-methoxy-7-oxo-7H-furo[3,2-g]chromen-4-yl) hexanamide (3k)	21
2.1.2.3.12. (3r,5r,7r)-N-(9-methoxy-7-oxo-7H-furo[3,2-g]chromen-4-yl) adamantane-1-carboxamide (3l)	21
2.1.2.3.13. N-(9-methoxy-7-oxo-7H-furo[3,2-g]chromen-4-yl)acetamide (3m)..	22
2.1.2.4. Synthesis of 4-6	23
2.1.2.4.1. 1-(5,9-dimethoxy-7-oxo-6,7-dihydro-5H-furo[3,2-g]chromen-4-yl)-3- phenylthiourea (4)	23
2.1.2.4.2. N-(9-methoxy-7-oxo-7H-furo[3,2-g]chromen-4-yl)benzene sulfonamide (5)	24
2.1.2.4.3. N-(9-methoxy-7-oxo-7H-furo[3,2-g]chromen-4-yl)-N- (phenylsulfonyl)benzenesulfonamide (6)	24

2.1.2.5. Synthesis of 7a-7b	25
2.1.2.5.1. 4-(benzylamino)-9-methoxy-7H-furo[3,2-g]chromen-7-one (7a) and 4-(dibenzylamino)-9-methoxy-7H-furo[3,2-g]chromen-7-one (7b)	25
2.2. Biological evaluation	26
2.2.1. Anticancer activity	26
CHAPTER III RESULTS & DISCUSSIONS	27
3.1. Synthesis of furocoumarin derivatives; amide group, thiourea group, sulfonamide group and benzyl-amino group at C-5 position	27
3.1.1. Amide synthesis by acylation	31
3.1.2. Synthesis of thiourea	34
3.1.3. Sulfonation	35
3.1.4. Benzylation	37
3.2. Synthesis the tetracyclic-furocoumarin derivatives	38
3.2.1. Synthesis of cyclopentanone-furocoumarin	38
3.2.2. Synthesis of benzo-furocoumarin	39
3.3. The results of the anticancer activity	40
3.3.1. Effect of substituent group at C-5 position	47
3.3.2. Effect of phenyl substituent and type of substituent group on aromatic ring ..	47
3.3.3. Effect of furan and thiophene substituent	48
3.3.4. Effect of alkyl substituent	48
CHAPTER IV CONCLUSION	49
REFERENCES	50
APPENDICES	53
APPENDIX A	54
APPENDIX B	87
Autobiography	96

LIST OF TABLES

	Page
Table 1 The structure of furocoumarin derivatives and their anti-breast, anti-prostate cancer activity and cytotoxicity (IC ₅₀ value in μM)	5
Table 2 structure of compounds and their activity in inhibiting the growth of HeLa cells (IC ₅₀ value in μM)	6
Table 3 The structure of methoxsalen derivatives and their anti-breast, anti-prostate cancer activity and cytotoxicity (IC ₅₀ value in μM)	7
Table 4 The synthesis of amide group at C-5 position of methoxsalens and their percent yield	31
Table 5 Conditions of synthesis cyclopentanone-furocoumarin	38
Table 6 The condition of synthesis benzo-furocoumarin	39
Table 7 The anticancer activity; breast cancer (MDA-MB-231 and T47-D), liver cancer (HepG2 and S102), leukemia (HL-60 and MOLT-3), lung cancer (A549 and H69AR), cholangiocarcinoma (HuCCA-1), HeLa cell and normal embryonic lung cell (MRC-5) in %Cytotoxicity at 50 $\mu\text{g}/\text{ml}$ and IC ₅₀ value (μM)	42

LIST OF FIGURES

	Page
Figure 1 Methoxsalen	2
Figure 2 Furanocoumarin isomers (IIa) psoralen and (IIb) angelicin	3
Figure 3 Xanthotoxin-triazole derivatives and their anti-gastric cancer activity (AGS cell lines) and the normal cell (L02 cell lines) IC ₅₀ value in μM	4
Figure 4 Imperatorin	4
Figure 5, 6 The structure of furocoumarin derivatives	4
Figure 7, 8 The structure of methoxsalen derivatives	7
Figure 9 The models of important structure-activity relationship (SAR)	8
Figure 10 (Xa) structure of pyrimidine bases, (Xb) Uracil; U, (Xc) Thymine; T and (Xd) Cytosine; C	9
Figure 11 (XIa) DNA cross-linking with furocoumarin derivatives and (XIb) tetracyclic furocoumarin derivatives, IC ₅₀ value of HeLa cell and skin phototoxicity	9
Figure 12 Overview of research scope	10
Figure 13 Modification of the functional groups at the C-5 position and their reagent	11
Figure 14 Synthesis the tetracyclic of furocoumarin derivatives	11
Figure 15 Synthesis the several functional group of furocoumarin derivatives	27
Figure 16 The nitration at C-5 position of methoxsalen	28
Figure 17 the mechanism of nitration	28
Figure 18 The reduction of nitro group to amine group	29
Figure 19 the mechanism of reduction	30
Figure 20 The synthesis of the <i>p</i> -NO ₂ -benzoyl substitution	33
Figure 21 The mechanism of acylation of amine	33
Figure 22 The mechanism of acylation of amine (3m)	34
Figure 23 Synthesis of thiourea 4	34

Figure 24 The mechanism of thiourea formation	35
Figure 25 Sulfonation of compound 5	35
Figure 26 Mechanism of sulfonation	36
Figure 27 Sulfonation	37
Figure 28 Benzylation of 7a and 7b	37
Figure 29 The mechanism benzylation	38
Figure 30 The structures and their anti-breast cancer activity (T47-D)	43
Figure 31 The anti-breast cancer activity as cytotoxicity percentage at 50 µg/mL (MDA-MB-231 and T47-D)	44
Figure 32 The anti-breast cancer activity as cytotoxicity percentage at 50 µg/mL (HepG2 and S102)	45
Figure 33 The anti-leukemia cancer activity as cytotoxicity percentage at 50 µg/mL (HL-60 and MOLT-3)	45
Figure 34 The anti-lung cancer activity as cytotoxicity percentage at 50 µg/mL (A549 and H69AR)	46
Figure 35 The anticancer activity and toxicity as cytotoxicity percentage at 50 µg/mL ; cholangiocarcinoma (HuCCA-1), HeLa cell and normal embryonic lung cell (MRC-5)	46
Figure 36 ¹ H NMR spectrum of 1	55
Figure 37 ¹³ C NMR spectrum of 1	55
Figure 38 HRMS spectrum of 1	56
Figure 39 ¹ H NMR spectrum of 2	57
Figure 40 HRMS spectrum of 2	58
Figure 41 ¹ H NMR spectrum of 3a	59
Figure 42 ¹³ C NMR spectrum of 3a	59
Figure 43 HRMS spectrum of 3a	60
Figure 44 ¹ H NMR spectrum of 3b	61
Figure 45 ¹³ C NMR spectrum of 3b	61

Figure 46 ^{19}F NMR spectrum of 3b	62
Figure 47 HRMS spectrum of 3b	63
Figure 48 ^1H NMR spectrum of 3c	64
Figure 49 ^{13}C NMR spectrum of 3c	64
Figure 50 ^{19}F NMR spectrum of 3c	65
Figure 51 HRMS spectrum of 3c	66
Figure 52 ^1H NMR spectrum of 3d	67
Figure 53 HRMS spectrum of 3d	68
Figure 54 ^1H NMR spectrum of 3e	69
Figure 55 ^{13}C NMR spectrum of 3e	69
Figure 56 HRMS spectrum of 3e	70
Figure 57 ^1H NMR spectrum of 3f	71
Figure 58 ^{13}C NMR spectrum of 3f	71
Figure 59 HRMS spectrum of 3f	72
Figure 60 ^1H NMR spectrum of 3g	73
Figure 61 ^{13}C NMR spectrum of 3g	73
Figure 62 HRMS spectrum of 3g	74
Figure 63 ^1H NMR spectrum of 3h	75
Figure 64 ^{13}C NMR spectrum of 3h	75
Figure 65 HRMS spectrum of 3h	76
Figure 66 ^1H NMR spectrum of 3i	77
Figure 67 ^{13}C NMR spectrum of 3i	77
Figure 68 HRMS spectrum of 3i	78
Figure 69 ^1H NMR spectrum of 3j	79
Figure 70 ^{13}C NMR spectrum of 3j	79
Figure 71 HRMS spectrum of 3j	80
Figure 72 ^1H NMR spectrum of 3k	81
Figure 73 ^{13}C NMR spectrum of 3k	81

Figure 74 HRMS spectrum of 3k	82
Figure 75 ¹ H NMR spectrum of 3l	83
Figure 76 ¹³ C NMR spectrum of 3l	83
Figure 77 HRMS spectrum of 3l	84
Figure 78 ¹ H NMR spectrum of 3m	85
Figure 79 ¹³ C NMR spectrum of 3m	85
Figure 80 HRMS spectrum of 3m	86
Figure 81 ¹ H NMR spectrum of 4	88
Figure 82 ¹³ C NMR spectrum of 4	88
Figure 83 HRMS spectrum of 4	89
Figure 84 ¹ H NMR spectrum of 5	90
Figure 85 ¹³ C NMR spectrum of 5	90
Figure 86 HRMS spectrum of 5	91
Figure 87 ¹ H NMR spectrum of 7a	92
Figure 88 ¹³ C NMR spectrum of 7a	92
Figure 89 HRMS spectrum of 7a	93
Figure 90 ¹ H NMR spectrum of 7b	94
Figure 91 ¹³ C NMR spectrum of 7b	94
Figure 92 HRMS spectrum of 7b	95

CHAPTER I

INTRODUCTION

1.1. Background and significance of research

It is well known that cancer is a terrifying disease that causes a sore number of deaths each year. In 2019, there were 1,762,450 new cancer cases and 606,880 deaths from cancer are expected in the United States.¹ Cancer develops due to the abnormal and uncontrolled cell division leading to mutation of cells in a greater rate than normal body cells.^{2,3} Cancer brings a lot of pain and suffering to people and it can highly spread if it is not inhibited.^{2,3} Therefore, doing research is very important for obtaining more treatment options and new knowledge. Nowadays, articles have introduced a variety of synthetic compounds as an anticancer potential drug. Furocoumarin derivatives such as bergamottin, 8-hydroxypsoralen, and methoxsalen are one of the interesting compounds which showed potential as a core structure for further development to become an anti-cancer agent.⁴ Furocoumarin or furanocoumarin is a class of heterocyclic compounds that have furan and coumarin. Some of their derivatives were found to have anticancer activity especially the one with modified amide group at the C-5 position of methoxsalen (**Figure 1**) that found significantly increased anti-breast cancer effects (MCF-7).⁵ However, there was still not much research about the amide group in that position. Therefore, the synthesis of the amide group is an interesting functional group that uses as a lead compound to develop the anti-cancer effects. The modification of this lead compound is one of the most significant objectives of this work.

Another aspect of drug development apart from the increasing efficacy is the reduction the side effect of the drug. In this regard, furocoumarin derivatives have been reported to cause DNA crosslink due to the double bonds at the edge of the molecule. When stimulated by light, the [2+2] cycloaddition occurs between the double bonds at both ends of furocoumarin and the thymine base of DNA leading to high cytotoxic towards normal cells.^{6,7} Hence, in this work, we also aim to block the double bonds at the furan edge by synthesising the tetracyclic furocoumarin derivatives, which might reduce the side effects and retain the anticancer activity.⁸

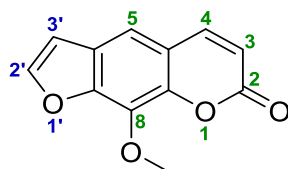


Figure 1 Methoxsalen⁴

1.2. Literature review

1.2.1. Cancer

Cancer is initiated by abnormalities in the cell-division cycle lead to the mutation of cells and then the abnormal cells distribute uncontrollably throughout the body. Cancer has come with a group of diseases affecting different organs and systems of the body. There are many types of cancer that are called following the organism that has the cancer cells or the tumor such as breast cancer, skin cancer, lung cancer, liver cancer, etc.^{2,3} Cancer patients may suffer from many symptoms resulting from the primary disease and the treatment process of diseases such as surgery with chemotherapy and radiation therapy. The symptoms from the side effects of the treatment process are nausea, diarrhea, fatigue, hair loss anxiety, and depression. All the symptoms can cause the patient unbearable and contribute to delay of the treatment process or lead to premature termination of treatment.⁹

1.2.2. SAR in drug discovery

SAR stands for structure-activity relationship is the study of the relationship between the structure of the molecule and biological activity.¹⁰ It is easier to research and develop the compounds that had SAR data because studying with the structure-activity relationship helps creating some guidelines. SAR helps to establish the relationship, so the synthesis of the molecular structure is designed more effectively because it considers the bioactive ability. The SAR model can be done by observing the relationship of biological activity to the molecular structure.¹⁰ In addition, SAR information might sometimes help us to understand the mechanism of biological processes, which will allow us to take into account various factors of molecular structure, such as functional groups, the electron density, steric effects, hydrophilicity and lipophilicity of the compounds, thereby reducing development time and increasing development efficiency of biological activity as well.

1.2.3. Furocoumarin derivatives

Furocoumarins are groups of compounds that exist in a variety of natural products that has a variety of biological activities such as inhibitory effects of Alzheimer's disease from the root of *Angelica dahurica*; (isoimperatorin, imperatorin), antioxidant activity from wampee or *Clausena lansium*; (8-hydroxypsoralen) and anticancer activity from kaffir lime or *Citrus hystrix*; (isoimperatorin, bergamottin).^{4,11-13} There are two furanocoumarin isomers, psoralen and angelicin (**Figure 2**).¹¹ This research will be focusing on psoralen isomer because it has a lot of SAR data and more potential to improve biological activity.

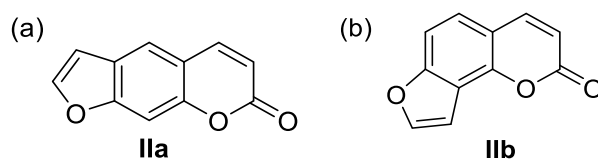


Figure 2 Furanocoumarin isomers (**IIa**) psoralen and (**IIb**) angelicin¹¹

1.2.3.1. Furocoumarin derivatives as anticancer

Furocoumarin derivatives have been considered as bioactive agents for their potential anticancer effects. Therefore, in order to develop new anti-cancer drug based on this scaffold, scientists have attempted to study the structure-activity relationship of the furocoumarin derivatives as followings.

1.2.3.1.1. Modification of the methoxy groups at the C-8 position

Methoxsalen or xanthotoxin (**Figure 1**) is an important structure that has been developed in several research works. Xanthotoxin-triazole derivatives were designed and synthesized to study their antiproliferative properties focusing on anti-gastric cancer activity. The antiproliferative activity was evaluated by the *in vitro* test with in the AGS cancer cell line and the L02 normal cell line, whereby the result was obtained by flow cytometric analysis and MTT assay. The derivatives that were *p*-substituted by electron-withdrawing group have a better antitumor activity than *p*-substitution, electron-donating group or non-substituted analogues (**Figure 3**).¹⁴

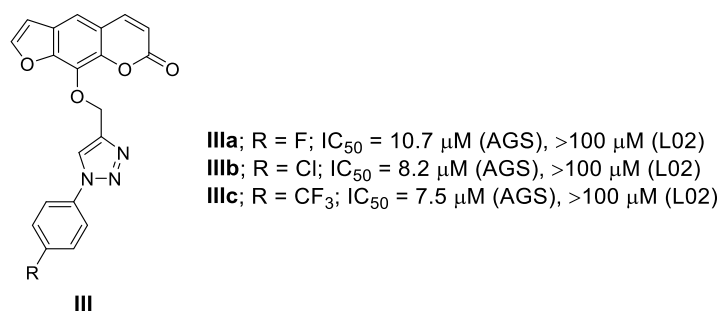


Figure 3 Xanthotoxin-triazole derivatives and their anti-gastric cancer activity (AGS cell lines) and the normal cell (L02 cell lines) IC₅₀ value in μM¹⁴

Another compound that has been modified at the C-8 position of furocoumarins is imperatorin (**Figure 4**). Imperatorin has been studied to be likely able to control the proliferation and angiogenesis of human colon cancer cell (HCT116, HeLa, and Hep3B cells).¹⁵ The results were received by promoter reporter gene assay, MTT assay, flow cytometric analysis, etc.¹⁵

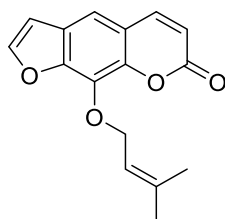


Figure 4 Imperatorin¹⁵

While the anti-breast and anti-prostate cancer activity of furocoumarin derivatives were researched as well. The bioactivity was evaluated by the *in vitro* test with the breast cancer cell lines (MCF-7 and MDA-MB-231), prostate cancer cell lines (PC-3) and the normal cell line (MCF-10A) via the MTT assay (**Figure 5, 6** and **Table 1**).⁵ The derivatives that contain alkyl substitution and benzyl substitution increased the activity. However, imperatorin, hydroxyl group, alkyl substitution that containing 1-naphthyl group and ester group at C-8 have not been showed the anti-breast and anti-prostate cancer activity.

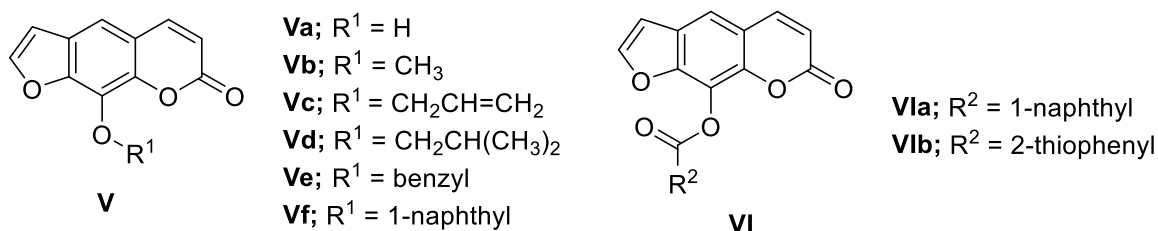
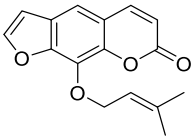


Figure 5, 6 The structure of furocoumarin derivatives⁵

Table 1 The structure of furocoumarin derivatives and their anti-breast, anti-prostate cancer activity and cytotoxicity (IC₅₀ value in μM)⁵

Compounds	IC ₅₀ value (μM)			
	MCF-7 ^a	MDA-MB-231 ^b	PC-3 ^c	MCF-10 ^d
imperatorin 	100	100	100	ND
Va	>100	100	100	ND
Methoxsalen Vb	20	>30	25	ND
Vc	12	10	15	100
Vd	8.15	10	7	>100
Ve	7.07	8.5	10	>100
Vf	>100	100	100	ND
Via	100	100	100	ND
Vib	>100	100	100	ND

^a Estrogenic breast cancer cell lines

^b Non-estrogenic breast cancer cell lines

^c Prostate cancer cell lines

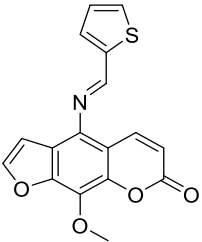
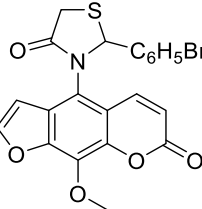
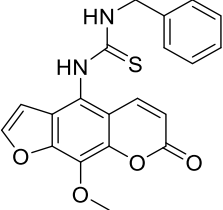
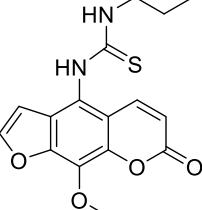
^d Normal cell lines

1.2.3.1.2. Modification of the functional groups at the C-5 position

Methoxsalen derivatives with substituents at C-5 position were designed and synthesized to study their antitumor activity in a variety of functional groups such as amine, thiourea, thiazolidine, thiazolidine-one, imidione group, etc. However, there were only two functional groups (imine and thiourea group) that were active in inhibiting the growth of HeLa

cells and none of the compounds showed activity inhibiting the growth of breast cancer (MCF-7) cells (**Table 2**).¹⁶

Table 2 structure of compounds and their activity in inhibiting the growth of HeLa cells (IC_{50} value in μM)¹⁶

Compounds	IC_{50} value (μM) HeLa cells
methoxsalen	29.10 (7.6 $\mu g/mL$)
	22.15 (7.2 $\mu g/mL$)
	84.69 (40 $\mu g/mL$)
	19.72 (7.5 $\mu g/mL$)
	69.20 (23 $\mu g/mL$)

On the other hand, the activity inhibiting the growth of breast and prostate cancer cells of methoxsalen derivatives were discovered with amine, amide groups, bromo substitution and *N,N*-dialkyl analogs (**Figure 7**). The bioactivity was evaluated by the *in vitro* test with the breast cancer cell lines (MCF-7 and MDA-MB-231), prostate cancer cell lines (PC-3) and the normal cell line (MCF-10A) via the MTT assay (**Table 3**).⁵

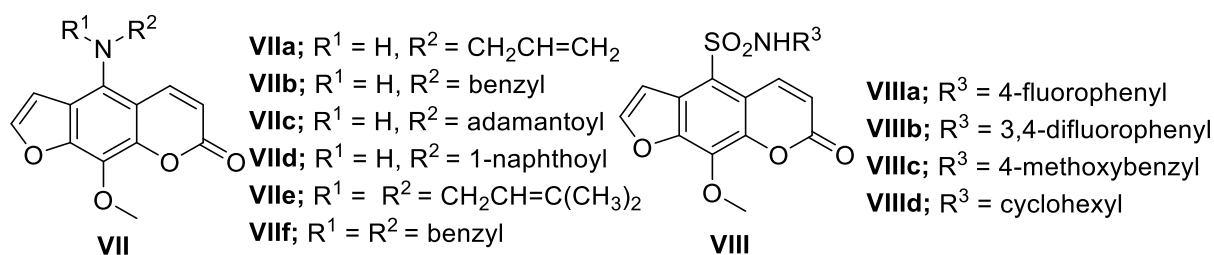
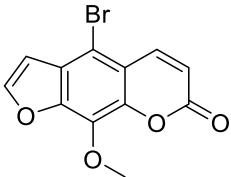
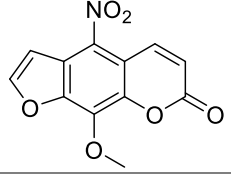
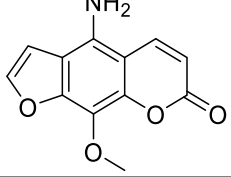
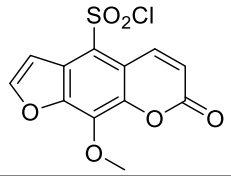


Figure 7, 8 The structure of methoxsalen derivatives⁵

Table 3 The structure of methoxsalen derivatives and their anti-breast, anti-prostate cancer activity and cytotoxicity (IC₅₀ value in μM)⁵

Compounds	IC ₅₀ value (μM)			
	MCF-7 ^a	MDA-MB-231 ^b	PC-3 ^c	MCF-10 ^d
	5.69	6	8	>100
	>100	100	90	ND
	>100	100	75	ND
VIIa	3.87	5	10	>100
VIIb	1.09	3	5	>100
VIIc	0.48	2	5	96
VIIId	>100	100	100	ND
VIIe	0.53	1	1	92
VIIIf	5	>15	1	>100
	>100	100	100	ND
VIIIa	>100	100	100	ND

Compounds	IC ₅₀ value (μM)			
	MCF-7 ^a	MDA-MB-231 ^b	PC-3 ^c	MCF-10 ^d
VIIIb	100	100	100	ND
VIIIc	100	100	100	ND
VIII d	>100	100	100	ND

^a Estrogenic breast cancer cell lines

^b Non-estrogenic breast cancer cell lines

^c Prostate cancer cell lines

^d Normal cell lines

1.2.3.2. SAR of furocoumarin derivatives

From the literature reviews mentioned above, the model of important structure-activity relationship (SAR) can be summarized as shown in **Figure 9**.⁵ The functional groups at C-5 position that have hardly showed the biological activity are sulfonamide, thiazolidine, thiazolidine-one, imidione group (**Table 2**).¹⁶ Furocoumarin derivatives that contain nitro group, primary amine or *N*-aryl sulphonamide substitution at C-5 position have no bioactivity.⁵ Furocoumarin derivatives with amide group at C-5 position were synthesized to obtain two derivatives, **VIIIc** and **VIII d**. The compound that has the most potent activity is **VIIIc** with the adamantoyl group, however another amide group (**VIII d**) containing 1-naphthoyl group has no activity.⁵ For the modification at C-8 position, alkyl and benzyl substitution increased the activity.⁵

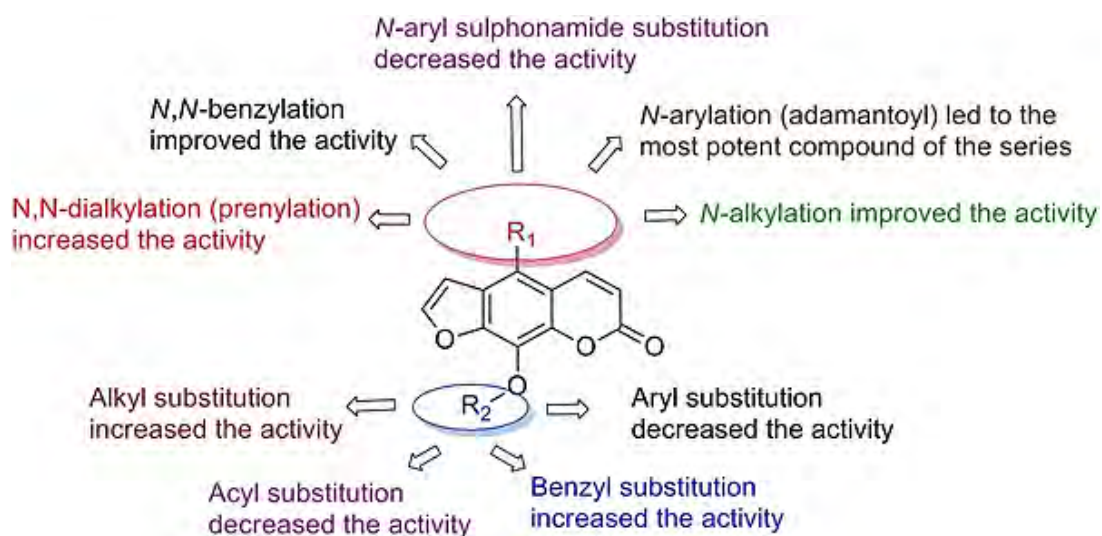


Figure 9 The models of important structure-activity relationship (SAR)⁵

1.2.4. Cytotoxic of furocoumarin derivatives

The furocoumarin derivatives possess modest cytotoxicity in the absence of light but it has the powerful cytotoxic effects upon photoactivation.^{6,17} Upon irradiation with UVA light, the 3,4- and 2',3'-double bonds of furocoumarin derivatives are activated, leading to a photocatalyzed reaction through [2+2] cycloaddition between the double bonds and the 5,6-double bond of pyrimidine bases of the DNA (**Figure 10**).^{6,18} This process can lead to DNA cross-linking (**Figure Xla**), which causes the synthesis of DNA cellular to be inhibited.^{6,7} Thereby cross-linking the DNA, has been invoked to explain the cytotoxicity,⁷ which causes serious side-effects both short-term (erythema, hyperpigmentation) and long-term (pre-malignant keratoses, skin cancers).⁸ According to these previous results, the cytotoxicity was relieved by blocking the double bonds by designing and synthesizing a series of tetracyclic furocoumarin derivatives (**Figure Xlb**).⁸

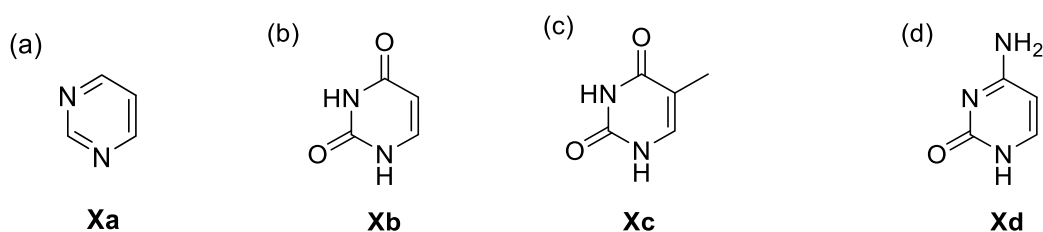


Figure 10 (**Xa**) structure of pyrimidine bases, (**Xb**) Uracil; U, (**Xc**) Thymine; T and (**Xd**) Cytosine; C¹⁸

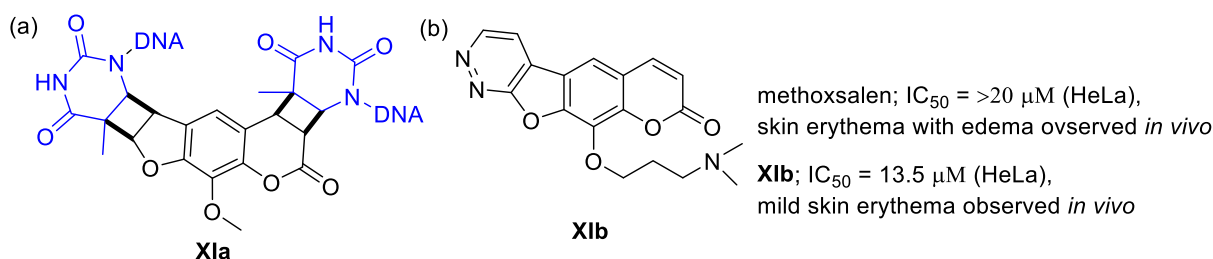


Figure 11 (**Xla**) DNA cross-linking with furocoumarin derivatives and (**Xlb**) tetracyclic furocoumarin derivatives, IC₅₀ value of HeLa cell and skin phototoxicity⁸

From all the literature reviews that are described, the modification at C-5 position of furocoumarin derivatives to give an amide group gave the highest anticancer activity. However, there were only 2 amide derivatives that have been explored. Therefore, this work will focus on the synthesis a novel amide derivatives and other functional groups at C-5 to further explore the structure-activity relationship of this promising scaffold to improve their anticancer

activity. Moreover, the reduction of side-effects will be attempted by synthesizing novel tetracyclic structures of furocoumarin derivatives.

1.3. Objectives and Scope of research

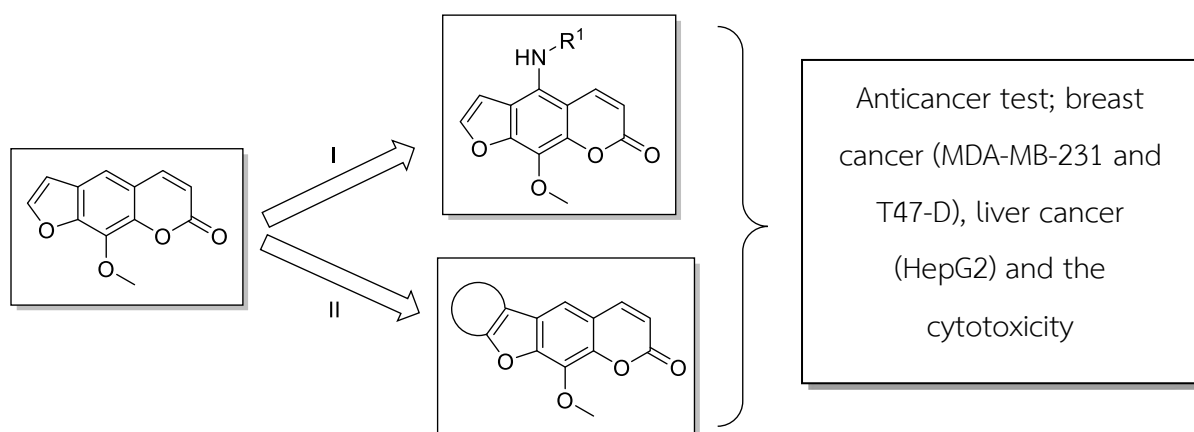
1.3.1. Objective

- 1.3.1.1. To design, synthesize and characterize novel furocoumarin derivatives.
- 1.3.1.2. To investigate the factors related to the structure of furocoumarin derivatives that can increase the anticancer activity and establish the structure-activity relationship (SAR).
- 1.3.1.3. To investigate the structure of furocoumarin derivatives that can reduce the side effects and retain the anticancer activity.

1.3.2. Scope of research

- 1.3.2.1. Synthesize various functional groups of furocoumarin derivatives such as amide group, urea group, thiourea group, sulfonamide group, sulfinamide group, carbamate group and benzyl-amino group at C-5 position.
- 1.3.2.2. Synthesize the tetracyclic of furocoumarin derivatives to reduce the side effects of anticancer activity.
- 1.3.2.3. Evaluate the bioactivity of the synthesized furocoumarin derivatives.
- 1.3.2.4. Establish the structure-activity relationship (SAR).

Overview of research scope



I = 1) Nitration, 2) Reduction, 3) Acylation and II = Cyclization

Figure 12 Overview of research scope

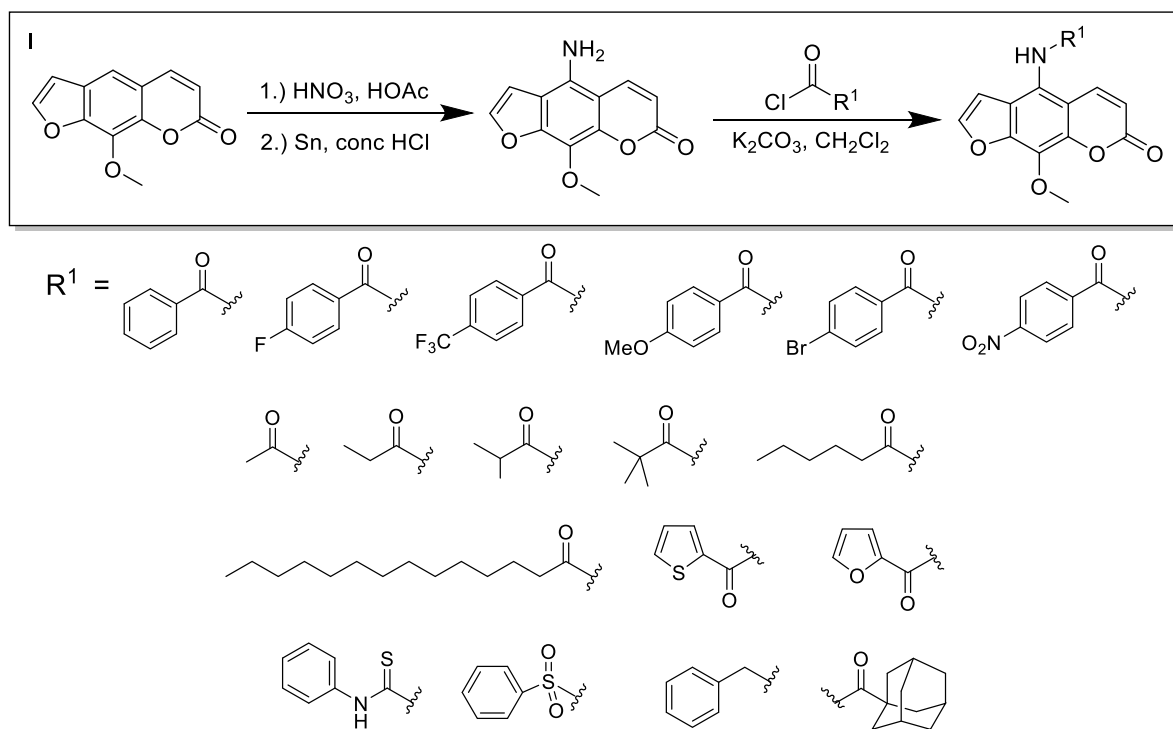


Figure 13 Modification of the functional groups at the C-5 position and their reagent

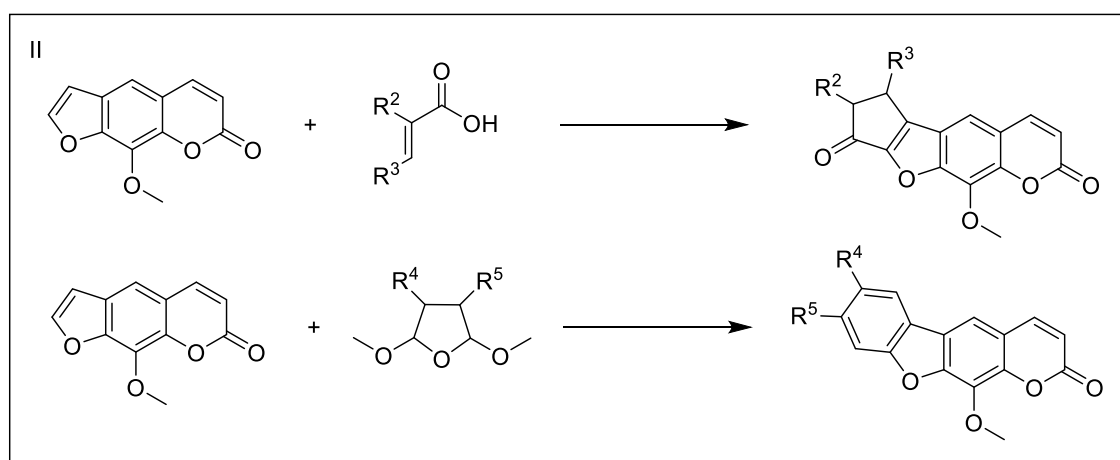


Figure 14 Synthesis the tetracyclic of furocoumarin derivatives

CHAPTER II

EXPERIMENTS

2.1. Chemical synthesis

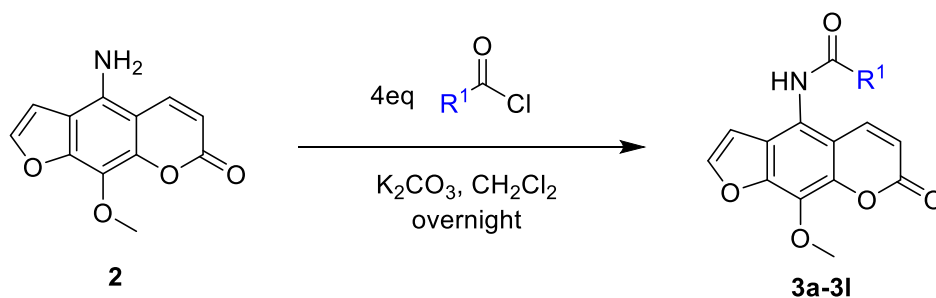
2.1.1. Materials and instrument for chemical synthetic section

All reagents and solvents were obtained from Sigma-Aldrich (St. Louis, MO, USA), TCI Chemicals (Tokyo, Japan), Fluorochem (Hadfield, Derbyshire, UK) and Merck (Darmstadt, Germany). All solvents for column chromatography from RCI Labscan (Samutsakorn, Thailand) were distilled before use.

Proton, carbon, fluorine nuclear magnetic resonance (^1H , ^{13}C and ^{19}F NMR) spectra were recorded on Bruker Avance (400 MHz) and Jeol Avance (500 MHz). Spectra were measured in DMSO- d_6 and CDCl_3 solvent and chemical shifts are reported as δ values in parts per million (ppm) relative to tetramethylsilane (δ 0.00) or the solvent residue in DMSO- d_6 (δ 2.50) or CDCl_3 (δ 7.26) as internal standard for ^1H NMR spectra. Data are reported as follows; chemical shift (multiplicity, coupling constants in Hz, integrate intensity, assignment). Abbreviations of multiplicity were as follows; s: singlet, d; doublet, t: triplet, q: quartet, m: multiplet, br: broad. Chemical shifts for ^{13}C NMR are reported as δ values in parts per million (ppm) relative to DMSO- d_6 (δ 39.52) and CDCl_3 (δ 77.16) as internal standard. High-resolution mass spectra (HRMS) data were obtained with Micro-TOF mass spectrometer. IR spectra were recorded using the Thermo Scientific™ Nicolet™ iS50 FTIR spectrometer with ATR module and are reported in wave number (cm^{-1}). Reactions were monitored by thin-layer chromatography (TLC) using aluminium Merck TLC plates coated with silica gel 60 F254. Normal phase column chromatography was performed using silica gel 60 (0.063-0.200 mm, 70-230 mesh ASTM, Merck, Darmstadt, Germany). Melting points were measured using a melting point apparatus (Griffin) and are uncorrected.

2.1.2. Experimental procedure for the synthesis

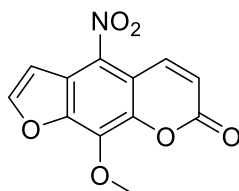
2.1.2.1. General procedure A



Compounds **3a-3m** were synthesized using a modified procedure.⁵ To a solution of substituted aniline (**2**) (1.0 equiv.) in CH_2Cl_2 were added acid chloride (4.0 equiv.) and K_2CO_3 (1.5 equiv.) at room temperature. The reaction mixture was refluxed overnight and monitored by TLC. Upon completion the reaction mixture was quenched with H_2O . The resulting mixture was neutralized by sat. NaHCO_3 and extracted with EtOAc. The combined organic layers were washed with brine, dried over anhydrous MgSO_4 , filtered, then concentrated *in vacuo* to give the amide product.

2.1.2.2. Synthesis of compounds 1 and 2

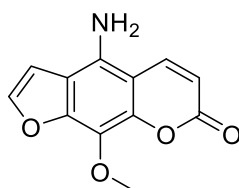
2.1.2.2.1. 9-methoxy-4-nitro-7H-furo[3,2-g]chromen-7-one (**1**)



Compound **1** was synthesized using a modified procedure.¹⁹ Methoxsalen (2.2 g, 10.0 mmol, 1.0 equiv.) was dissolved in glacial acetic acid (21ml). The resulting solution was stirred at room temperature, then conc. HNO_3 (17.1 ml) was slowly added. The precipitate formed was filtered and washed with DI water. The solid was dried *in vacuo* to give the nitro compound **1** (2.262 g, 8.66 mmol, 85% yield) as a yellow solid.

$^1\text{H NMR}$ (400 MHz, CDCl_3) δ 8.78 (d, $J = 10.2$ Hz, 1H), 7.86 (d, $J = 2.3$ Hz, 1H), 7.42 (d, $J = 2.3$ Hz, 1H), 6.63 (d, $J = 10.2$ Hz, 1H), 4.49 (s, 3H); $^{13}\text{C NMR}$ (101 MHz, CDCl_3) δ 149.58, 139.37, 118.78, 107.58, 61.66; **IR** (neat): 3156 (C=C), 1736 (C=O), 1571 (C=C), 1497 (N=O), 1314 (N=O), 1282 (C-O), 1265 (C-O) cm^{-1} ; **HRMS** (ESI⁺): m/z calcd for $\text{C}_{12}\text{H}_6\text{NO}_6\text{Na}$ [M-H+Na]⁺ 283.0093, found 283.2629; **Mp**: not determined.

2.1.2.2.2. 4-amino-9-methoxy-7H-furo[3,2-g]chromen-7-one (2)

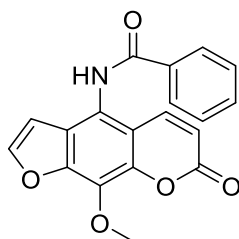


Compound **2** was synthesized using a modified procedure.²⁰ To a solution of compound **1** (2.09 g, 8.0 mmol, 1.0 equiv.) in methanol (15 mL) under nitrogen atmosphere, tin powder (3.80 g, 40.0 mmol, 5.0 equiv.) and conc. hydrochloric acid (40 mL) were added. The resulting mixture was stirred under a nitrogen atmosphere at reflux at 70 °C for 2 hrs. After being cooled to room temperature, the mixture was neutralized by 10% NaOH (250 mL) and the excess tin powder was filtered. The mother liquor was extracted with EtOAc (3 x 100 mL). The combined organic layers were washed with brine, dried with anhydrous MgSO₄, filtered and concentrated *in vacuo* to give the amine compound **2** (1.298 g, 5.61 mmol, 70% yield) as a green solid.

¹H NMR ¹H NMR (400 MHz, DMSO) δ 7.46 (d, *J* = 9.8 Hz, 1H), 6.99 (d, *J* = 2.2 Hz, 1H), 6.33 (d, *J* = 2.3 Hz, 1H), 5.63 (s, 2H), 5.25 (d, *J* = 9.8 Hz, 1H), 3.03 (s, 3H); ¹³C NMR: not determined; IR (neat): 3478 (N-H), 3383 (N-H), 3137 (C=C), 3107 (C=C), 2957 (C-H), 1701 (C=O), 1647 (N-H), 1587 (C=C), 1480 (C=C), 1446 (C=C), 1050 (C-O) cm⁻¹; HRMS (ESI⁺): *m/z* calcd for C₁₂H₉NO₄Na⁺ [M+Na]⁺ 254.0429, found 254.0428; Mp: not determined.

2.1.2.3. Synthesis of 3a-3m

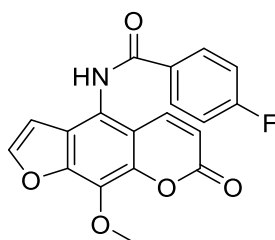
2.1.2.3.1. N-(9-methoxy-7-oxo-7H-furo[3,2-g]chromen-4-yl)benzamide (3a)



The title compound was synthesized following **General procedure A** using the amine compound **2** (24 mg, 0.1 mmol, 1.0 equiv.) in CH₂Cl₂ (2.0 mL), benzoyl chloride (56.0 μ L, 0.4 mmol, 4.0 equiv.) and K₂CO₃ (21 mg, 0.15 mmol, 1.5 equiv.). The crude product was purified by silica gel column chromatography (eluent: EtOAc/hexanes = 1:9-1:1) to provide the amide compound **3a** (30 mg, 0.09 mmol, 86% yield) as an off-white solid.

$^1\text{H NMR}$ (400 MHz, DMSO) δ 10.60 (s, 1H), 8.09 – 7.99 (m, 4H), 7.61 (d, $J = 7.5$ Hz, 1H), 7.54 (t, $J = 7.5$ Hz, 2H), 6.92 (d, $J = 2.3$ Hz, 1H), 6.41 (d, $J = 9.8$ Hz, 1H), 4.16 (s, 3H); $^{13}\text{C NMR}$ (101 MHz, DMSO) δ 166.44, 159.65, 147.44, 147.18, 142.87, 141.70, 133.90, 132.18, 130.85, 128.66, 128.16, 123.84, 121.77, 113.92, 112.94, 106.53, 61.38; **IR** (neat): 3235 (N-H), 3060 (C=C), 2944 (C-H), 1726 (C=O), 1647 (C=O), 1593 (C=C), 1145 (C-O) cm^{-1} ; **HRMS** (ESI⁺): m/z calcd for $\text{C}_{19}\text{H}_{13}\text{NO}_5\text{Na}^+$ $[\text{M}+\text{Na}]^+$ 358.069, found 358.0681; **Mp**: not determined.

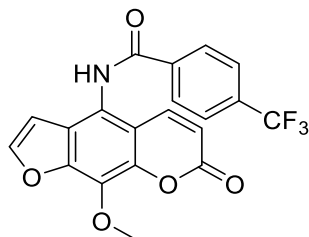
2.1.2.3.2. 4-fluoro-*N*-(9-methoxy-7-oxo-7*H*-furo[3,2-*g*]chromen-4-yl)benzamide (3b)



The title compound was synthesized following **General procedure A** using the amine compound **2** (24 mg, 0.1 mmol, 1.0 equiv.) in CH_2Cl_2 (2.0 mL), 4-fluorobenzoyl chloride (50.0 μL , 0.4 mmol, 4.0 equiv.) and K_2CO_3 (21 mg, 0.15 mmol, 1.5 equiv.) to provide the amide compound **3b** (36 mg, 0.10 mmol, 98% yield) as a gray solid.

$^1\text{H NMR}$ (400 MHz, DMSO) δ 10.60 (s, 1H), 8.11 (dd, $J = 8.5, 5.4$ Hz, 2H), 8.05 (d, $J = 2.3$ Hz, 1H), 8.02 (d, $J = 9.8$ Hz, 1H), 7.36 (t, $J = 8.6$ Hz, 2H), 6.90 (d, $J = 2.3$ Hz, 1H), 6.39 (d, $J = 9.7$ Hz, 1H), 4.14 (s, 3H); $^{13}\text{C NMR}$ (101 MHz, DMSO) δ 166.01, 165.61, 159.86, 147.67, 147.38, 143.07, 141.90, 131.16 (d, $J = 9.3$ Hz), 130.61 (d, $J = 2.9$ Hz), 124.06, 121.83, 115.93, 115.72, 114.16, 113.16, 106.73, 61.59; $^{19}\text{F NMR}$ (376 MHz, DMSO) δ -108.18 (td, $J = 9.2, 4.9$ Hz); **IR** (neat): 3395 (N-H), 3163 (C=C), 2950 (C-H), 1725 (C=O), 1674 (C=O), 1592 (C=C), 1475 (N-H), 1257 (C-O), 1168 (C-O), 1139 (C-O), 748 (C-F) cm^{-1} ; **HRMS** (ESI⁺): m/z calcd for $\text{C}_{19}\text{H}_{12}\text{FNO}_5\text{Na}^+$ $[\text{M}+\text{Na}]^+$ 376.0597, found 376.0590; **Mp**: not determined.

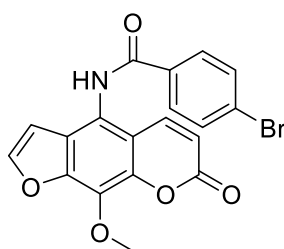
2.1.2.3.3. *N*-(9-methoxy-7-oxo-7*H*-furo[3,2-*g*]chromen-4-yl)-4-(trifluoromethyl)benzamide (**3c**)



The title compound was synthesized following **General procedure A** using the amine compound **2** (24 mg, 0.1 mmol, 1.0 equiv.) in CH₂Cl₂ (2.0 mL), 4-trifluoromethylbenzoyl chloride (60.0 μL, 0.4 mmol, 4.0 equiv.) and K₂CO₃ (21 mg, 0.15 mmol, 1.5 equiv.) to provide the amide compound **3c** (40 mg, 0.992 mmol, 96% yield) as an off-white solid.

¹H NMR (400 MHz, DMSO) δ 10.78 (s, 1H), 8.20 (d, *J* = 8.0 Hz, 2H), 8.04 (dd, *J* = 6.0, 3.8 Hz, 2H), 7.88 (d, *J* = 8.1 Hz, 2H), 6.90 (d, *J* = 2.3 Hz, 1H), 6.38 (d, *J* = 9.9 Hz, 1H), 4.12 (s, 3H); ¹³C NMR (101 MHz, DMSO) δ 165.43, 159.65, 147.57, 147.17, 142.88, 141.65, 137.82, 132.13, 131.82, 131.05, 129.16, 125.66 (q, *J* = 3.6 Hz), 123.86, 121.23, 114.08, 112.96, 106.52, 61.41; ¹⁹F NMR (376 MHz, DMSO) δ -61.34; IR (neat): 3230 (N-H), 3123 (C=C), 2945 (C-H), 1724 (C=O), 1652 (C=O), 1590 (C=C), 1521 (N-H), 1145 (C-O), 1108 (C-O), 824 (C-F) cm⁻¹; HRMS (ESI⁺): *m/z* calcd for C₂₀H₁₂F₃NO₅Na⁺ [M+Na]⁺ 426.0565, found 426.0570; Mp: not determined

2.1.2.3.4. 4-bromo-*N*-(9-methoxy-7-oxo-7*H*-furo[3,2-*g*]chromen-4-yl)benzamide (**3d**)

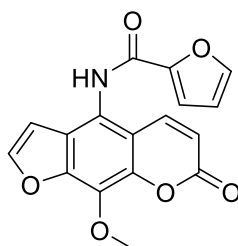


The title compound was synthesized following **General procedure A** using the amine compound **2** (24 mg, 0.1 mmol, 1.0 equiv.) in CH₂Cl₂ (2.0 mL), 4-bromobenzoyl chloride (88.0 mg, 0.4 mmol, 4.0 equiv.) and K₂CO₃ (21 mg, 0.15 mmol, 1.5 equiv.). The crude product was purified by silica gel column chromatography (eluent: 100% DCM - 3% MeOH in DCM) to provide the amide compound **3d** (38 mg, 0.09 mmol, 88% yield) as a gray solid.

¹H NMR (400 MHz, DMSO) δ 10.66 (s, 1H), 8.07 – 7.95 (m, 4H), 7.76 (d, *J* = 8.1 Hz, 2H), 6.91 (s, 1H), 6.40 (d, *J* = 9.8 Hz, 1H), 4.15 (s, 3H); ¹³C NMR not determined; IR (neat): 3211 (N-H), 3149

(C=C), 2924 (C-H), 1734 (C=O), 1647 (C=O), 1590 (N-H), 1142 (C-O), 1116 (C-O), 752 (C-Br) cm^{-1} ; **HRMS** (ESI⁺): m/z calcd for $\text{C}_{19}\text{H}_{12}\text{BrNO}_5\text{Na}^+$ [M+Na]⁺ 435.9797, found 437.9762; **Mp**: not determined.

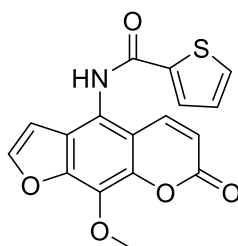
2.1.2.3.5. *N*-(9-methoxy-7-oxo-7*H*-furo[3,2-*g*]chromen-4-yl)furan-2-carboxamide (3e)



The title compound was synthesized following **General procedure A** using the amine compound **2** (72 mg, 0.3 mmol, 1.0 equiv.) in CH_2Cl_2 (6.0 mL), 2-furoyl chloride (120.0 μL , 1.20 mmol, 4.0 equiv.) and K_2CO_3 (63 mg, 0.45 mmol, 1.5 equiv.). The crude product was purified by silica gel column chromatography (eluent: 100% DCM - 1% MeOH in DCM) to provide the amide compound **3e** (39 mg, 0.120 mmol, 39% yield) as a yellow-green solid.

¹H NMR (500 MHz,) δ 10.52 (s, 1H), 7.97 (d, J = 2.3 Hz, 1H), 7.93 – 7.85 (m, 2H), 7.28 (d, J = 3.4 Hz, 1H), 6.79 (d, J = 2.3 Hz, 1H), 6.63 (dd, J = 3.6, 1.8 Hz, 1H), 6.32 (d, J = 9.8 Hz, 1H), 4.06 (s, 1H); **¹³C NMR** (126 MHz, $\text{DMSO-}D_6$) δ 159.95, 157.54, 147.79, 147.40, 147.36, 146.49, 143.07, 141.90, 131.19, 124.17, 120.99, 115.86, 114.25, 113.26, 112.73, 106.77, 61.64; **IR** (neat): 3257 (N-H), 3142 (C=C), 3065 (C=C), 2955 (C-H), 1720 (C=O), 1653 (C=O), 1590 (C=C), 1466 (N-H), 1423 (C=C), 1137 (C-O), 1170 (C-O) cm^{-1} ; **HRMS** (ESI⁺): m/z calcd for $\text{C}_{17}\text{H}_{11}\text{NO}_6\text{Na}^+$ [M+Na]⁺ 348.0484, found 348.0484; **Mp**: not determined.

2.1.2.3.6. *N*-(9-methoxy-7-oxo-7*H*-furo[3,2-*g*]chromen-4-yl) thiophene-2-carboxamide (3f)



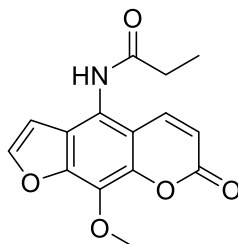
The title compound was synthesized following **General procedure A** using the amine compound **2** (72 mg, 0.3 mmol, 1.0 equiv.) in CH_2Cl_2 (6.0 mL), thiophene-2-carbonyl

chloride (130.0 μL , 1.20 mmol, 4.0 equiv.) and K_2CO_3 (63 mg, 0.45 mmol, 1.5 equiv.). The crude product was purified by silica gel column chromatography (eluent: 100% hexanes - EtOAc/hexanes = 1:3). Then the solid was recrystallized in EtOH/water. After that the resulting solid was purified by short silica gel column chromatography (eluent: 5% MeOH in DCM) to provide the amide compound **3f** (52 mg, 0.152 mmol, 49% yield) as a green solid.

$^1\text{H NMR}$ (500 MHz,) δ 10.63 (s, 1H), 8.09 (d, J = 3.3 Hz, 1H), 8.08 (d, J = 2.2 Hz, 1H), 8.01 (d, J = 9.8 Hz, 1H), 7.88 (dd, J = 5.0, 0.9 Hz, 1H), 7.24 (dd, J = 4.9, 3.8 Hz, 1H), 6.90 (d, J = 2.2 Hz, 1H), 6.42 (d, J = 9.9 Hz, 1H), 4.16 (s, 3H); $^{13}\text{C NMR}$ (126 MHz, $\text{DMSO-}D_6$) δ 161.08, 159.84, 147.77, 147.31, 143.01, 141.79, 139.07, 132.64, 131.12, 130.37, 128.63, 124.03, 121.24, 114.27, 113.13, 106.68, 61.56; **IR** (neat): 3236 (N-H), 3123 (C=C), 2921 (C-H), 1725 (C=O), 1635 (C=O), 1590 (C=C), 1525 (N-H), 1414 (C=C), 1140 (C-O), 1098 (C-O), 718 (C-S) cm^{-1} ; **HRMS** (ESI⁺): m/z calcd for $\text{C}_{17}\text{H}_{11}\text{NO}_5\text{Na}^+$ [M+Na]⁺ 364.0256, found 364.0261; **Mp**: not determined.

2.1.2.3.7. *N*-(9-methoxy-7-oxo-7H-furo[3,2-*g*]chromen-4-yl)propionamide

(**3g**)

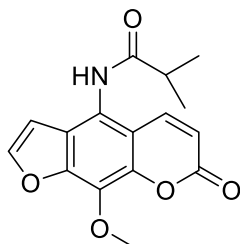


The title compound was synthesized following **General procedure A** using the amine compound **2** (72 mg, 0.3 mmol, 1.0 equiv.) in CH_2Cl_2 (6.0 mL), propionyl chloride (105.0 μL , 1.20 mmol, 4.0 equiv.) and K_2CO_3 (63 mg, 0.45 mmol, 1.5 equiv.). The crude product was collected and washed with cool hexanes to provide the amide compound **3g** (57 mg, 0.20 mmol, 64% yield) as a gray solid.

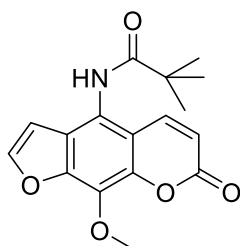
$^1\text{H NMR}$ (500 MHz,) δ 10.06 (s, 1H), 8.03 (s, 1H), 7.96 (d, J = 9.8 Hz, 1H), 6.83 (s, 1H), 6.40 (d, J = 9.8 Hz, 1H), 4.10 (s, 3H), 2.42 (d, J = 7.4 Hz, 2H), 1.12 (t, J = 7.4 Hz, 3H); $^{13}\text{C NMR}$ (126 MHz, $\text{DMSO-}D_6$) δ 173.17, 159.77, 147.29, 147.20, 142.91, 141.73, 130.47, 123.11, 121.97, 113.68, 112.20, 106.63, 61.40, 28.90, 10.01; **IR** (neat): 3243 (N-H), 3118 (C=C), 2980 (C-H), 1719 (C=O), 1655 (C=O), 1591 (C=C), 1515 (N-H), 1425 (C=C), 1162 (C-O), 1135 (C-O) cm^{-1} ; **HRMS** (ESI⁺): m/z calcd for $\text{C}_{15}\text{H}_{13}\text{NO}_5\text{Na}^+$ [M+Na]⁺ 310.0691, found 310.0683; **Mp**: not determined.

2.1.2.3.8. *N*-(9-methoxy-7-oxo-7*H*-furo[3,2-*g*]chromen-4-yl)isobutyramide

(3h)



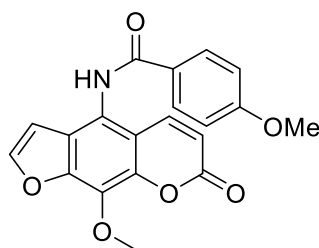
The title compound was synthesized following **General procedure A** using the amine compound **2** (72 mg, 0.3 mmol, 1.0 equiv.) in CH₂Cl₂ (6.0 mL), isobutyryl chloride (130.0 μL, 1.20 mmol, 4.0 equiv.) and K₂CO₃ (63 mg, 0.45 mmol, 1.5 equiv.). The resulting solid was recrystallized in EtOH/water, then the solid was collected and washed with hexanes. The crude product was purified by silica gel column chromatography (eluent: EtOAc/hexanes = 1:3-1:1) to provide the amide compound **3h** (13 mg, 0.043 mmol, 14% yield) as a white solid. ¹H NMR (500 MHz, CHLOROFORM-*D*) δ 7.70 (d, *J* = 9.8 Hz, 1H), 7.62 (d, *J* = 2.2 Hz, 1H), 7.50 (s, 1H), 6.64 (d, *J* = 2.2 Hz, 1H), 6.31 (d, *J* = 9.7 Hz, 1H), 4.25 (s, 3H), 2.79 – 2.67 (m, 1H), 1.35 (d, *J* = 6.9 Hz, 6H); ¹³C NMR (126 MHz, CHLOROFORM-*D*) δ 10.06 (s, 1H), 8.03 (s, 1H), 7.96 (d, *J* = 9.8 Hz, 1H), 6.83 (s, 1H), 6.40 (d, *J* = 9.8 Hz, 1H), 4.10 (s, 3H), 2.42 (d, *J* = 7.4 Hz, 2H), 1.12 (t, *J* = 7.4 Hz, 3H); IR (neat): 3248 (N-H), 3167 (C=C), 3129 (C=C), 2971 (C-H), 1732 (C=O), 1650 (C=O), 1588 (C=C), 1518 (N-H), 1161 (C-O), 1142 (C-O), 1128 (C-O) cm⁻¹; HRMS (ESI⁺): *m/z* calcd for C₁₆H₁₅NO₅Na⁺ [M+Na]⁺ 324.0848, found 324.0843; Mp: not determined.

2.1.2.3.9. *N*-(9-methoxy-7-oxo-7*H*-furo[3,2-*g*]chromen-4-yl)pivalamide (3i)

The title compound was synthesized following **General procedure A** using the amine compound **2** (72 mg, 0.3 mmol, 1.0 equiv.) in CH₂Cl₂ (6.0 mL), pivaloyl chloride (150.0 μL, 1.20 mmol, 4.0 equiv.) and K₂CO₃ (63 mg, 0.45 mmol, 1.5 equiv.). The crude product was recrystallized in EtOH/water to provide the amide compound **3i** (31 mg, 0.098 mmol, 32% yield) as a yellow solid.

$^1\text{H NMR}$ (500 MHz,) δ 9.65 (s, 1H), 8.05 (s, 1H), 7.83 (d, $J = 9.3$ Hz, 1H), 6.74 (s, 1H), 6.42 (d, $J = 9.3$ Hz, 1H), 4.12 (s, 3H), 1.28 (s, 9H); $^{13}\text{C NMR}$ (126 MHz, DMSO- D_6) δ 178.00, 159.92, 147.59, 147.26, 142.93, 141.65, 130.81, 124.07, 122.39, 114.10, 113.23, 106.49, 61.54, 31.08, 27.69; **IR** (neat): 3215 (N-H), 3134 (C=C), 2984 (C-H), 1730 (C=O), 1640 (C=O), 1590 (C=C), 1505 (N-H), 1475 (C=C), 1376 (C-C), 1154 (C-O), 1133 (C-O) cm^{-1} ; **HRMS** (ESI $^+$): m/z calcd for $\text{C}_{17}\text{H}_{17}\text{NO}_5\text{Na}^+$ $[\text{M}+\text{Na}]^+$ 338.1004, found 338.1004; **Mp**: not determined.

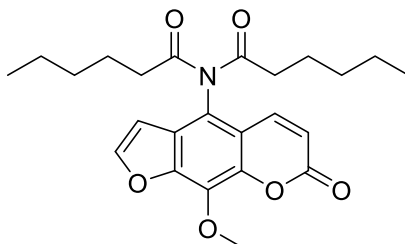
2.1.2.3.10. 4-methoxy-*N*-(9-methoxy-7-oxo-7*H*-furo[3,2-*g*]chromen-4-yl)benzamide (3j)



The title compound was synthesized following **General procedure A** using the amine compound **2** (72 mg, 0.3 mmol, 1.0 equiv.) in CH_2Cl_2 (6.0 mL), 4-methoxybenzoyl chloride (165.0 μL , 1.20 mmol, 4.0 equiv.) and K_2CO_3 (63 mg, 0.45 mmol, 1.5 equiv.). The resulting solid was recrystallized in EtOH/water. Then the crude product was purified by silica gel column chromatography (eluent: EtOAc/hexanes = 1:9-1:1) to provide the amide compound **3j** (35 mg, 0.096 mmol, 31% yield) as a white solid.

$^1\text{H NMR}$ (500 MHz,) δ 10.44 (s, 1H), 8.05 (d, $J = 2.3$ Hz, 1H), 8.03 (d, $J = 8.8$ Hz, 2H), 7.99 (d, $J = 9.9$ Hz, 1H), 7.06 (dd, $J = 9.3, 2.3$ Hz, 2H), 6.88 (d, $J = 2.1$ Hz, 1H), 6.40 (d, $J = 9.8$ Hz, 1H), 4.15 (s, 3H), 3.82 (s, 3H); $^{13}\text{C NMR}$ (126 MHz, DMSO- D_6) δ 166.01, 162.66, 159.92, 147.60, 147.37, 143.06, 142.01, 130.91, 130.35, 126.12, 124.02, 122.27, 114.10, 114.02, 113.11, 106.78, 61.57, 55.90; **IR** (neat): 3214 (N-H), 3128 (C=C), 2950 (C-H), 1725 (C=O), 1644 (C=O), 1607 (C=C), 1592 (N-H), 1498 (C=C), 1478 (C=C), 1254 (C-O), 1023 (C-O) cm^{-1} ; **HRMS** (ESI $^+$): m/z calcd for $\text{C}_{24}\text{H}_{29}\text{NO}_6\text{Na}^+$ $[\text{M}+\text{Na}]^+$ 388.0797, found 388.0804; **Mp**: not determined.

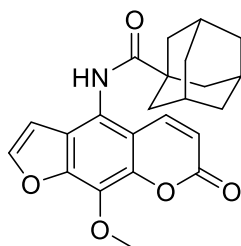
2.1.2.3.11. *N*-hexanoyl-*N*-(9-methoxy-7-oxo-7*H*-furo[3,2-*g*]chromen-4-yl)hexanamide (**3k**)



The title compound was synthesized following **General procedure A** using the amine compound **2** (72 mg, 0.3 mmol, 1.0 equiv.) in CH₂Cl₂ (6.0 mL), caproyl chloride (224.0 μL, 1.20 mmol, 4.0 equiv.) and K₂CO₃ (63 mg, 0.45 mmol, 1.5 equiv.). The crude product was purified by silica gel column chromatography (eluent: EtOAc/hexanes = 1:9-1:2). Then the resulting solid was collected and washed with cool hexanes to provide the amide compound **3k** (21 mg, 0.064 mmol, 21% yield) as a white solid.

¹H NMR (500 MHz, CHLOROFORM-*D*) δ 7.71 (d, *J* = 2.3 Hz, 1H), 7.54 (d, *J* = 9.8 Hz, 1H), 6.61 (d, *J* = 2.3 Hz, 1H), 6.44 (d, *J* = 9.9 Hz, 1H), 4.35 (s, 3H), 2.52 (t, 4H), 1.60 (p, *J* = 7.4 Hz, 4H), 1.31 – 1.16 (m, 8H), 0.84 (t, *J* = 7.0 Hz, 6H); ¹³C NMR (126 MHz, CHLOROFORM-*D*) δ 175.66, 159.31, 147.73, 147.04, 143.03, 137.87, 133.32, 125.49, 120.44, 116.62, 114.73, 103.82, 61.29, 37.99, 31.06, 24.22, 22.26, 13.74; IR (neat): 3441 (N-H), 3126 (C=C), 2953 (C-H), 2926 (C-H), 2858 (C-H), 1726 (C=O), 1685 (C=O), 1589 (C=C), 1480 (N-H), 1163 (C-O), 1135 (C-O) cm⁻¹; HRMS (ESI⁺): *m/z* calcd for C₂₄H₃₁NO₅Na⁺ [M+Na]⁺ 450.1893, found 450.1885; Mp: not determined.

2.1.2.3.12. (3*r*,5*r*,7*r*)-*N*-(9-methoxy-7-oxo-7*H*-furo[3,2-*g*]chromen-4-yl)adamantane-1-carboxamide (**3l**)

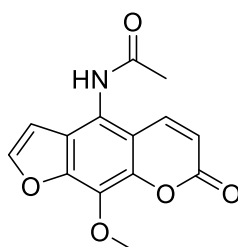


The title compound was synthesized following **General procedure A** using the amine compound **2** (116 mg, 0.5 mmol, 1.0 equiv.) in CH₂Cl₂ (6.0 mL), 1-adamantanecarbonyl chloride (200.0 μL, 2.0 mmol, 4.0 equiv., synthesized from reaction between 1-adamantanecarboxylic acid (1.0 mmol, 1.0 equiv.), thionyl chloride (20.0 mmol, 20.0 equiv.) and a few drops of DMF in anhydrous toluene at 80 °C for 2 hrs, the crude mixture was

evaporated and used without further purification)) and K_2CO_3 (104 mg, 0.75 mmol, 1.5 equiv.). The crude product was purified by silica gel column chromatography (eluent: 100% hexanes - EtOAc/hexanes = 1:4) to provide the amide compound **3l** (29 mg, 0.074 mmol, 15% yield) as an off-white solid.

1H NMR (500 MHz,) δ 7.62 (s, 1H), 7.59 (d, J = 9.8 Hz, 1H), 7.58 (d, J = 2.2 Hz, 1H), 6.55 (d, J = 2.2 Hz, 1H), 6.23 (d, J = 9.8 Hz, 1H), 4.22 (s, 3H), 2.13 (s, 3H), 2.04 (d, J = 2.5 Hz, 6H), 1.79 (q, J = 12.5 Hz, 6H); ^{13}C NMR (126 MHz, CHLOROFORM- D) δ 177.59, 160.13, 147.40, 146.35, 143.00, 139.76, 131.69, 123.79, 119.53, 114.38, 113.00, 105.18, 61.47, 41.62, 39.53, 36.47, 28.19; IR: cannot be retrieved; HRMS (ESI $^+$): m/z calcd for not determined; Mp: not determined

2.1.2.3.13. *N*-(9-methoxy-7-oxo-7H-furo[3,2-*g*]chromen-4-yl)acetamide (**3m**)



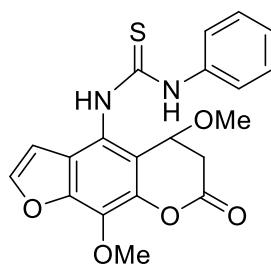
The title compound was synthesized using a modified procedure.²¹ The solution of amine compound **2** (24 mg, 0.1 mmol, 1.0 equiv.) in CH_2Cl_2 (2.0 mL); acetic anhydride in DCM (200 μ L, 0.2 mmol, 2.0 equiv.), pyridine (16 μ L, 0.2 mmol, 2.0 equiv.) and DMAP (2.5 mg, 0.02 mmol, 0.2 equiv.) were added at 0 $^{\circ}C$. After being heated to room temperature, the reaction mixture was stirred under a nitrogen atmosphere for 21 hrs. and then acetic anhydride in DCM (800 μ L, 0.8 mmol, 8.0 equiv.) and K_2CO_3 (27.6 mg, 0.2 mmol, 2.0 equiv.) were added. The reaction mixture was stirred overnight and monitored by TLC. Upon completion the reaction mixture was quenched with H_2O . The resulting mixture was neutralized by sat. $NaHCO_3$ and extracted with EtOAc (3 x 20 mL). The combined organic layers were washed with brine, dried over anhydrous $MgSO_4$, filtered, then concentrated *in vacuo*. The resulting solid was recrystallized in EtOH/water to provide the amide compound **3m** (12 mg, 0.044 mmol, 42% yield) as a white solid.

1H NMR (500 MHz, $DMSO-D_6$) δ 10.06 (s, 1H), 7.95 (d, J = 2.2 Hz, 1H), 7.91 (d, J = 9.9 Hz, 1H), 6.79 (d, J = 2.2 Hz, 1H), 6.32 (d, J = 9.8 Hz, 1H), 4.03 (s, 3H), 2.05 (s, 3H); ^{13}C NMR (126 MHz, $DMSO-D_6$) δ 169.53, 159.81, 147.32, 147.27, 142.93, 141.80, 130.55, 123.16, 121.95, 113.73, 112.23, 106.67, 61.44, 23.20; IR (neat): 3324 (N-H), 3114 (C=C), 2955 (C-H), 1709 (C=O), 1687

(C=O), 1593 (C=C), 1506 (N-H), 1163 (C-O), 1134 (C-O), 1058 (C-O) cm^{-1} ; **HRMS** (ESI⁺): m/z calcd for $\text{C}_{14}\text{H}_{11}\text{NO}_5\text{Na}^+$ $[\text{M}+\text{Na}]^+$ 296.0535, found 296.0533; **Mp**: not determined.

2.1.2.4. Synthesis of 4-6

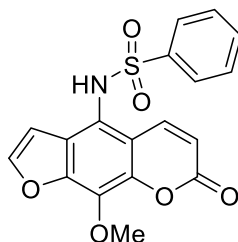
2.1.2.4.1. 1-(5,9-dimethoxy-7-oxo-6,7-dihydro-5H-furo[3,2-g]chromen-4-yl)-3-phenylthiourea (4)



The title compound was synthesized using a modified procedure.²² The solution of amine compound **2** (47 mg, 0.2 mmol, 1.0 equiv.) in MeOH (1.0 mL); phenylisothiocyanate (90 μL , 2.22 mmol, 3.1 equiv.) was added. The reaction mixture was stirred under the Ar atmosphere at 65 °C overnight. After being cooled to room temperature, the reaction mixture was quenched with H_2O . The resulting mixture was extracted with CH_2Cl_2 (3 x 20 mL). The combined organic layers were washed with brine, dried over anhydrous MgSO_4 , filtered, then concentrated *in vacuo*. The resulting solid was purified by preparative thin-layer chromatography (eluent: EtOAc/hexanes = 2:3) to provide the thiourea compound **4** (40 mg, 0.100 mmol, 49% yield) as a dark green solid.

¹H NMR: (400 MHz, CDCl_3) δ 8.82 (s, 1H), 7.52 (d, 1H), 7.48 – 7.42 (m, 4H), 7.41 (t, $J = 18.7$ Hz, 1H), 6.88 (d, $J = 2.3$ Hz, 1H), 6.23 (s, 1H), 5.50 (t, 1H), 4.15 (s, 3H), 3.55 (s, 3H), 2.91 (dd, $J = 14.8$, 4.9 Hz, 1H), 2.83 (dd, $J = 14.8$, 5.3 Hz, 1H); ¹³C NMR: (101 MHz, CDCl_3) δ 176.38, 170.25, 145.99, 143.97, 143.65, 140.35, 129.17, 128.59, 128.35, 128.08, 121.95, 108.60, 103.20, 102.95, 60.90, 57.22, 51.87, 38.42; **IR**: cannot be retrieved; **HRMS** (ESI⁺): m/z calcd for $\text{C}_{20}\text{H}_{18}\text{N}_2\text{O}_5\text{SH}^+$ $[\text{M}+\text{H}]^+$ 399.1015, found 399.1011; **Mp**: not determined.

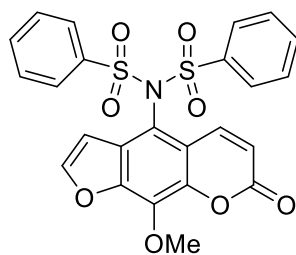
2.1.2.4.2. *N*-(9-methoxy-7-oxo-7*H*-furo[3,2-*g*]chromen-4-yl)benzene sulfonamide (5)



The title compound was synthesized using a modified procedure.²³ The solution of amine compound **2** (47 mg, 0.2 mmol, 1.0 equiv.) in pyridine (400 μ L); benzenesulfonyl chloride (30 μ L, 0.22 mmol, 1.1 equiv.) and DMAP (2.5 mg, 0.02 mmol, 0.1 equiv.) were added. The reaction mixture was stirred under the Ar atmosphere at room temperature for 2 hrs. 20 mins. The reaction mixture was quenched with H₂O. The resulting mixture was extracted with CH₂Cl₂ (3 x 20 mL). The combined organic layers were washed with brine, dried over anhydrous MgSO₄, filtered, then concentrated *in vacuo*. The resulting solid was purified by preparative thin-layer chromatography (eluent: EtOAc/hexanes = 4:1) to provide the sulfonamide compound **5** (62.3 mg, 0.170 mmol, 82% yield) as a dark green solid.

¹H NMR: (300 MHz, Acetone) δ 9.07 (s, 1H), 8.05 (d, *J* = 9.9 Hz, 1H), 7.70 (d, *J* = 2.3 Hz, 1H), 7.59 (d, *J* = 7.6 Hz, 4H), 7.45 (t, 2H), 6.35 (d, *J* = 2.3 Hz, 1H), 6.26 (d, *J* = 9.9 Hz, 1H), 4.18 (s, 4H); ¹³C NMR: (75 MHz, Acetone) δ 160.24, 148.28, 148.02, 144.63, 142.03, 140.43, 134.30, 133.38, 130.45, 128.41, 126.58, 120.12, 116.50, 115.11, 106.31, 61.89; IR (neat): 3201 (N-H), 3160 (C=C), 2951 (C-H), 1697 (C=O), 1615 (C=O), 1588 (C=C), 1474 (C=C), 1338 (S=O), 1164 (C-O), 1130 (C-O), 1053 (C-O), 724 (C-S) cm⁻¹; HRMS (ESI⁺): *m/z* calcd for C₁₈H₁₃NO₆SNa⁺ [M+Na]⁺ 394.0362, found 394.0365; Mp: not determined.

2.1.2.4.3. *N*-(9-methoxy-7-oxo-7*H*-furo[3,2-*g*]chromen-4-yl)-*N*-(phenylsulfonyl)benzenesulfonamide (6)



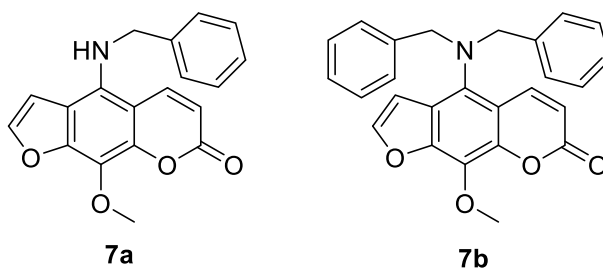
The title compound was synthesized using a modified procedure.²⁴ The solution of amine compound **2** (72 mg, 0.3 mmol, 1.0 equiv.) in CH₂Cl₂ (2.0 mL); benzenesulfonyl chloride

(40 μL , 0.3 mmol, 1.0 equiv.), triphenylphosphine (120 mg, 0.45 mmol, 1.5 equiv.) and TEA (63 μL , 0.6 mmol, 2.0 equiv.) were added. The reaction mixture was stirred under the Ar atmosphere at 0 $^{\circ}\text{C}$ for 2 hrs. and then heated to room temperature for another 2 hrs. The reaction mixture was quenched with H_2O . The resulting mixture was extracted with CH_2Cl_2 (3 x 20 mL). The combined organic layers were washed with brine, dried over anhydrous MgSO_4 , filtered, then concentrated *in vacuo*. The resulting solid was purified by silica gel column chromatography (eluent: 100% hexanes - EtOAc/hexanes = 1:1) to provide the sulfonamide compound **6** (<20 mg, %yield; not determined).

^1H NMR: cannot be retrieved; ^{13}C NMR: cannot be retrieved; IR: cannot be retrieved; HRMS: cannot be retrieved; Mp: not determined.

2.1.2.5. Synthesis of 7a-7b

2.1.2.5.1. 4-(benzylamino)-9-methoxy-7H-furo[3,2-g]chromen-7-one (7a) and 4-(dibenzylamino)-9-methoxy-7H-furo[3,2-g]chromen-7-one (7b)



Compounds **7a** and **7b** were synthesized using a modified procedure.⁵ To a solution of substituted aniline (**2**) (72 mg, 0.3 mmol, 1.0 equiv.) in anhydrous acetone (1.5 mL) were added benzyl bromide (43 μL , 0.36 mmol, 1.2 equiv.) and K_2CO_3 (63 mg, 0.45 mmol, 1.5 equiv.). The reaction mixture was stirred under the Ar atmosphere at reflux at 55 $^{\circ}\text{C}$ for 3 h. After cooling to room temperature, the reaction mixture was filtered and washed with acetone. The solvent was removed on a rotary evaporator, and the crude product was purified by preparative thin-layer chromatography (eluent: EtOAc/hexanes = 2:3) to give the benzylamino **7a** (21.1 mg, 0.066 mmol, 21% yield) as a yellow solid and **7b** (70 mg, 0.17 mmol, 55% yield) as a yellow solid.

(**7a**) ^1H NMR: (400 MHz, CDCl_3) δ 7.84 (d, J = 9.9 Hz, 1H), 7.53 (d, J = 2.3 Hz, 1H), 7.35 (q, J = 8.5, 7.5 Hz, 5H), 6.82 (d, J = 2.3 Hz, 1H), 6.18 (d, J = 9.9 Hz, 1H), 4.65 (s, 2H), 4.11 (s, 3H); ^{13}C NMR: (101 MHz, CDCl_3) δ 160.60, 150.30, 144.72, 144.38, 138.81, 134.43, 128.98, 127.90, 127.49,

126.52, 114.34, 112.89, 111.19, 105.91, 104.61, 61.72, 52.49; **IR**: cannot be retrieved; **HRMS** (ESI⁺): m/z calcd for C₁₉H₁₅NO₄H⁺ [M+H]⁺ 322.1080, found 322.1078; **Mp**: not determined.

(7b) ¹H NMR: (400 MHz, CDCl₃) δ 8.22 (d, *J* = 9.7 Hz, 1H), 7.58 (d, *J* = 2.2 Hz, 1H), 7.33 – 7.19 (m, 6H), 7.19 – 7.09 (m, 4H), 6.67 (d, *J* = 2.3 Hz, 1H), 6.24 (d, *J* = 9.8 Hz, 1H), 4.28 (s, 4H), 4.22 (s, 3H); **¹³C NMR**: (101 MHz, CDCl₃) δ 160.33, 148.33, 145.02, 143.28, 141.21, 137.40, 135.45, 130.11, 128.75, 128.16, 127.30, 123.10, 113.95, 112.99, 105.86, 61.28, 58.05; **IR**: cannot be retrieved; **HRMS** (ESI⁺): m/z calcd for C₂₆H₂₁NO₄Na⁺ [M+Na]⁺ 434.1369, found 434.1365; **Mp**: not determined.

2.2. Biological evaluation

2.2.1. Anticancer activity

The biological evaluation was performed by Dr. Jutatip Boonsombat and Dr. Sanit Thongnест from Chulabhorn Research Institute. The synthesized novel products (**1**, **2**, **3a-3k** and **3m**) and methoxsalen were evaluated for anticancer activity. However, the synthesized novel products (**3l**, **4-6**, **7a** and **7b**) were not evaluated due to the COVID-19 situation. Approximately 7-8 mg of each solid product was packed in clean eppendorf tube for anticancer activity: breast cancer (MDA-MB-231 cell and T47-D cell), liver cancer (HepG2 cell and S102), leukemia (HL-60 and MOLT-3), lung cancer (A549 and H69AR), cholangiocarcinoma (HuCCA-1), HeLa cell and normal embryonic lung cell (MRC-5). Approximately 4-5 mg of each solid product was packed in clean eppendorf tube for cytotoxicity of cancer cell lines. The results of anticancer activity were received as %cytotoxicity at 50 µg/mL and IC₅₀ value (µM) obtained by MTT assay and XTT assay.

CHAPTER III

RESULTS & DISCUSSIONS

3.1. Synthesis of furocoumarin derivatives; amide group, thiourea group, sulfonamide group and benzyl-amino group at C-5 position.

There are three steps for this synthesis; (a) the nitration at C-5 position of methoxsalens, (b) the reduction of nitro group to primary amine and (c) the functionalization at the primary amine such as acylation, synthesis of thiourea, sulfonation, or benzylation. The overview of the synthesis is illustrated in **Figure 15**.

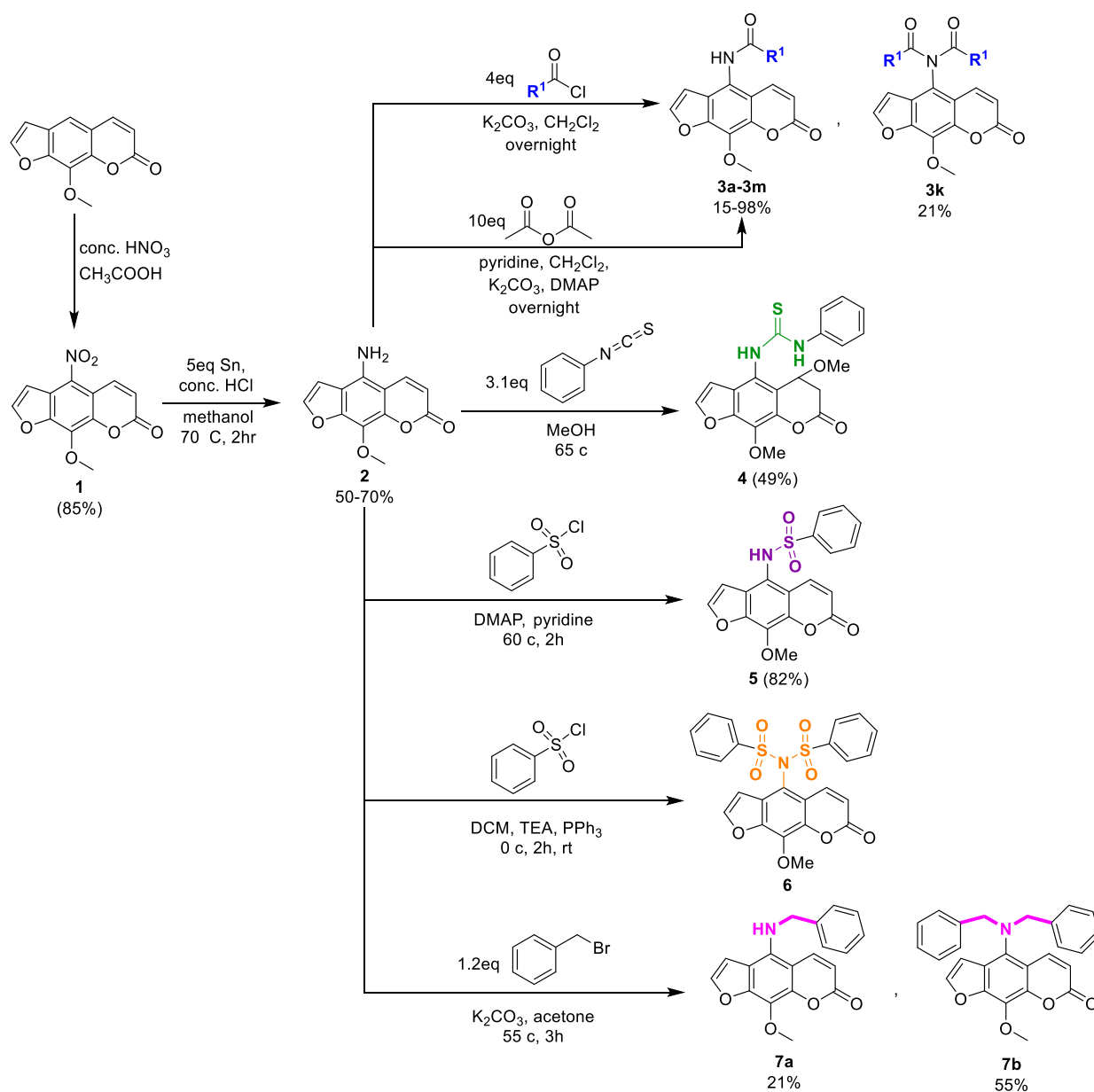


Figure 15 Synthesis the several functional group of furocoumarin derivatives

All the final compounds were characterized by ^1H NMR spectroscopy, ^{13}C NMR spectroscopy, high-resolution mass spectrometry (HRMS) and IR spectroscopy. The compounds **4-6**, **7a**, and **7b** had characterized by the laboratory at Chulabhorn Research Institute. The results confirmed that compounds have the structure as illustrated. However, the data were unable to show because the data is in the laboratory at Chulalongkorn University due to the COVID-19 situation, the data are inaccessible.

The first step (a) is the nitration¹⁹ (**Figure 16**). During the addition of conc. HNO_3 to the mixture of methoxsalen and acetic acid, the solution of the reaction mixture rapidly changed to the yellow solid in a few seconds. Then, the precipitate formed was filtered, washed with DI water and concentrated *in vacuo* to obtain the nitro compound **1** in good yield (85%).

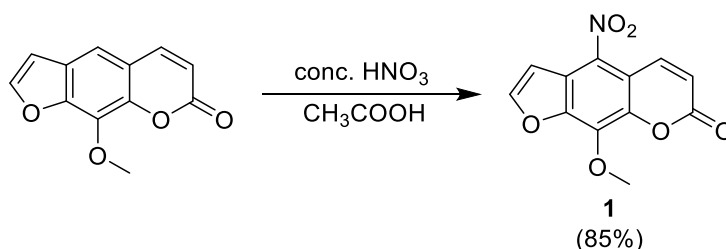


Figure 16 The nitration at C-5 position of methoxsalen

The nitration at C-5 position of methoxsalen occurs when lone pair of HNO_3 was protonated by acetic acid, then the protonated form of HNO_3 eliminated H_2O to generate the nitronium ion that was been attacked by methoxsalen containing the electron-donating group at C-5 position (**Figure 17**).²⁵

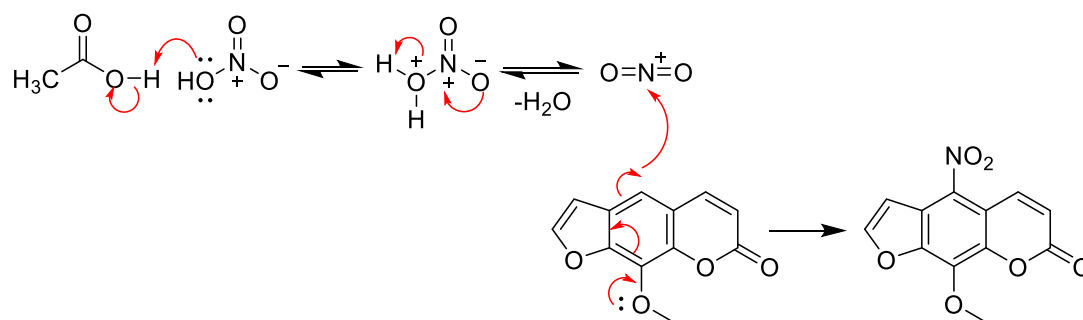


Figure 17 the mechanism of nitration

For the characterization, the ^1H NMR peak of the proton at C-5 position disappeared as it is replaced by the NO_2 group. Moreover, all of the peaks were deshielded because of the higher electronegativity of the NO_2 group compared to the H atom. For the IR spectra, the N–O stretching in an aromatic ring occurred at 1497 cm^{-1} and 1314 cm^{-1} , which is slightly lower

than usual because of the delocalization. Therefore, it confirms that compound **1** has the structure as shown (Figure 16).

The second step (b) is the reduction of nitro group to amine group (Figure 18).²⁰ When Zn powder was used as the reagent, **2** was obtained in a moderate yield (50%) even when the reaction was stirred overnight. Next, the reagent was changed to Sn powder with a shorter reaction time gave the amine compound **2** in moderate to good yield (50-70%). The yields were lower than expected probably due to the poor solubility of those molecules and especially the loss of the product in the filtration step. In the filtration step, it has the mixture of SnCl₂ as a white solid and the excess tin powder in the crude product, therefore, the filter paper was easily clogged.

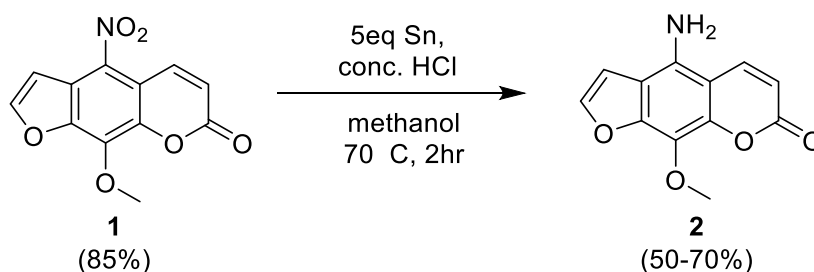


Figure 18 The reduction of nitro group to amine group

The mechanism of reduction starts with Sn donated electron pair to the nitro group, then the negatively charged electron on oxygen atom was protonated, next, the Sn pushed off, later on, nitro group was protonated and eliminated H₂O to give the nitroso group. Sn donated electron pair to nitroso (N=O) and then generate the hydroxylamine, that was donated electron pair by Sn, next eliminated H₂O and finally, Sn pushed off to obtain the amine compound **2** (Figure 19).²⁶

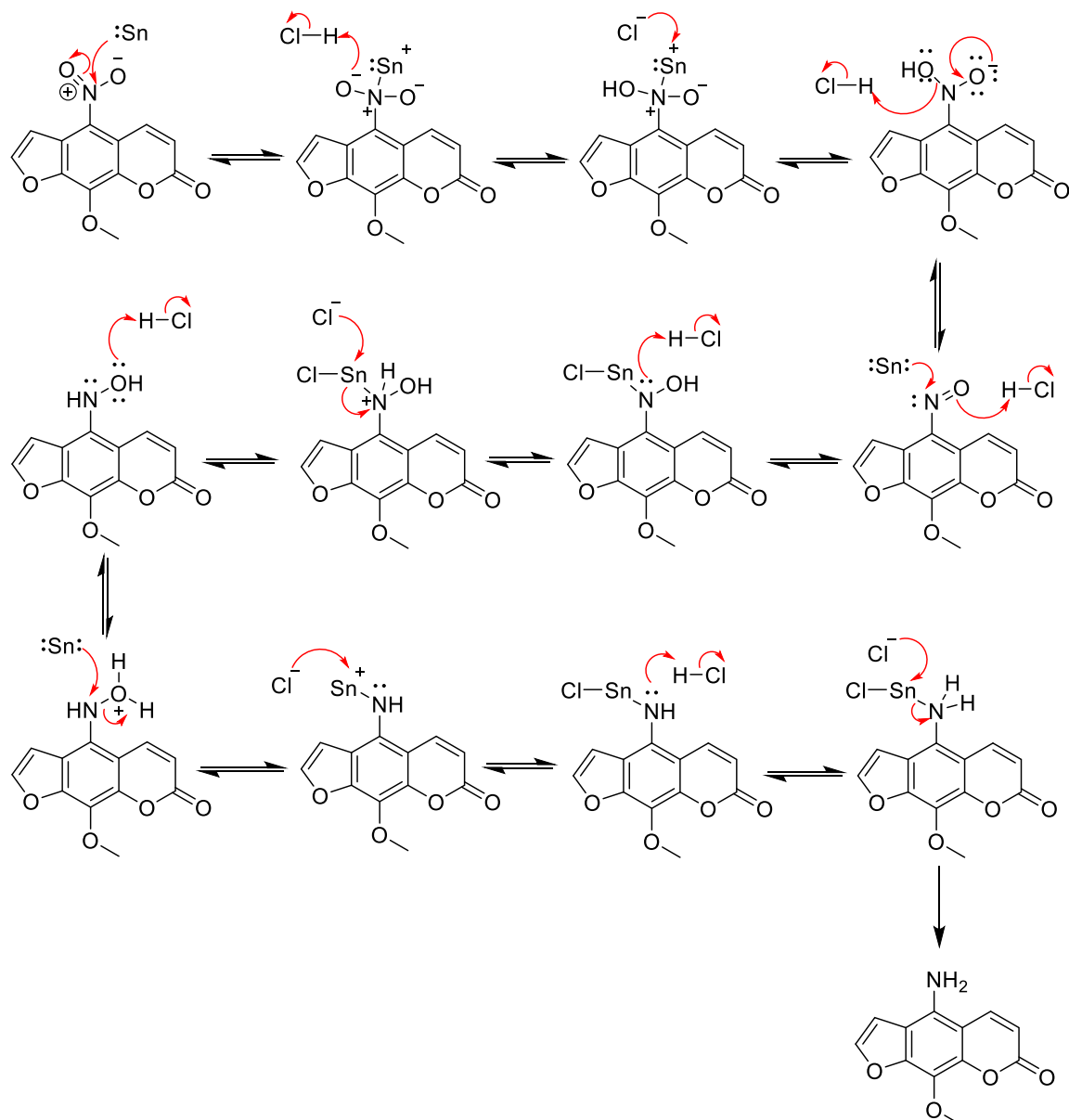


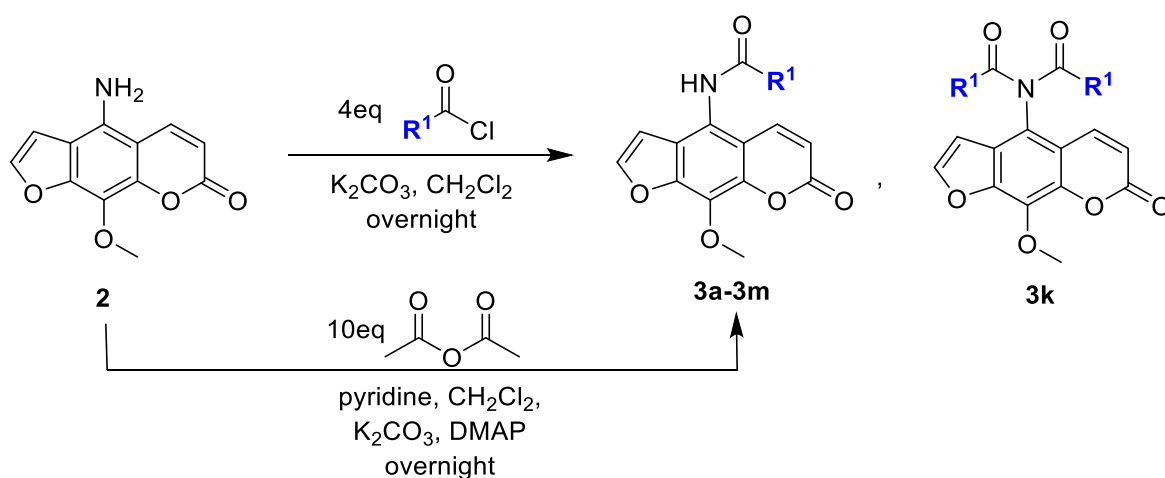
Figure 19 the mechanism of reduction

For the characterization, ¹H NMR spectrum showed a singlet peak of amine group at 5.63 ppm with the integration = 2. The other peaks were more shielded compared to those of the starting material because the higher electron density of NH₂ than the nitro group due to lone pair of N atom of the amine group. For the IR spectra, the N–H stretching in primary amine occurred at 3478 cm⁻¹ and 3383 cm⁻¹. The mass spectra found peak at m/z = 254.0428, which is [M+Na]⁺ (254.0429). Therefore, the characterization data confirmed that compound **2** has the structure as shown (**Figure 18**).

3.1.1. Amide synthesis by acylation

The third step (c) is the acylation of the amine group to amide group.⁵ Various acid chlorides were used as reagents and K_2CO_3 as a base for deprotonation. Compounds were synthesized following **General procedure A** to obtain the amide compounds **3a-3l** in low to excellent yields (15-98%) (**Table 4**). The reaction was able to occur at room temperature because the chloride ion is a good leaving group and the carbon atom of carbonyl group is highly electrophilic.

Table 4 The synthesis of amide group at C-5 position of methoxsalens and their percent yield



Compounds	R^1	Yield (%)
3a	$-C_6H_5$	86
3b	$-C_6H_5(p-F)$	98
3c	$-C_6H_5(p-CF_3)$	96
3d	$-C_6H_5(p-Br)$	88
3e	$-C_4H_9O$	39
3f	$-C_4H_9S$	46
3g	$-CH_2CH_3$	64
3h	$-CH(CH_3)_2$	25
3i	$-C(CH_3)_3$	32
3j	$-C_6H_5(p-OCH_3)$	31
3k	$-(CH_2)_4CH_3$	21
3l	-1-adamantyl	15
3m	$-CH_3$	42

There are three groups of substituents. First, the compounds **3a-3d** and **3j** contain phenyl substituents; **3b-3d** bearing phenyl substituents containing the electron-withdrawing groups, while **3j** bearing the electron-donating group. Second, the furan and thiophene substituents are in **3e** and **3f**, respectively. Last, the alkyl substituents are in **3g-3i**, **3k** and **3m**. For compound **3k**, we initially intended to synthesize a secondary amide containing one alkyl long chain substituent, however, the acylation occurred twice to obtain the tertiary amide, maybe due to the excess of acid chloride and the higher reactivity of alkyl substituted acid chloride.

Compound **3m** was initially synthesized following **General procedure A** but was not successful, probably due to the decomposed of acetyl chloride. The crude reaction was monitored by TLC and there was no expected spot corresponding to the product. There are two spots on TLC plate; the spot of starting material and the thin spot in baseline that may belong to carboxylic acid that decomposed from acid chloride. Although the catalyst is present in the reaction mixture with increased the temperature and reaction time nevertheless, no reaction occurred. Therefore, the synthesis of **3m** was instead achieved by using acetic anhydride as a reagent, DMAP as a catalyst and pyridine as a base to provide the amide compound **3m** in a moderate yield (42%) (**Table 4**).

Some products were relatively low yielded, probably due to the poor solubility of those molecules. Moreover, performing the reaction in a small scale could exaggerate the product loss, especially during the repeated purification step. However, the reaction without further purification has excellent yields (**3b** and **3c**) and the reaction with benzoyl chloride analogues has better yields than alkyl chloride.

Unfortunately, the synthesis of the *p*-NO₂-benzoyl substrate as the electron-donating group was unsuccessful despite several attempts, probably due to the high reactivity of *p*-nitrobenzoyl chloride, leading to reagent decomposition. Since we did not have the *p*-nitrobenzoyl chloride reagent, it was synthesized from the reaction between *p*-nitrobenzoic acid and thionyl chloride or oxalyl chloride, hence the improvement of this synthesis maybe required (**Figure 20**).

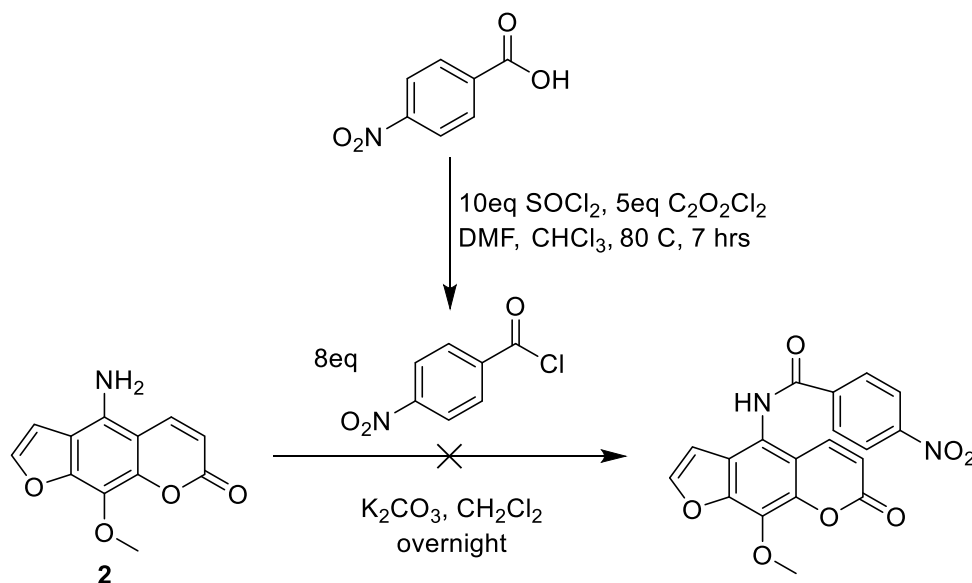


Figure 20 The synthesis of the *p*-NO₂-benzoyl substitution

The mechanism of the acylation using acid chloride is as followed: the addition stage of the reaction involves a nucleophilic attack on the electrophilic carbon atom of carbonyl by the lone pair on the nitrogen atom of amine group. Then, the elimination stage, the carbon-oxygen double bond reforms and a chloride ion is pushed off. Next, the removal of a hydrogen ion from the nitrogen by a chloride ion to obtain amide group at C-5 position (Figure 21).

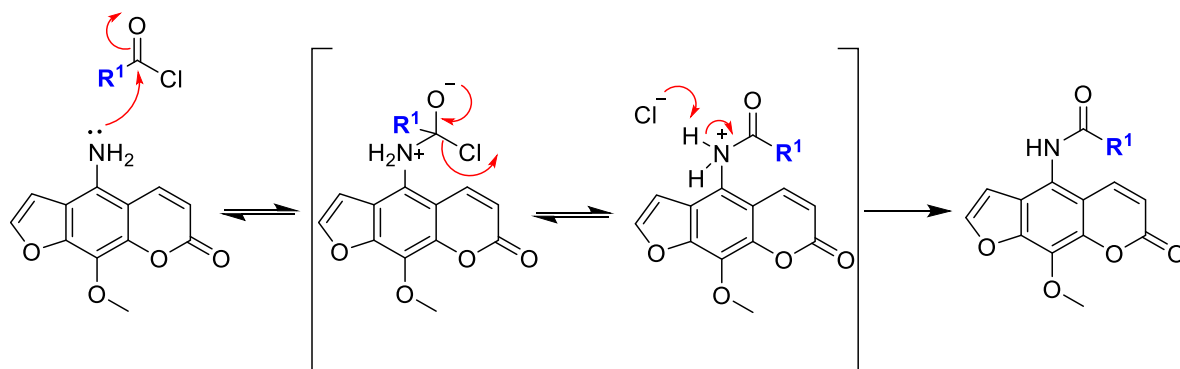


Figure 21 The mechanism of acylation of amine

The mechanism of **3m** has DMAP as the catalyst.²⁷ The lone pair on the nitrogen atom of DMAP attacked the electrophilic carbon atom of acid anhydride, and the acetate ion pushed off. Next, the nucleophilic addition occurred again. The lone pair on the nitrogen atom of amine group attacked the electrophilic carbon atom of carbonyl to generate the tetrahedral intermediate, then the intermediate was deprotonated by acetate ion to give the amide compound **3m** (Figure 22).

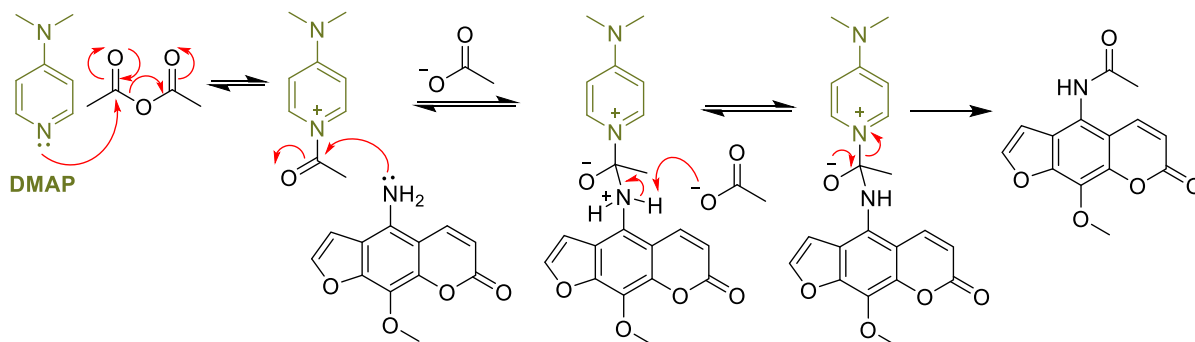


Figure 22 The mechanism of acylation of amine (**3m**)

The characterization of the compounds **3a-3m** from ^1H NMR spectrum, the singlet peak of amine group at 5.63 ppm disappeared. ^1H peak of secondary amide was found near 7.50-10.98 ppm but disappeared in the compound **3k** because it is tertiary amide. All peaks were deshielded because N atom was less electron-donating due to the carbonyl in amide group affect the electron density of H atom to be decreased. The ^{19}F NMR spectra of **3b** showed the triplet of doublets (td) peak of ^{19}F , which coupling with the hydrogen atom. For IR spectra, secondary amide occurred the N-H stretching near $3441\text{-}3211\text{ cm}^{-1}$, C=O stretching near $1687\text{-}1635\text{ cm}^{-1}$, C-F stretching at 748 and 824 cm^{-1} (**3b** and **3c**), C-Br stretching at 752 cm^{-1} (**3d**) and C-S stretching at 718 cm^{-1} (**3f**). The mass spectra of each compound found m/z at $[\text{M}+\text{Na}]^+$. Therefore, the characterization data confirmed that compounds **3a-3m** have the structure as shown (Table 4).

3.1.2. Synthesis of thiourea

The addition of primary amine compound **2** to phenylisothiocyanate gave the thiourea group. The reaction used phenylisothiocyanate as the reagent and MeOH as a solvent. Unfortunately, the desired thiourea product was not obtained. However, the major product of this reaction is the by-product **4** in a moderate yield (49%) and the others are excess reagent and a little of impurity (Figure 23).²²

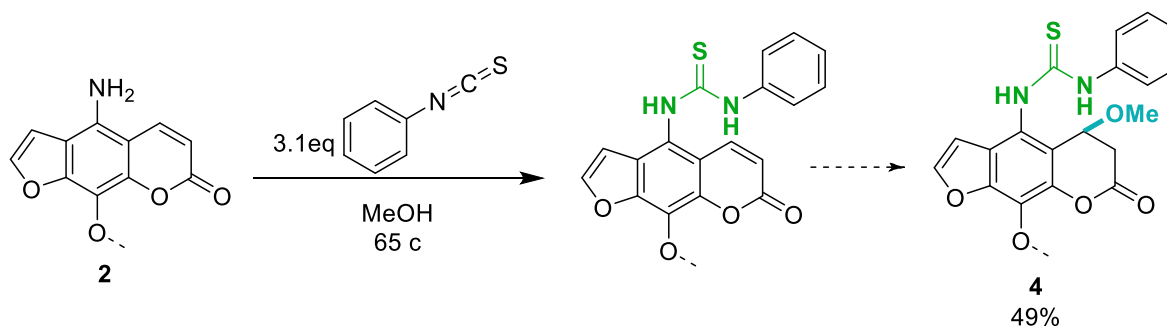


Figure 23 Synthesis of thiourea **4**

The mechanism of this reaction could involve a nucleophilic attack of the primary amine compound **2** at the phenylisothiocyanate giving the thiourea. Nevertheless, all the characterizations can be confirmed that the product of this reaction was unexpected. Unfortunately, the characterization data were unable to show because the data are inaccessible due to the COVID-19 situation. The side product **4** was arise, probably due to the 1,4-addition (conjugate addition or Michael addition). The solvent of this reaction which is MeOH, acts as a nucleophile by lone pair on oxygen atom, attacking the β -carbon atom containing the double bond on the right ring of coumarin. The 1,4-addition occurred to give an enolate ion, and the protonation may occur on oxygen atom and then tautomerization occurs to obtain the compound **4** (Figure 24).²⁸

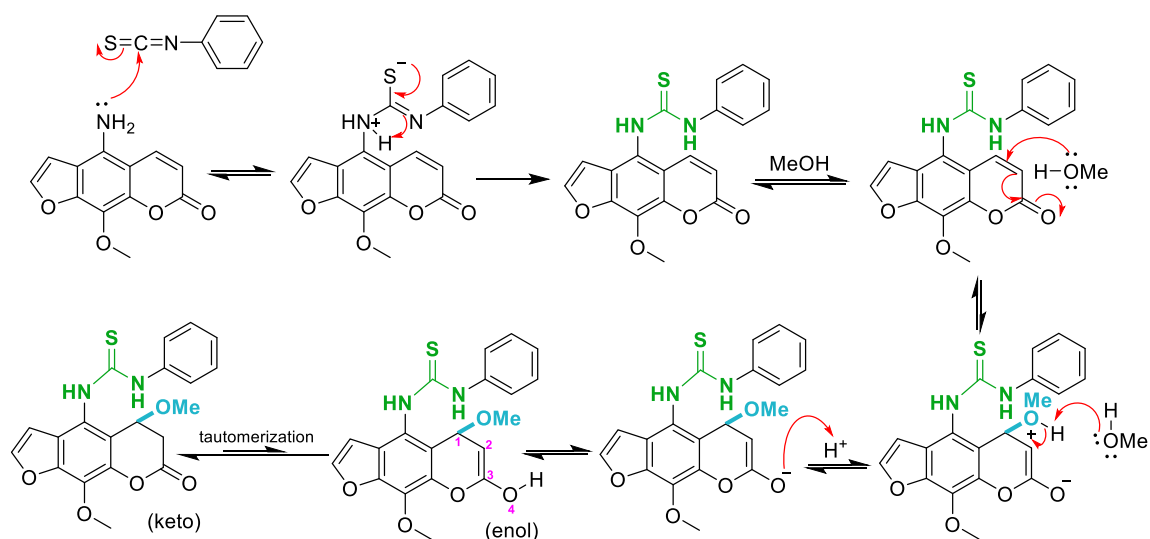


Figure 24 The mechanism of thiourea formation

3.1.3. Sulfonation

The sulfonation occurred between the amine compound **2** and benzenesulfonyl chloride by using DMAP as the catalyst to provide the sulfonamide compound **5** in a good yield (82%) (Figure 25).²³

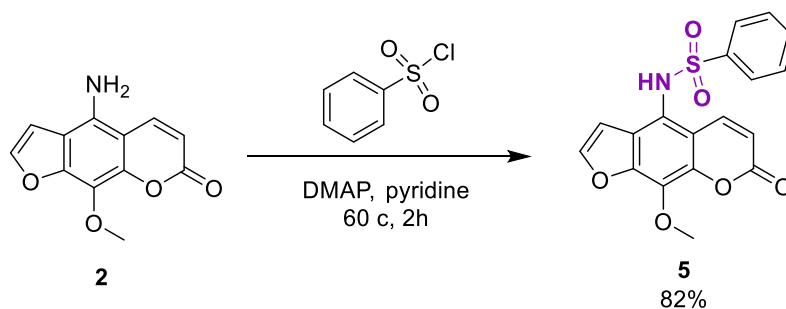


Figure 25 Sulfonation of compound 5

The mechanism of sulfonation (**4**) could involve a nucleophilic attack of the primary amine compound **2**. The electrophilic sulfur atom of benzenesulfonyl chloride followed by a proton transfer of H on N atom of amino to the negatively charged oxygen atom and HCl was eliminated from the intermediate generate to give the sulfonamide (**5**) (**Figure 26**). For the mechanism of the DMAP catalyst occurred in the same manner as that shown in **Figure 22**.

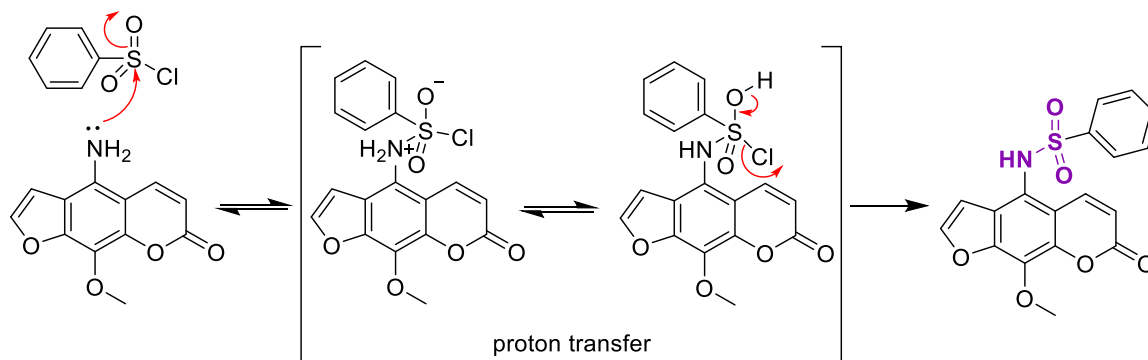


Figure 26 Mechanism of sulfonation

The reaction of the amine compound **2** with benzenesulfonyl chloride in triphenylphosphine by using TEA as the catalyst was performed, and we expected the formation of sulfinamide as our desired product.²⁴ However, after purification by silica gel column chromatography, the sulfonamide compounds **5**, together with the unexpected side-product **6**, were obtained (**Figure 27**). The structure of the products of this reaction can be confirmed by all the characterizations. Unfortunately, the data were unable to show because the data are inaccessible due to the COVID-19 situation.

The major compound was **5** (22 %yield) because of the steric effects due to the sulfonation occurred only one side. The minor product **6** received in quantity of <20 mg and yield cannot be precisely presented, since the data is in the laboratory at Chulabhorn Research Institute, which is inaccessible due to the COVID-19 situation (**Figure 27**). The yields were relatively low, probably due to the poor solubility of those molecules and the steric effects of molecules. Moreover, performing the reaction in a small scale could exaggerate the product loss, especially during the repeated purification step.

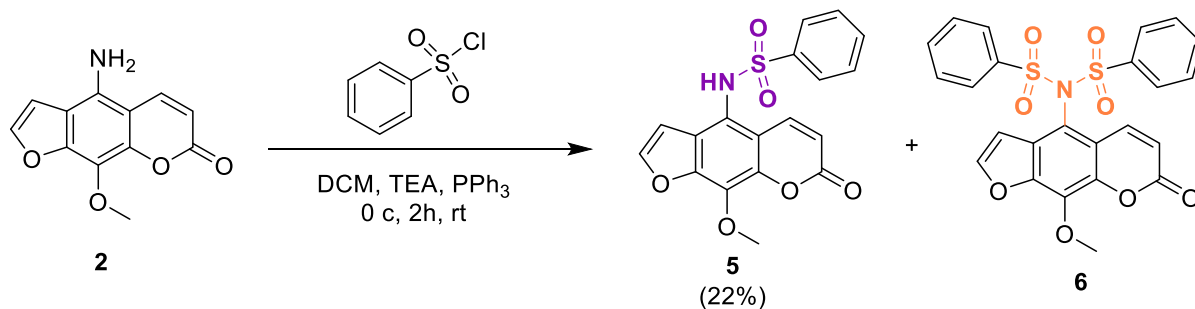
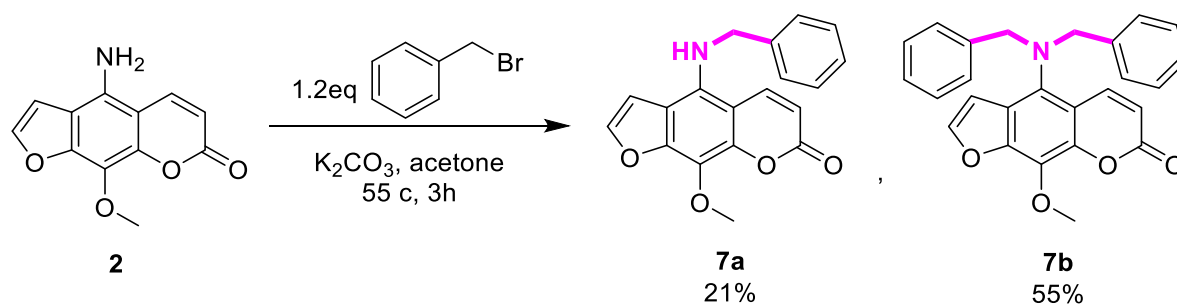


Figure 27 Sulfonation

3.1.4. Benzylation

Benylation of amine compound **2** with benzyl bromide in acetone using K_2CO_3 as a base to give the benzyl-amino **7a** and **7b** in moderate yields (21% and 55%, respectively) (Figure 28).⁵

Figure 28 Benzylation of **7a** and **7b**

The characterizations revealed that the products of this reaction are secondary amine **7a** and tertiary amine **7b**. The major product is tertiary amine **7b** which occurred by nucleophilic substitution at both sides. From the structures, the secondary amine compound **7a** (HN-R) has more nucleophilicity than primary amine **2** (NH_2) led to **7a** can attack the electrophilic carbon atom of benzyl bromide to give **7b** in the higher yield. In the facts that the effects of the alkyl group (benzyl group) act as an electron-donating group due to secondary amine **7a** is the greater nucleophile compared to compound **2** thus, secondary amine **7a** is better starting material than compound **2**.

The mechanism benzylation occurred by nucleophilic substitution reaction ($\text{S}_{\text{N}}2$). The nucleophile amine compound **2** attacked the electrophilic carbon atom, forcing the leaving group as Br atom to leave (Figure 29).

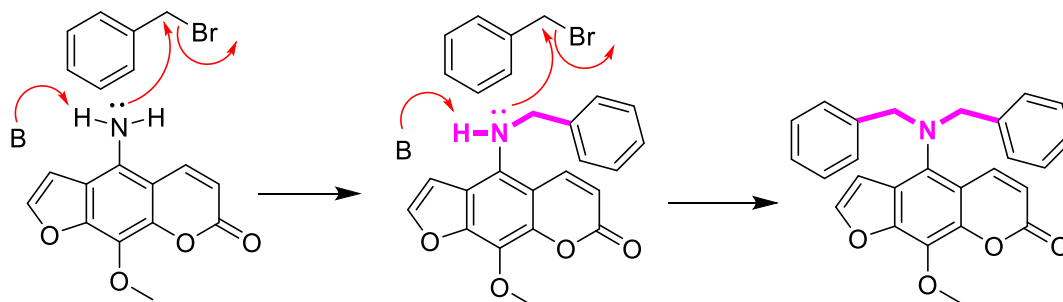


Figure 29 The mechanism benzylation

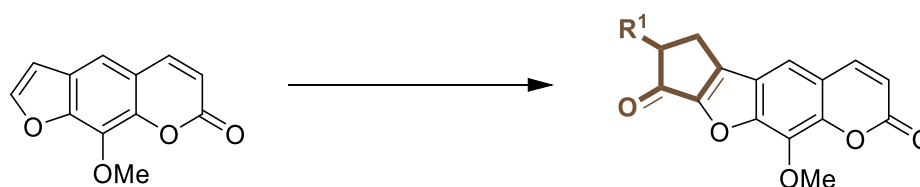
3.2. Synthesis the tetracyclic-furocoumarin derivatives

All the crude compounds were monitored by TLC and ^1H NMR spectroscopy to confirm that the majority of the product is the starting material. However, the ^1H NMR spectra are unable to be showed because the data is in the laboratory at Chulalongkorn University due to the COVID-19 situation, the data are inaccessible.

3.2.1. Synthesis of cyclopentanone-furocoumarin

The conditions were varied for reactions of cyclopentanone-furocoumarin by using acrylic acid or methacrylic acid as the reagents (Table 5). The reactions cannot be conducted in all the proposed conditions, probably due to the stability of the rings.

Table 5 Conditions of synthesis cyclopentanone-furocoumarin



Entry	Conditions	R ¹	Reagents	Yields (%)
1	PPA, DCM 70 °C	-H	4eq	0
2	PPA, DCE 70 °C	-H	6eq	0
3	Eaton's reagent 60-80 °C	-H	1.2eq	0
4	Eaton's reagent 65 °C	-CH ₃		0

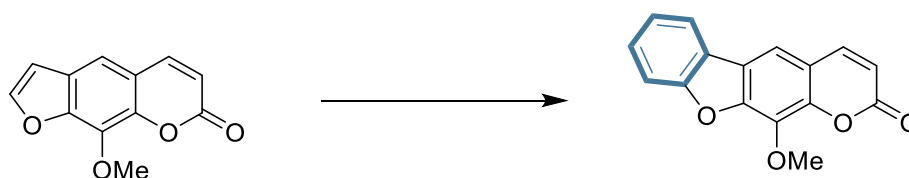
The reaction between methoxsalen and acrylic acid as a reagent and polyphosphoric acid (PPA) as a catalyst in DCM did not give the desired product (**Entry 1**).^{29,30} DCM was used as the solvent and stirred at 70 °C causes some solvent loss due to the low boiling point of DCM (boiling point of DCM = 39.6 °C).³¹ For **Entry 2**, the solvent was changed to DCE, which has higher boiling point and the excess of reagent (6 equiv.) was used. Nevertheless, no reaction occurred, probably due to steric effects of the aromatic ring and the decomposition of the PPA catalyst.

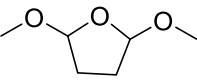
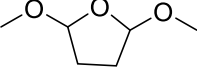
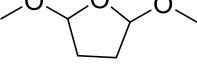
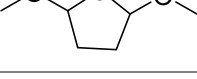
The Eaton's reagent (which was synthesized from reaction between methanesulfonic acid and phosphoric oxide)³² was used as a catalyst in the reaction between methoxsalen and acrylic acid (**Entry 3**).³³ The reaction mixture was stirred at 60-80 °C, but this reaction did not give the desired product. Next, the reagent was changed to methacrylic acid (**Entry 4**).³⁴ The reaction time was increased from the methodology, but in the TLC plate, there was no candidate product spot.

3.2.2. Synthesis of benzo-furocoumarin

The conditions were varied for the reactions of benzo-furocoumarin by using 2,5-dimethoxytetrahydrofuran as the reagent. All the reactions did not give the desired product (**Table 6**).

Table 6 The condition of synthesis benzo-furocoumarin



Entry	Condition	Reagent	Yield (%)
1	ZnBr ₂ , DCM 0 °C, rt	2eq 	0
2	CH ₃ SO ₃ H, DCM 0 °C, rt	2eq 	0
3	ZnBr ₂ , DCE 0 °C, reflux 60 °C	2eq 	0
4	CH ₃ SO ₃ H, DCE 0 °C, reflux 60 °C	2eq 	0

The 2,5-dimethoxytetrahydrofuran was used in the reaction of methoxsalen in DCM. The ZnBr_2 was used as a catalyst and stirred at room temperature, no reaction occurred (**Entry 1**).³⁵ Then in **Entry 2**, the catalyst was changed to $\text{CF}_3\text{SO}_3\text{H}$. The reaction mixture turned into an orange solution after adding $\text{CF}_3\text{SO}_3\text{H}$, but finally there was no reaction occurred. Although the reagent or solvent was changed, and the temperature and reaction time were increased (**Entry 3** and **Entry 4**). The results were confirmed by using the TLC plate and $^1\text{H-NMR}$ spectroscopy. There were starting material spot, the reagent spot and a thin spot of impurity. For ^1H NMR spectra, methoxsalen was found as the major compound.

All the synthesized tetracyclic-furocoumarin were unsuccessful despite several attempts, probably due to the stability and steric hindrance of the aromatic rings. Other possible reasons are the limitation of reagents or catalysts, air humidity in Thailand and the difference of starting material from the reference methodology. Thus, the synthesis of tetracyclic-furocoumarin was required to further improve the procedure.

3.3. The results of the anticancer activity

The biological evaluation was performed by Dr. Jutatip Boonsombat and Dr. Sanit Thongnest from Chulabhorn Research Institute. The synthesized novel products (**1**, **2**, **3a-3k** and **3m**) and methoxsalen were evaluated for anticancer activity; breast cancer (MDA-MB-231 and T47-D), liver cancer (HepG2 and S102), leukemia (HL-60 and MOLT-3), lung cancer (A549 and H69AR), cholangiocarcinoma (HuCCA-1), HeLa cell and normal embryonic lung cell (MRC-5). However, some of the synthesized novel products (**3l**, **4-6**, **7a** and **7b**) were not tested due to the COVID-19 situation.

The primary screening for anticancer activity used the cytotoxicity percentage at 50 $\mu\text{g/mL}$ against breast cancer (MDA-MB-231 and T47-D), liver cancer (HepG2 and S102), leukemia (HL-60 and MOLT-3), lung cancer (A549 and H69AR), cholangiocarcinoma (HuCCA-1), HeLa cell and normal embryonic lung cell (MRC-5) obtained by MTT assay and XTT assay (**Table 7**). Cyto- mean “of the cell” so cytotoxicity means the quality of being toxic to cells. Thus, the better anticancer activity should have higher cytotoxicity percentage at 50 $\mu\text{g/mL}$. Secondary screening was further investigated when each compound passed the primary screening and classified as being active (cytotoxicity percentage more than 50% at 50 $\mu\text{g/mL}$). The

compounds were screened at various concentrations to determine its IC_{50} value. IC_{50} value stands for concentration of drug compound at 50% of inhibition, which indicate the potency of compound in inhibiting. The lower IC_{50} value refers to the higher activity of that compound due to the small quantity of compound being able to inhibit the bioactivity of interest. Nowadays, IC_{50} value of drug compounds are reported in very low in degree of μM or nM . In this work, the compounds receiving cytotoxicity percentage at $50 \mu g/mL$ refers to the compounds have lower anticancer activity because $50 \mu g/mL$ is the lowest concentration that can obtain the bioactivity.

Table 7 The anticancer activity; breast cancer (MDA-MB-231 and T47-D), liver cancer (HepG2 and S102), leukemia (HL-60 and MOLT-3), lung cancer (A549 and H69AR), cholangiocarcinoma (HuCCA-1), HeLa cell and normal embryonic lung cell (MRC-5) in %Cytotoxicity at 50 µg/ml and IC₅₀ value (µM).

Compounds	IC50 [µM] (%Cytotoxicity at 50 µg/ml)										
	MDA-MB-231 ^a	T47-D ^b	HepG2 ^c	S102 ^d	HL-60 ^e	MOLT-3 ^f	A549 ^g	H69AR ^h	HuCCA-1 ⁱ	HeLa ^j	MRC-5 ^k
methoxsalen	I (6.10)	I (16)	I (18.94)	I (7.60)	I (46)	177.44 ± 14.66	I (15)	I (18)	I (24)	180.95 ± 7.32	I (12.74)
1	I (38.60)	161.72 ± 2.38	139.82 ± 18.91	I (42.11)	I (17)	I (29)	87.87 ± 7.60	81.01 ± 8.23	87.41 ± 9.39	84.61 ± 6.50	I (49.4)
2	I (2.77)	I (28)	I (10.16)	I (2.50)	I (39)	I (42)	I (10)	I (26)	I (22)	I (40)	I (5.25)
3a	I (24.85)	I (45)	I (18.94)	I (15.10)	I (42)	56.54 ± 5.16	I (12)	I (5)	I (3)	I (31)	I (15.75)
3b	I (33.86)	I (49)	I (21.17)	I (13.80)	I (38)	68.07 ± 12.85	I (35)	I (30)	I (40)	133.85 ± 0.58	I (11.2)
3c	I (35.27)	13.64 ± 0.26	I (42.80)	I (4.85)	I (6)	I (33)	I (23)	I (10)	I (27)	I (30)	I (41.1)
3d	91.33 ± 7.84	10.14 ± 0.53	71.68 ± 4.64	I (32.50)	98.62 ± 6.71	42.47 ± 7.80	31.92 ± 5.19	I (25)	I (48)	I (34)	I (45.07)
3e	I (0.45)	I (24)	I (1.70)	I (0.00)	I (9)	127.50 ± 9.53	I (6)	I (5)	I (7)	I (18)	I (4.35)
3f	I (8.45)	I (25)	I (10.50)	I (8.00)	I (28)	77.87 ± 17.69	I (8)	I (0)	I (0)	I (32)	I (2.95)
3g	I (3.12)	I (22)	I (16.40)	I (0.25)	I (13)	I (19)	I (6)	I (4)	I (5)	I (24)	I (3.6)
3h	I (4.32)	I (36)	I (28.70)	I (3.10)	I (11)	I (36)	I (10)	I (36)	I (20)	I (44)	I (18.25)
3i	I (0.90)	I (21)	I (4.00)	I (0.00)	I (0)	I (20)	I (6)	I (0)	I (22)	I (4)	I (5.55)
3j	I (19.32)	I (38)	I (31.16)	I (10.25)	123.72 ± 12.62	44.37 ± 2.09	I (9)	I (6)	I (33)	133.60 ± 3.31	I (5.55)
3k	I (5.15)	I (15)	I (6.97)	I (17.95)	I (0)	I (11)	I (16)	I (0)	I (30)	I (12)	I (10.05)
3m	I (6.30)	I (20)	I (8.25)	I (7.95)	I (19)	I (15)	I (4)	I (4)	I (6)	I (27)	I (11.5)
doxorubicin hydrochloride	2.59 ± 0.50	1.12 ± 0.12	0.43 ± 0.018	2.05 ± 0.08	0.14 ± 0.02	0.01	-	34.48 ± 2.44	1.18 ± 0.08	0.17 ± 0.01	2.26 ± 0.22
etoposide	-	-	49.08 ± 3.79	-	1.34 ± 0.10	0.04	0.34 ± 0.01	-	-	-	-

^a = Hormone-independent breast cancer; ^b = Hormone-dependent breast cancer; ^c = Human liver cancer cell line; ^d = Thai liver cancer; ^e = Promyeloblast;

^f = Acute lymphoblastic leukemia; ^g = Lung carcinoma; ^h = small cell lung cancer cell; ⁱ = Cholangiocarcinoma; ^j = Cervical Carcinoma; ^k = Normal embryonic lung cell; I = Inactive at 50 µg/ml

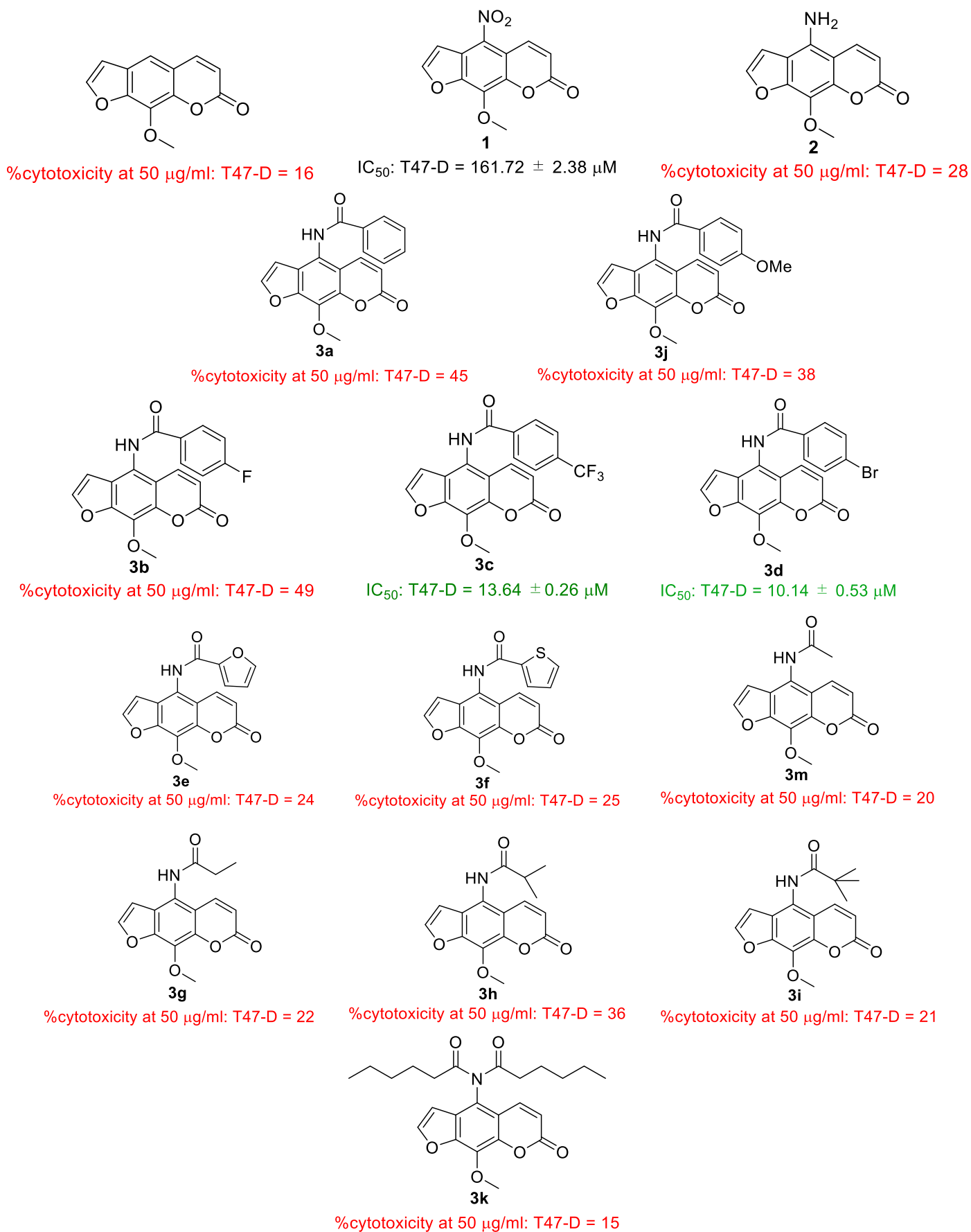


Figure 30 The structures and their anti-breast cancer activity (T47-D)

According to **Table 7**, most of the synthesized compounds unexpectedly had quite poor anticancer activity. Although the amide-containing compounds had been reported to possess significant anti-breast cancer effects.⁵ They were not quite effective in this study as the anticancer activity in breast cancer (MDA-MB-231 and T47-D), liver cancer (HepG2 and S102), leukemia (HL-60 and MOLT-3), lung cancer (A549 and H69AR), cholangiocarcinoma (HuCCA-1) and HeLa cell due to the activity was received in moderate to high of IC₅₀ value and low of cytotoxicity percentage. Referring to **Table 7** and **Figure 30**, compound **3d** which containing *p*-bromine on phenol substitution has significantly the greatest anticancer activity against. To compare the activity, the cytotoxicity percentage at 50 µg/mL of each compound is plotted in bar graphs (**Figure 31-35**) (noted that some compounds that has higher anti-cancer activity such as **3d** are included in the graph with stars on the bar graph since the data that we have is in IC₅₀ values, not the cytotoxicity percentage. Compounds had cytotoxicity percentage at 50 µM/mL of 0%, meaning that they showed no potent anticancer activity).

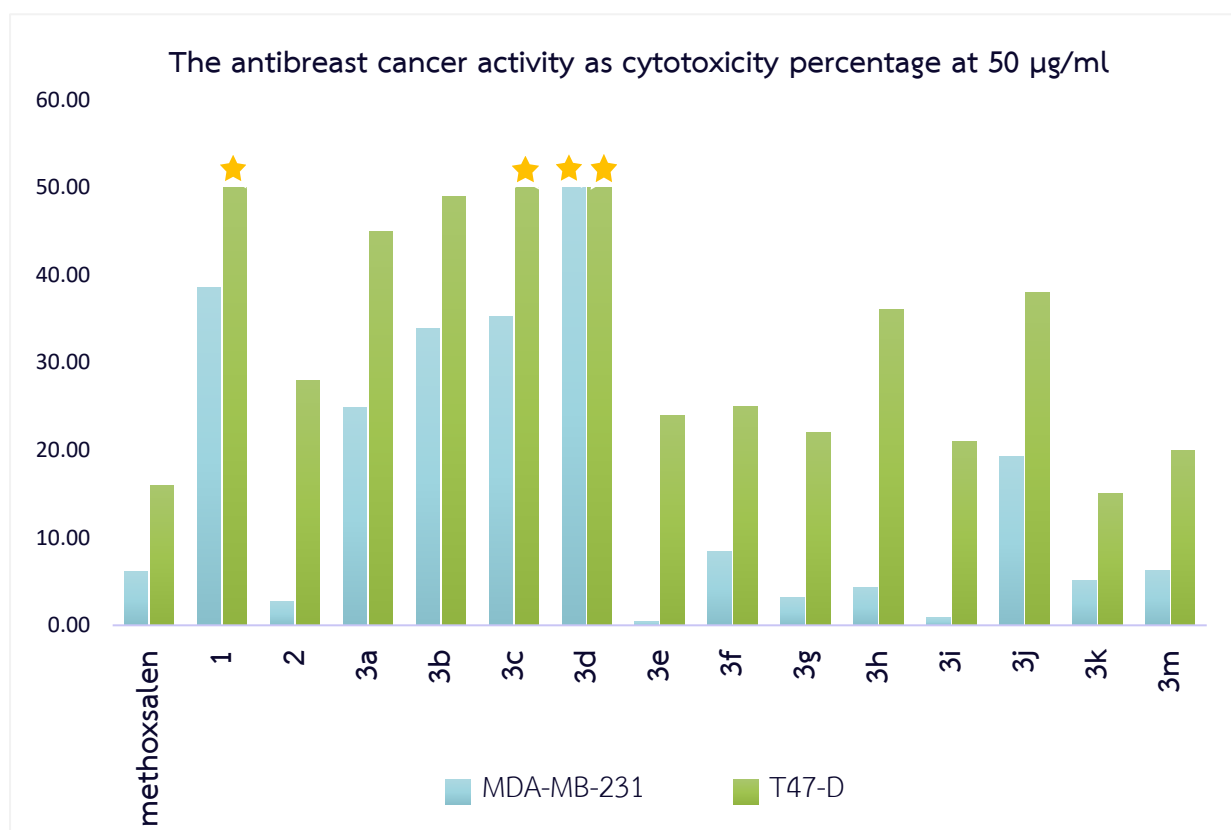


Figure 31 The anti-breast cancer activity as cytotoxicity percentage at 50 µg/mL (MDA-MB-231 and T47-D)

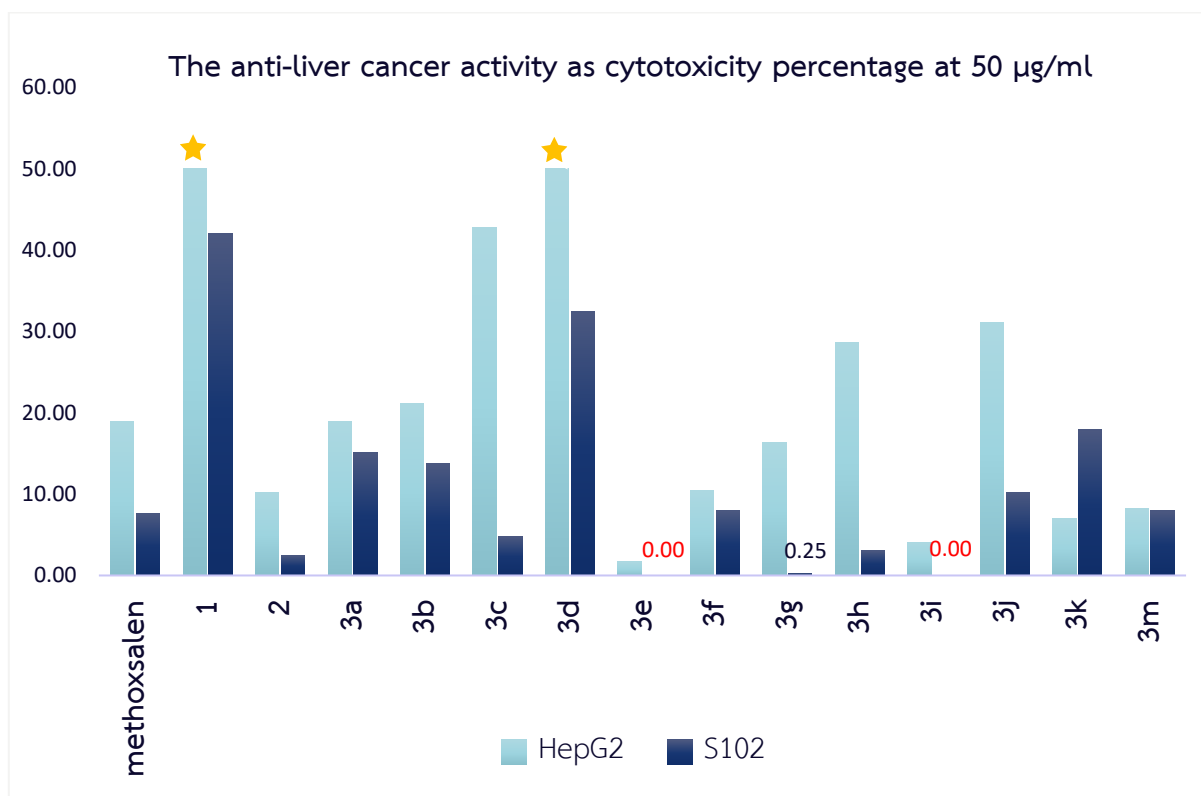


Figure 32 The anti-breast cancer activity as cytotoxicity percentage at 50 $\mu\text{g/ml}$
(HepG2 and S102)

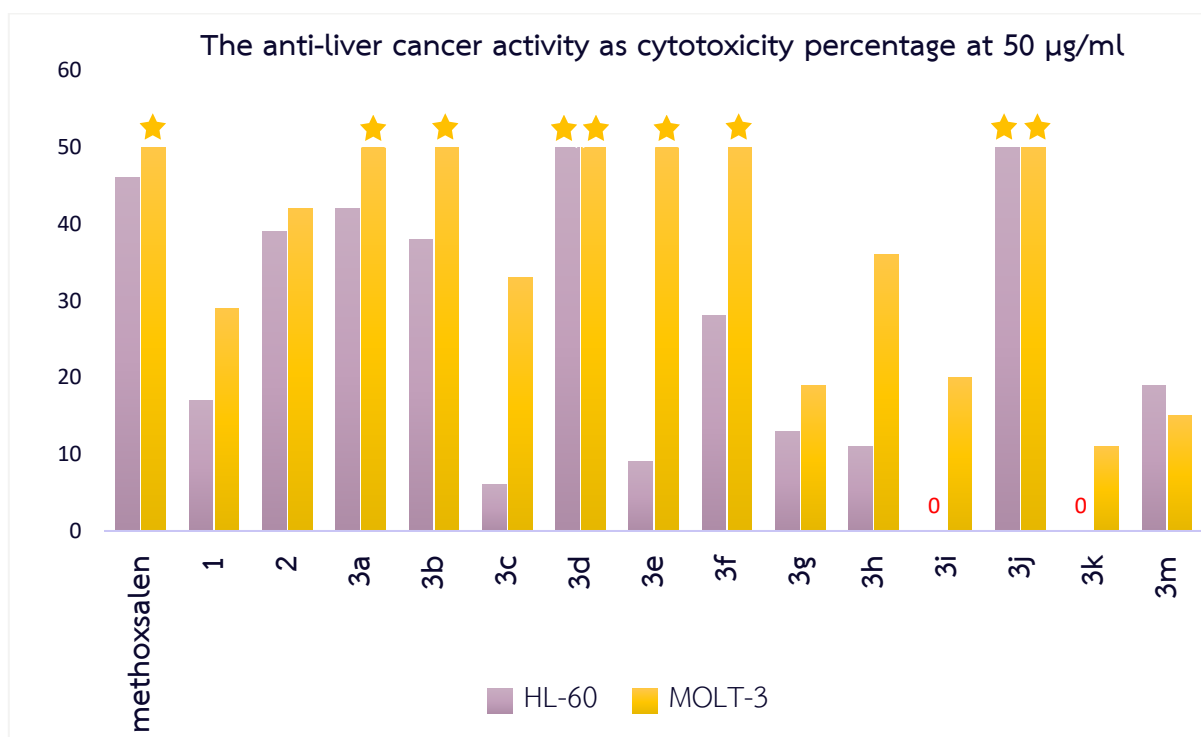


Figure 33 The anti-leukemia cancer activity as cytotoxicity percentage at 50 $\mu\text{g/ml}$
(HL-60 and MOLT-3)

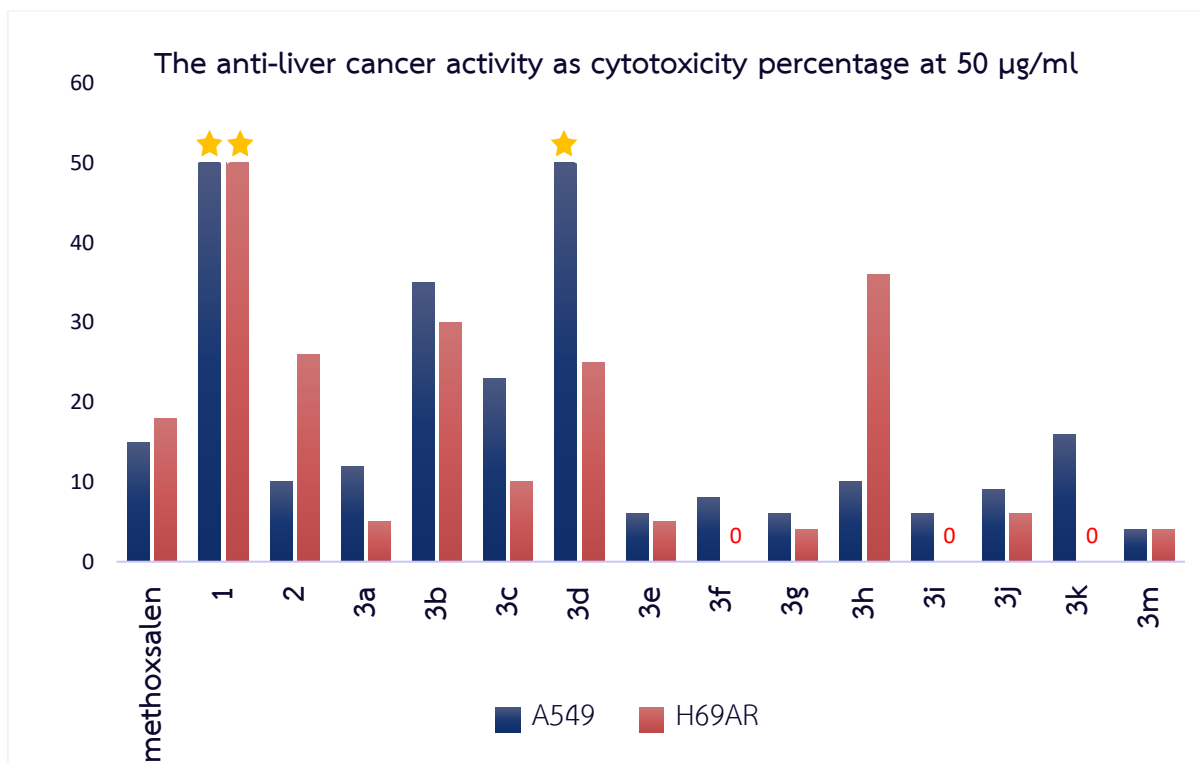


Figure 34 The anti-lung cancer activity as cytotoxicity percentage at 50 $\mu\text{g/ml}$
(A549 and H69AR)

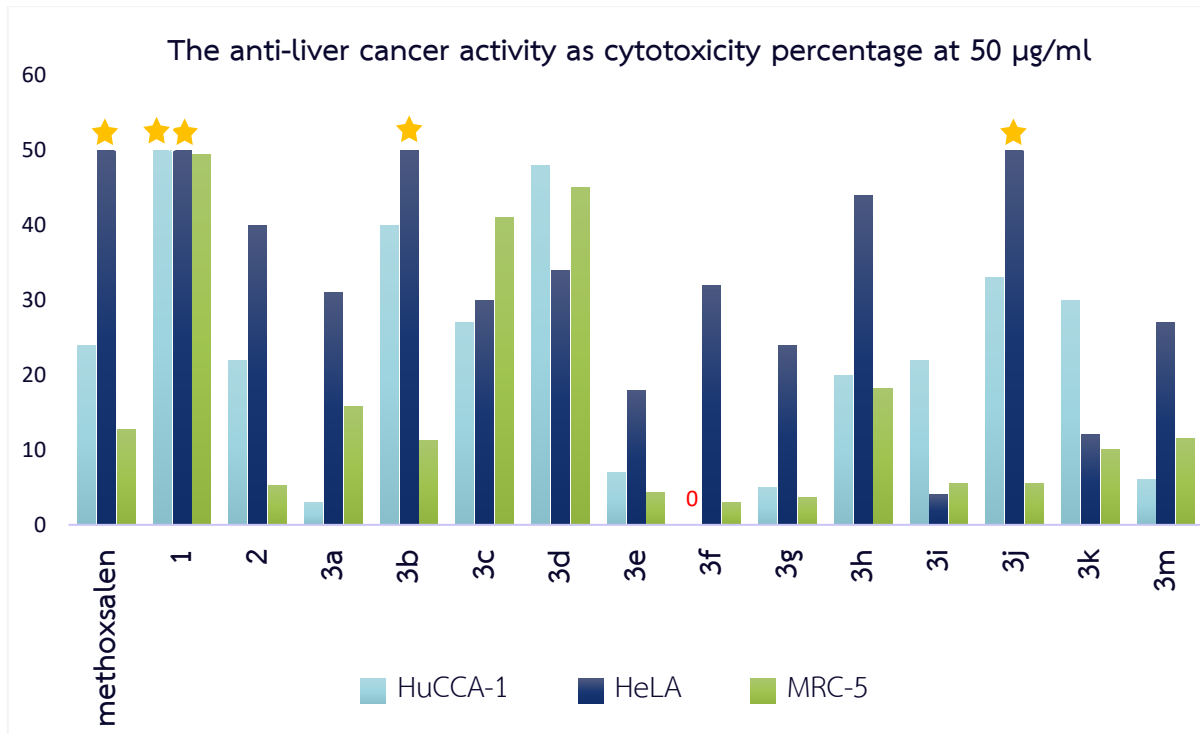


Figure 35 The anticancer activity and toxicity as cytotoxicity percentage at 50 $\mu\text{g/ml}$
; cholangiocarcinoma (HuCCA-1), HeLa cell and normal embryonic lung cell (MRC-5)

From the results above, it could be concluded that there are four types of substitution at C-5 position of methoxsalen that affect to the anticancer activity.

3.3.1. Effect of substituent group at C-5 position

Compound **1** bearing nitro substituent, showed the improvement in anticancer activity compared to methoxsalen and compound **2**. For breast cancer (MDA-MB-231), liver cancer (HepG2 and S102), lung cancer (A549), cholangiocarcinoma (HuCCA-1) and HeLa cell could be concluded that the ability of anticancer activity of nitro substituent (**1**) is the best, followed by methoxsalen, then the electron-donating group substituent (**2**). The results from MTT assay revealed that the substitution of nitro group (**1**) containing the electron-withdrawing group had the better activity compared to **2**, which contains the electron-donating group and the non-substitution methoxsalen. In breast cancer type T47-D, the amine substituent (**2**) had a better activity than methoxsalen. However, methoxsalen showed the best anticancer activity followed by compound **2**, next the electron-withdrawing group substituent (**1**) in leukemia cells (HL-60 and MOLT-3). The results also found that the non-substitution methoxsalen, compound **2** were quite ineffective against cancer cells; MDA-MB-231, T47-D, HepG2, S102 and A549 cell.

3.3.2. Effect of phenyl substituent and type of substituent group on aromatic ring

According to **Table 7** and **Figure 30-35**, the phenyl substituent **3a-3d** and **3j** had a better tend of activity than methoxsalen, compounds **1** and **2**. Mostly, the phenyl substituent containing the electron-withdrawing group (**3b**, **3c** and **3d**) were found to show a greater activity than phenyl substituent and phenyl substituent containing the electron-donating group like **3j** in breast cancer (MDA-MB-231 and T47-D), liver cancer (HepG2), lung cancer (A549 and H69AR) and cholangiocarcinoma (HuCCA-1). It could be concluded that the ability of anticancer activity of bromo substituent on benzene ring (**3d**) is the best, followed by other electron-withdrawing group substituents (**3b** and **3c**), then the electron-donating group substituent (**3j**). On the other hand, phenyl substituent containing the electron-donating group like **3j** showed the best anticancer activity followed by **3b** and **3d** that containing the electron-withdrawing groups in HeLa cells. Compound **3d** with the bromo substituent on benzene ring

showed the most potent activity against breast cancer (T47-D cell line) with IC_{50} value of $10.14 \pm 0.53 \mu\text{M}$ compared to other compounds in this work.

3.3.3. Effect of furan and thiophene substituent

Referring to the bioactivity, compound **3e** had no anticancer activity against liver cancer type S102 cell. Besides, compound **3f** had no anticancer activity against lung cancer (H69AR cell) and cholangiocarcinoma (HuCCA-1), due to compound **3e** and **3f** bearing 0% cytotoxicity at $50 \mu\text{M/mL}$. Compounds **3e** and **3f** were quite ineffective in most cancer cells, probably due to both furan and thiophene substituent are electron-donating groups. Nevertheless, compounds **3e** and **3f** were quite effective in leukemia cell type MOLT-3 with IC_{50} value of 127.50 ± 7.80 and $77.87 \pm 17.69 \mu\text{M}$, respectively.

3.3.4. Effect of alkyl substituent

Effect of alkyl substituent on amide compounds (**3g-3i**, **3k** and **3m**) are similar to the effect of furan and thiophene substituent, the anticancer activities were quite ineffective in all of cancer cells. Compounds **3i** and **3k** had cytotoxicity percentage at $50 \mu\text{M/mL}$ of 0% in leukemia cell type HL-60 and lung cancer type H69AR cell. Moreover, **3i** also had no anticancer activity against liver cancer type S102 cell. On a final note, all of the alkyl substituents (**3g-3i**, **3k** and **3m**) showed quite poor potent anticancer activity, maybe because they are all electron-donating groups.

In consonance with the effects of substituent, the compounds containing electron-withdrawing groups have better significance in anticancer activity for breast cancer type T47-D cell, leukemia type MOLT-3 and lung cancer type A549. Unfortunately, the compounds **3l**, **7a** and **7b** which have the same structure from the literature⁵ and the compounds **4-6** were not evaluated due to the COVID-19 situation. If there had evaluated, we would have had more data to discuss the factors of the structures that cause activity.

Nevertheless, the anticancer activity received in moderate to high of IC_{50} value and low cytotoxicity percentage, therefore the furocoumarin derivatives required the further synthesis to improve the activity.

CHAPTER IV

CONCLUSION

In conclusion, twenty-two novel of furocoumarin derivatives were successfully synthesized over three steps with yields ranging from 15% to 98%. All final products were characterized by proton, carbon-13 and fluorine-19 nuclear magnetic resonance spectroscopy (^1H , ^{13}C and ^{19}F NMR), high-resolution mass spectrometry (HRMS), and fourier-transform infrared spectroscopy (FTIR). The synthesized novel products (**1**, **2**, **3a-3k** and **3m**) and methoxsalen were evaluated for anticancer activity; breast cancer (MDA-MB-231 and T47-D), liver cancer (HepG2 and S102), leukemia (HL-60 and MOLT-3), lung cancer (A549 and H69AR), cholangiocarcinoma (HuCCA-1), HeLa cell and normal embryonic lung cell (MRC-5) from Chulabhorn Research Institute. According to the results, phenyl substituent containing bromine atom on benzene ring compound **3d** has significantly greater anticancer activity against, following by another synthesized compounds. With the structure-activity relationship (SAR), the compounds containing electron-withdrawing groups have better activity especially on the phenyl substituent as **3d**. The furan, thiophene and alkyl substituent at secondary amide were not quite effective as the anticancer activity in most cancer cells. Unfortunately, some of the compounds (**3l**, **4-6**, **7a** and **7b**) were not evaluated the anticancer activity and synthesis of tetracyclic-furocoumarins to reduce the side effects were unsuccessfully, even though several conditions were varied. Therefore, the furocoumarin derivatives require the further synthesis to improve the activity.

REFERENCES

1. Siegel, R.L.; Miller, K.D.; Jemal, A. Cancer Statistics, 2019. *CA A Cancer J Clin.* **2019**, *69*, 7–34.
2. Gupta S.P. Quantitative Structure-Activity Relationship Studies on Anticancer Drugs. *Chem. Rev.* **1994**, *94* (6), 1507–1551.
3. Stratton, M.R.; Campbell, P.J.; Futreal, P.A. The Cancer Genome. *Nature* **2009**, *458*, 719–724.
4. Prasad, K.N.; Xie, H.; Hao, J.; Yang, B.; Qiu, S.; Wei, X.; Chen, F.; Jiang, Y. Antioxidant and Anticancer Activities of 8-Hydroxypsoralen Isolated from Wampee [*Clausena lansium* (Lour.) Skeels] Peel. *Food Chem.* **2010**, *118*, 62–66.
5. Chauthe, S.K.; Mahajan, S.; Rachamalla, M.; Tikoo, K.; Singh, I.P. Synthesis and Evaluation of Linear Furanocoumarins as Potential Anti-breast and Anti-prostate Cancer Agents. *Med. Chem. Res.* **2015**, *24*, 2476–2484.
6. Guillon, C.D.; Jan, Y.-H.; Foster, N.; Ressler, J.; Heck, D.E.; Laskin, J.D.; Heindel, N.D. Synthetically Modified Methoxsalen for Enhanced Cytotoxicity in Light and Dark Reactions. *Bioorg. Med. Chem. Lett.* **2019**, *29*, 619–622.
7. Via, L.D.; Gia, O.; Magno, S.M.; Santana, L.; Teijeira, M.; Uriarte, E. New Tetracyclic Analogues of Photochemotherapeutic Drugs 5-MOP and 8-MOP: Synthesis, DNA Interaction, and Antiproliferative Activity. *J. Med. Chem.* **1999**, *42*, 4405–4413.
8. Via, L.D.; González-Gómez J.C.; Pérez-Montoto L.G.; Santana, L.; Uriarte, E.; Magno, S.M.; Gia, O. A New Psoralen Derivative with Enlarged Antiproliferative Properties. *Bioorg. Med. Chem. Lett.* **2009**, *19*, 2874–2876.
9. Cleeland, C.S.; Bennett, G.J.; Dantzer, R.; Dougherty, P.M.; Dunn, A.J., Meyers C.A.; Miller, A.H.; Payne, R.; Reuben, J.M.; Wang, X.S.; Lee, B.N. Are the Symptoms of Cancer and Cancer Treatment due to a Shared Biologic Mechanism Cancer. *Cancer News* **2003**, *97*, 2919–2925.
10. Testa, B.; Kier, L. B. The Concept of Molecular Structure in Structure–Activity Relationship Studies and Drug Design. *Med. Res. Rev.* **1991**, *11* (1), 35–48.
11. Fowlks, W. L. The Chemistry of the Psoralens. *J Invest. Dermatol.* **1959**, *1*, 249–254.

12. Marumoto, S.; Miyazawa, M. β -Secretase Inhibitory Effects of Furanocoumarins from the Root of *Angelica dahurica*. *Phytother. Res.* **2010**, *24*, 510–513.
13. Zhang, B.-L.; Fan, C.-Q.; Dong, L.; Wang, F.-D.; Yue, J.-M. Structural Modification of a Specific Antimicrobial Lead Against *Helicobacter pylori* Discovered from Traditional Chinese Medicine and a Structure Activity Relationship Study. *Eur. J. Med. Chem.* **2010**, *45*, 5258–5264.
14. Shen, Q.K.; Liu, C.F.; Zhang, H.J.; Tian, Y.S.; Quan, Z.S. Design and Synthesis of New Triazoles Linked to Xanthotoxin for Potent and Highly Selective Anti-Gastric Cancer Agents. *Bioorg. Med. Chem. Lett.* **2017**, *47*, 4871–4875.
15. Mi, C.; Ma, J.; Wang, K.S.; Zuo, H.X.; Wang, Z.; Li, M.Y.; Piao, L.X.; Xu, G.H.; Li, X.; Quan, Z.S.; Jin, X. Imperatorin Suppresses Proliferation and Angiogenesis of Human Colon Cancer Cell by Targeting HIF-1 α via the mTOR/p70S6K/4E-BP1 and MAPK Pathways. *J. Ethnopharmacol.* **2017**, *203*, 27–3.
16. Hafez, O.M.; Amin, K.M.; Latif, N.A.; Mohamed, T.K.; Ahmed, E.Y.; Maher, T. Synthesis and Antitumor Activity of Some New Xanthotoxin Derivatives. *Eur. J. Med. Chem.* **2009**, *44*, 2967–2974.
17. Kaufman, K.O.; Erb, D.J.; Blok, T.M.; Carlson, R.W.; Knoald, D.J.; Bride, L.M.; Zeitlow, T. Synthetic Aminomethyl Psoralens via Chloromethylation or Benzylic Bromination. *J. Heterocyclic Chem.* **1982**, *19*, 1051–1056.
18. Kociok-Köhn, G.; Molloy, K.C.; Price, G.J.; Smith, D.R.G. The Structures of Uncommon Cationic *N*-alkenyl Purine and Pyrimidine Bases. *J. Heterocyclic Chem.* **2016**, *53*, 64–68.
19. Katritzky, A.R.; Taylor, R. Chapter 3 Nitration. *Adv. Heterocycl. Chem.* **1990**, *47*, 39–58.
20. Horwitz, N.E.; Phelan, B.T. Nelson, J.N.; Krzyaniak, M.D.; Wasielewski, M.R.; *J. Phys. Chem. A* **2016**, *120*, 2841–2853.
21. Panini, P.; Chopra, D. Quantitative Insights into Energy Contributions of Intermolecular Interactions in Fluorine and Trifluoromethyl Substituted Isomeric *N*-phenylacetamides and *N*-methylbenzamides. *CrystEngComm* **2013**, *15*, 3711–3733.
22. Alawode, O.E.; Robinson, C.; Rayat, S. Clean Photodecomposition of 1-Methyl-4-phenyl-1H-tetrazole-5(4H)-thiones to Carbodiimides Proceeds via a Biradical. *J. Org. Chem.* **2011**, *76*, 216–222.

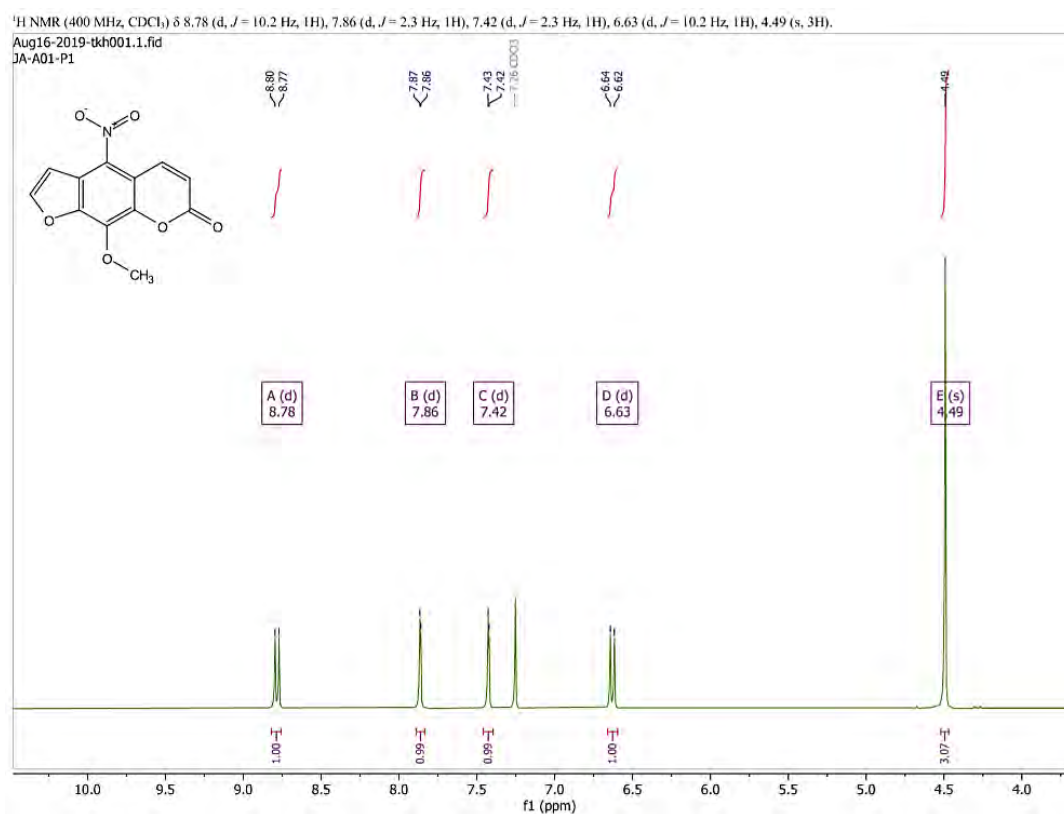
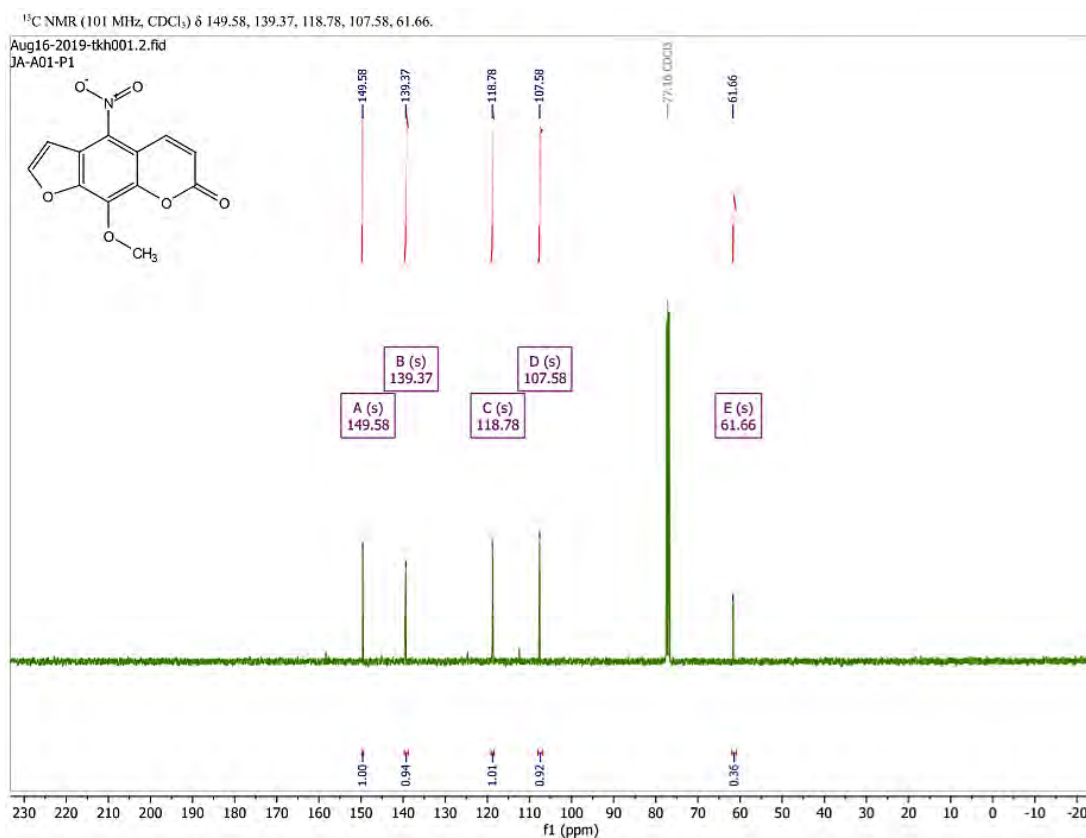
23. Murase, H.; Senda, K.; Senoo, M.; Hata, T.; Urabe, H. Rhodium-Catalyzed Intramolecular Hydroarylation of 1-Halo-1-alkynes: Regioselective Synthesis of Semihydrogenated Aromatic Heterocycles *Eur. J. Med. Chem.* **2014**, *20*, 317–322.
24. Harmata, M.; Zheng, P.; Huang, C.; Gomes, M.G.; Ying, W.; Ranyanil, K.O.; Balan, G.; Calkins, N.L. Expedient Synthesis of Sulfinamides from Sulfonyl Chlorides. *J. Org. Chem.* **2007**, *72*, 683–685.
25. Laali, K.K.; Volkar J.G. Electrophilic Nitration of Aromatics in Ionic Liquid Solvents. *J. Org. Chem.* **2000**, *66*, 35–40.
26. Wu, Z.; Zhai, Y.; Zhao, W.; Wei, Z.; Yu, H.; Han, S.; Wei, Y. An Efficient Way for The N-Formylation of Amines by Inorganic-Ligand Supported Iron Catalysis. *Green Chem.* **2020**, *22*, 737–741.
27. Neises, B.; Steglich, W. Simple Method for the Esterification of Carboxylic Acids. *Angew. Chem. Int. Ed.* **1978**, *17*, 522–524.
28. Kharasch, M.S.; Kritchevsky, J.; Mayo, F.R. The Addition of Hydrogen Chloride to Butadiene. *J. Org. Chem.* **1937**, *2*, 489–496.
29. Ewen, J.A.; Elder, M.J.; Jones, R.L.; Rheingold, A.L.; Liable-Sands, L.M.; Sommer, R.D. Chiral Ansa Metallocenes with Cp Ring-Fused to Thiophenes and Pyrroles: Syntheses, Crystal Structures, and Isotactic Polypropylene Catalyst *J. Am. Chem. Soc.* **2001**, *123*, 4763–4773.
30. Grant, H.G. A simple synthesis of (\pm)-1-Methyl benzofurocyclopentan-3-one. *J. Heterocyclic Chem.* **1978**, *15*, 1235–1236.
31. Young, J.A. Chemical Laboratory Information Profile. *J. Chem. Educ.* **2004**, *81*, 1415.
32. Ren, R.X.; Zueva, L.D.; Ou, W. Formation of ϵ -caprolactam via Catalytic Beckmann Rearrangement Using P₂O₅ in Ionic Liquids. *Tetrahedron Lett.* **2001**, *42*, 8441–8443.
33. Jones, R.; Elder, M. Preparation of Heterocyclic Ketones Germany Patent WO 2004056796 July 8, 2004.
34. Jones, R.; Elder, M. Procedure for the Production of Heterocyclic Ketones Especially Cyclopenta[b]thiophen-6-ones Germany Patent DE 10260095 July 1, 2004.
35. Rafiq, S.M.; Sivasakthikumar, R.; Mohanakrishnan, A.K. Lewis Acid/Brønsted Acid Mediated Benz-Annulation of Thiophenes and Electron-Rich Arenes. *Org. Lett.* **2014**, *16*, 2720–2723.

APPENDICES

APPENDIX A

NMR and HRMS spectra of 1-2 and 3a-3m

9-methoxy-4-nitro-7H-furo[3,2-g]chromen-7-one (1)

Figure 36 ¹H NMR spectrum of 1Figure 37 ¹³C NMR spectrum of 1

Generic Display Report

Analysis Info

Analysis Name D:\Data\Data Service\200318\A01_RB3_01_3870.d
Method nv_pos_0min_profile_wguardcol_50-1500_191021.m
Sample Name A01
Comment

Acquisition Date 3/16/2020 4:48:01 PM

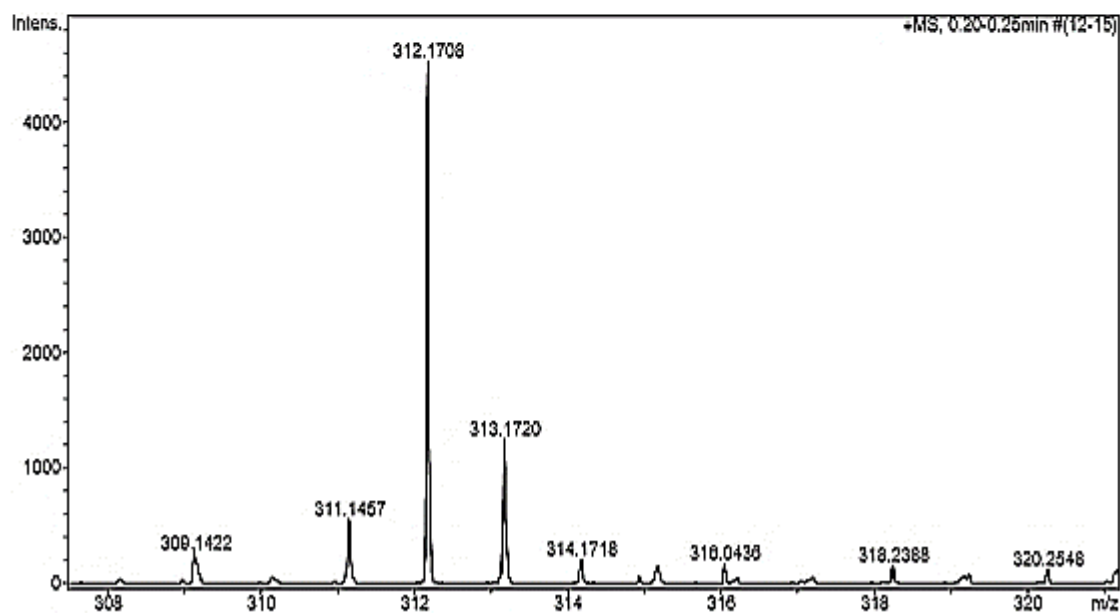
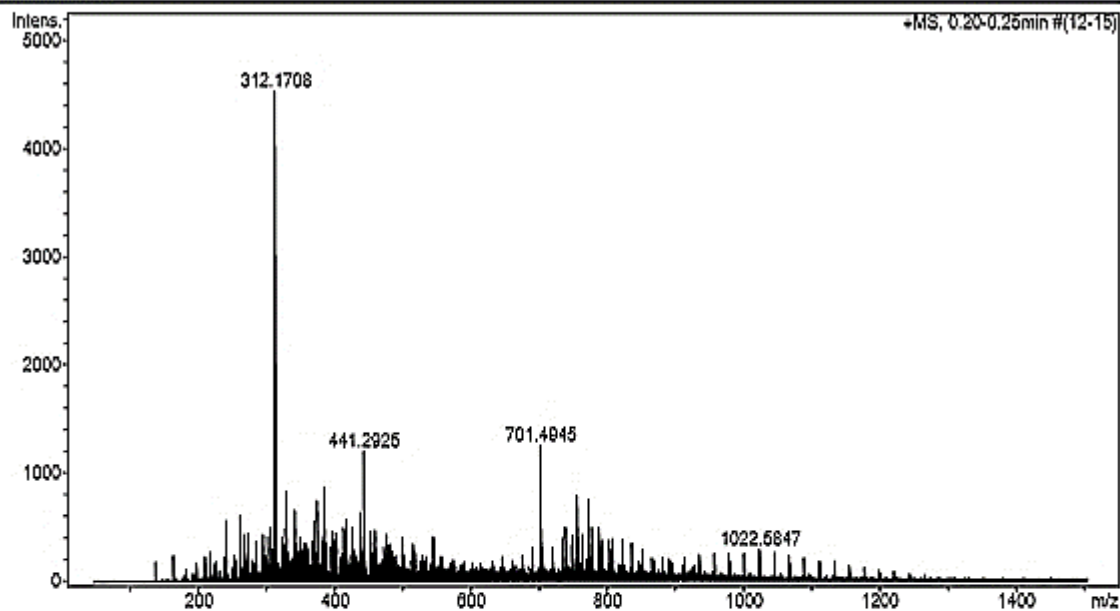
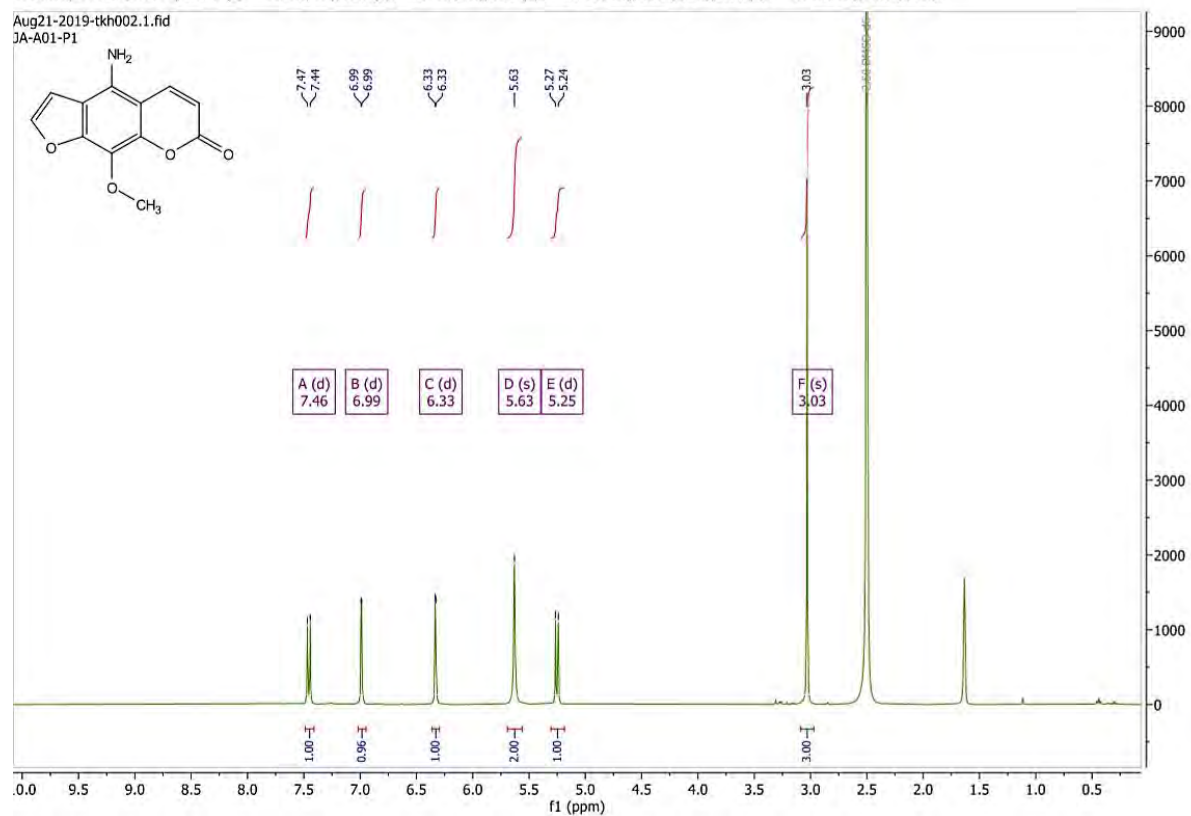
Operator CU.
Instrument microTOF-Q II

Figure 38 HRMS spectrum of 1

4-amino-9-methoxy-7H-furo[3,2-g]chromen-7-one (2)

¹H NMR (400 MHz, DMSO) δ 7.46 (d, $J = 9.8$ Hz, 1H), 6.99 (d, $J = 2.2$ Hz, 1H), 6.33 (d, $J = 2.3$ Hz, 1H), 5.63 (s, 2H), 5.25 (d, $J = 9.8$ Hz, 1H), 3.03 (s, 3H).

Figure 39 ¹H NMR spectrum of 2

Generic Display Report

Analysis Info

Analysis Name D:\Data\Data Service\200316\A02_RB4_01_3864.d
Method nv_pos_6min_profile_wguardcol_50-1500_191021.m
Sample Name A02
Comment

Acquisition Date 3/16/2020 4:08:45 PM

Operator CU.
Instrument micrOTOF-Q II

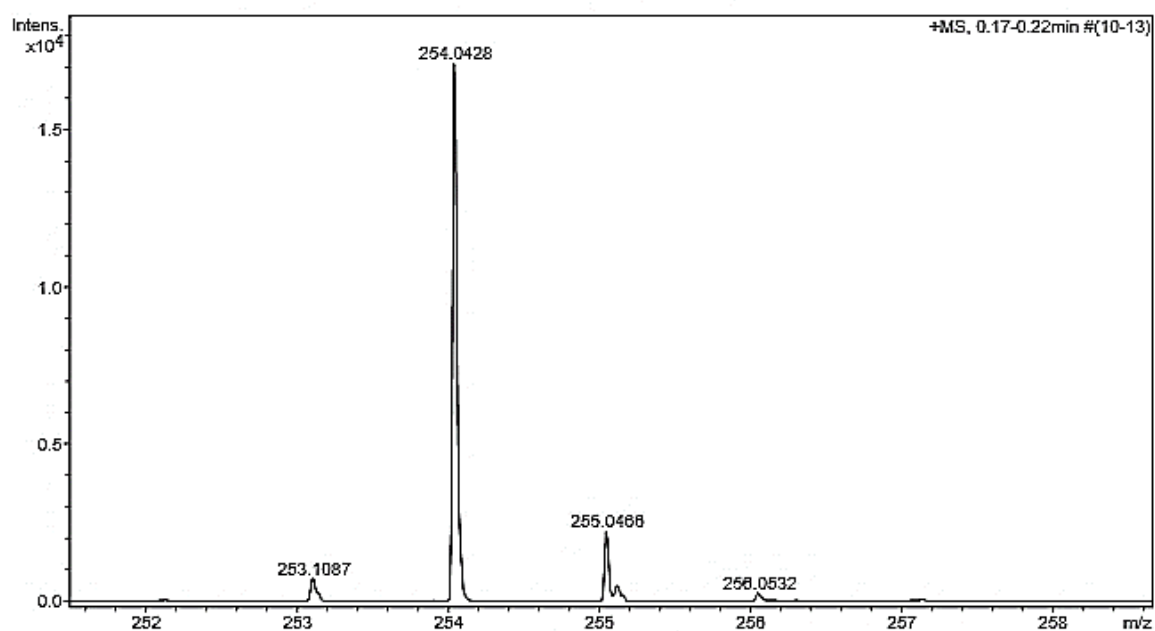
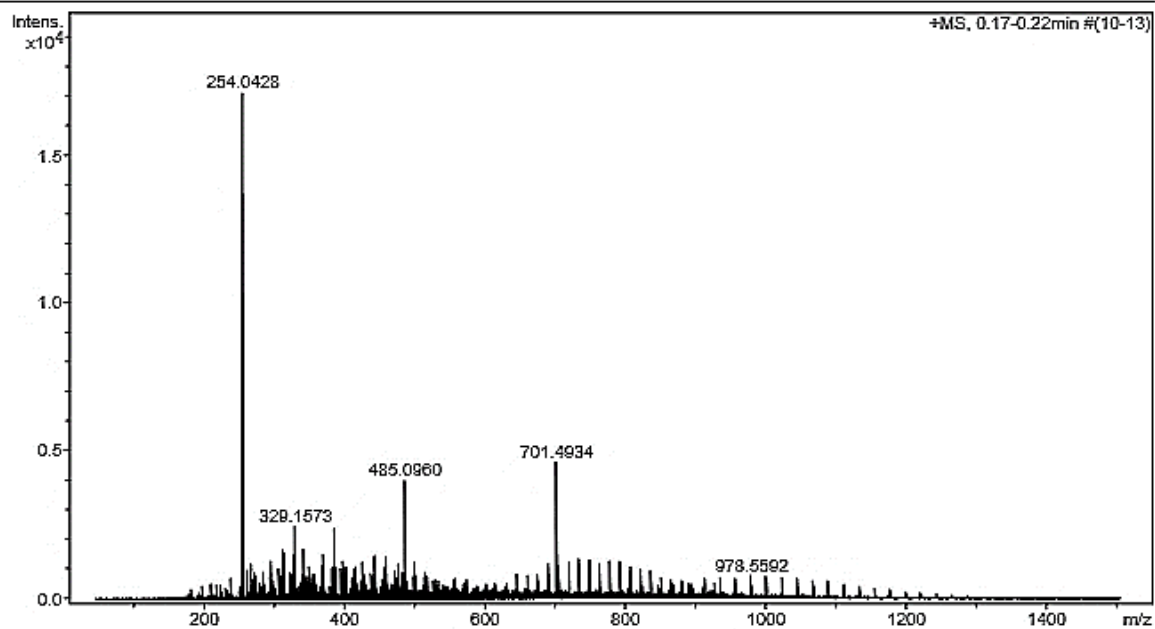
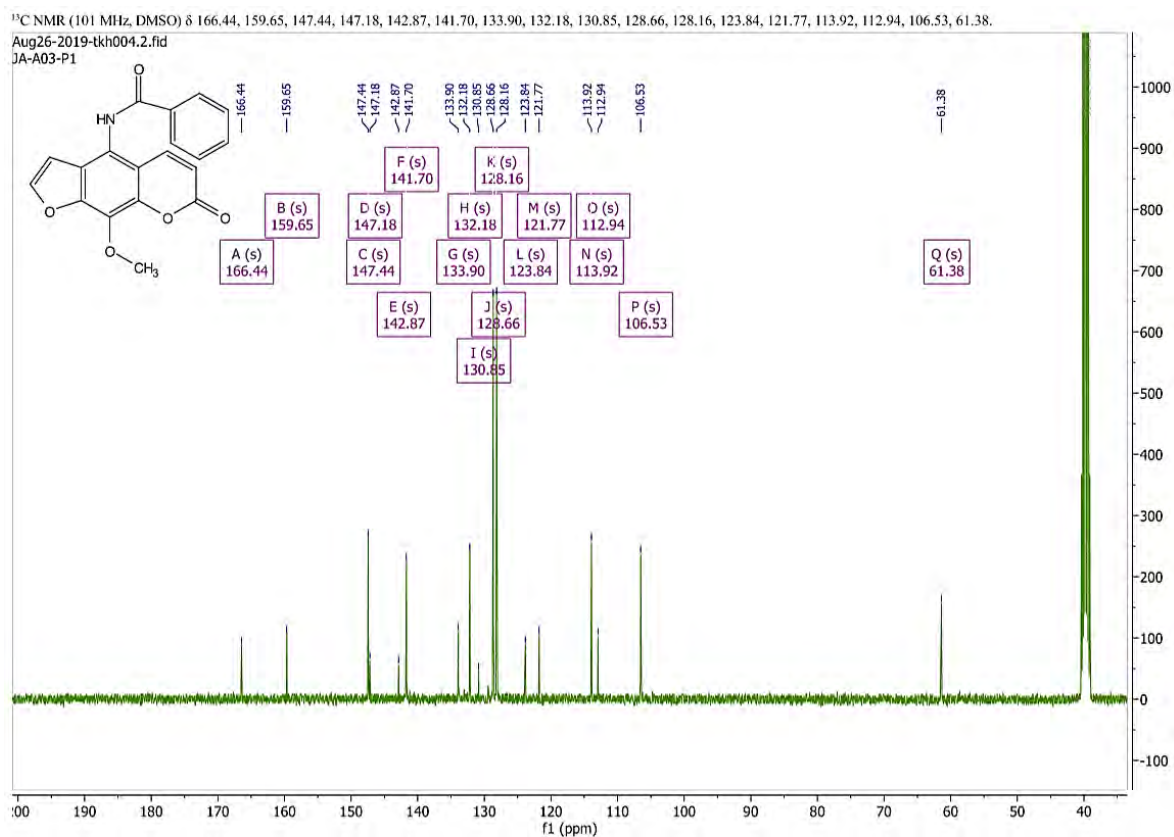
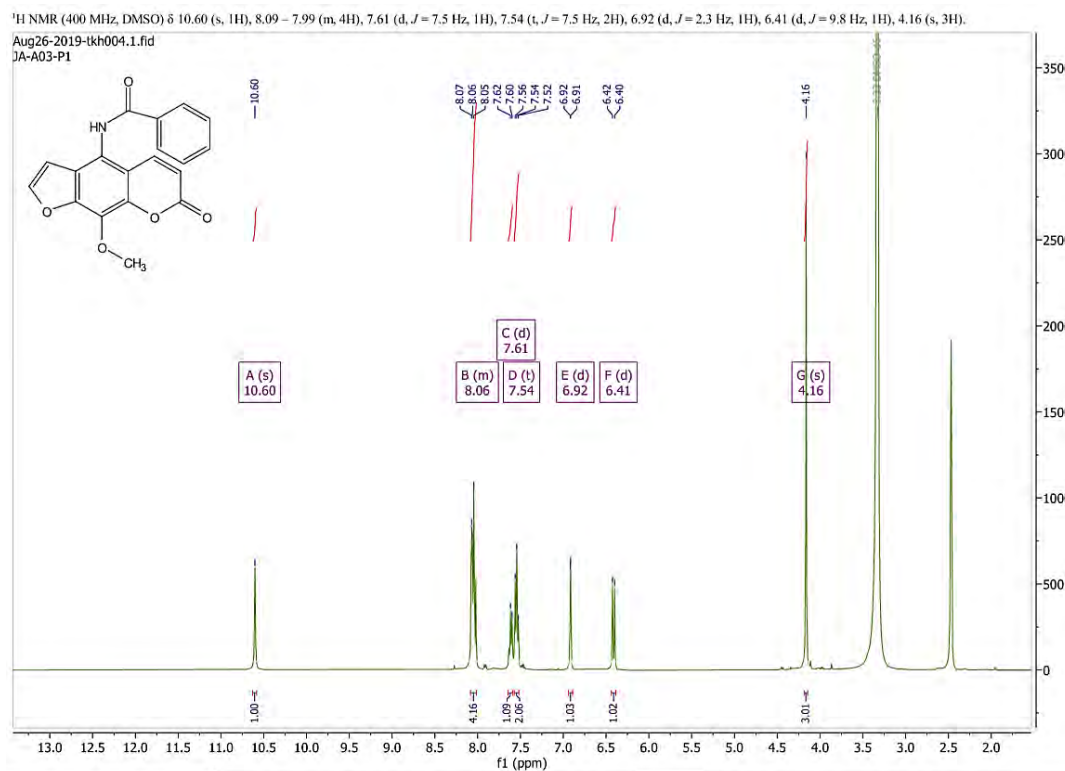


Figure 40 HRMS spectrum of 2

N-(9-methoxy-7-oxo-7*H*-furo[3,2-*g*]chromen-4-yl)benzamide (3a)



Generic Display Report

Analysis Info

Analysis Name D:\Data\Data Service\200316\A03_RB5_01_3867.d
Method nv_pos_6min_profile_wguardcol_50-1500_191021.m
Sample Name A03
Comment

Acquisition Date 3/16/2020 4:28:10 PM

Operator CU
Instrument micrOTOF-Q II

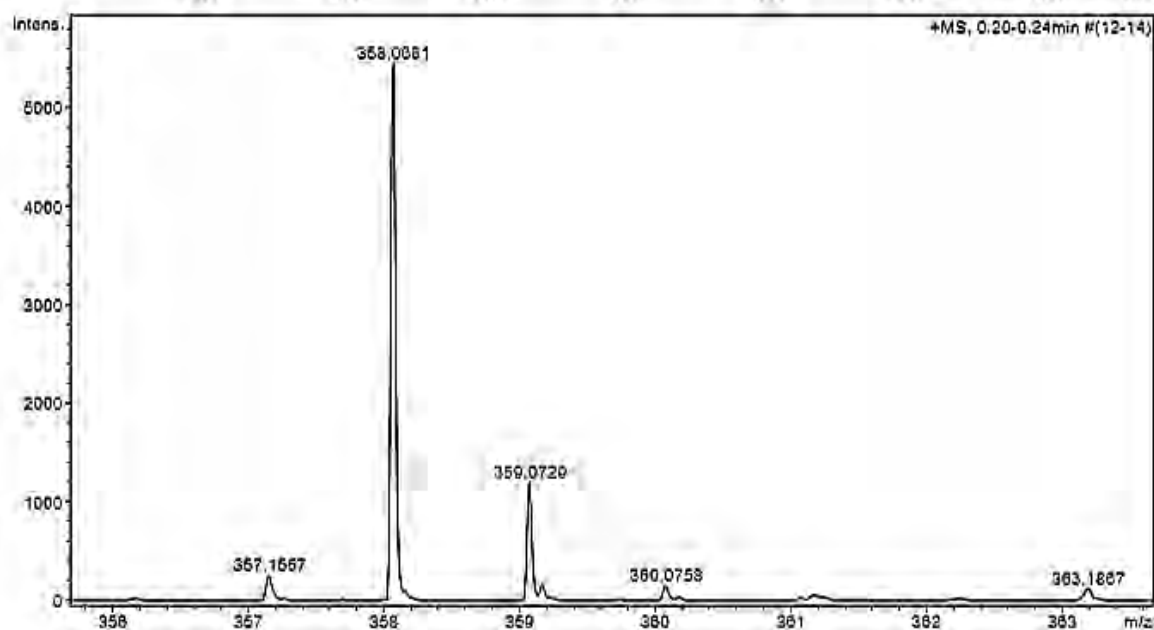
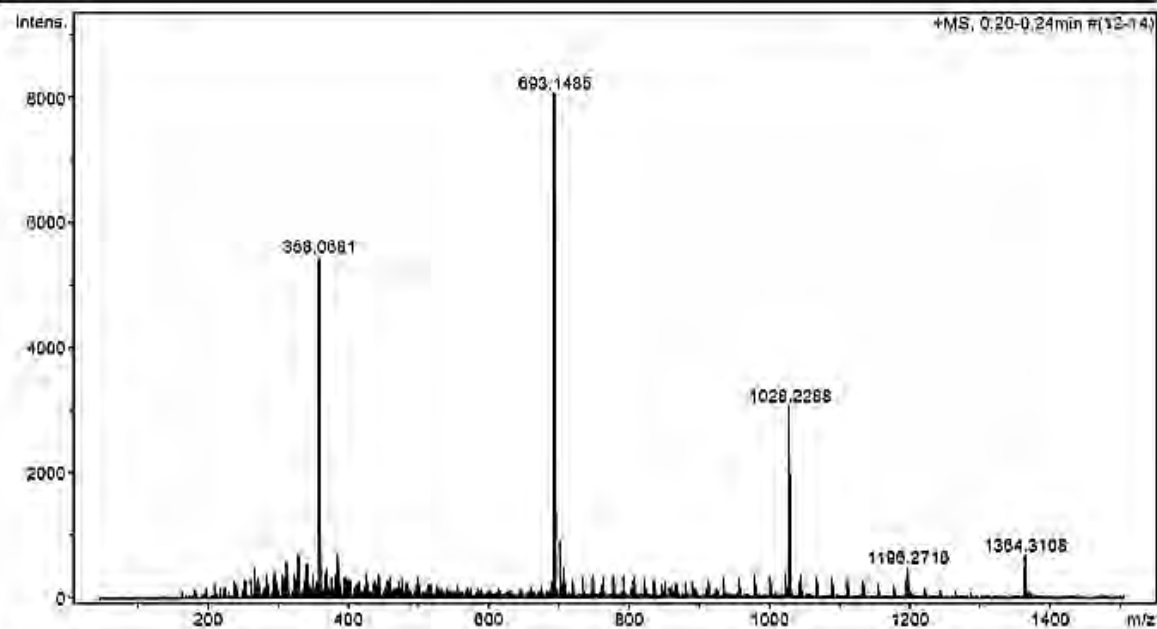
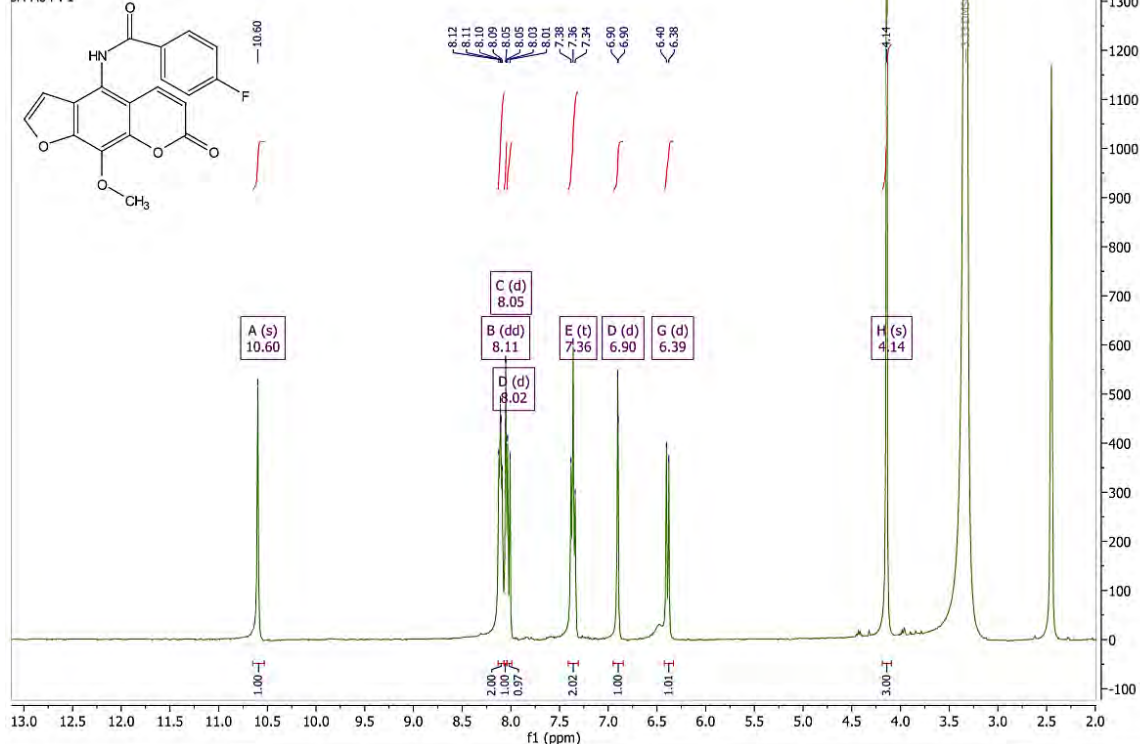


Figure 43 HRMS spectrum of 3a

4-fluoro-*N*-(9-methoxy-7-oxo-7*H*-furo[3,2-*g*]chromen-4-yl)benzamide (3b)

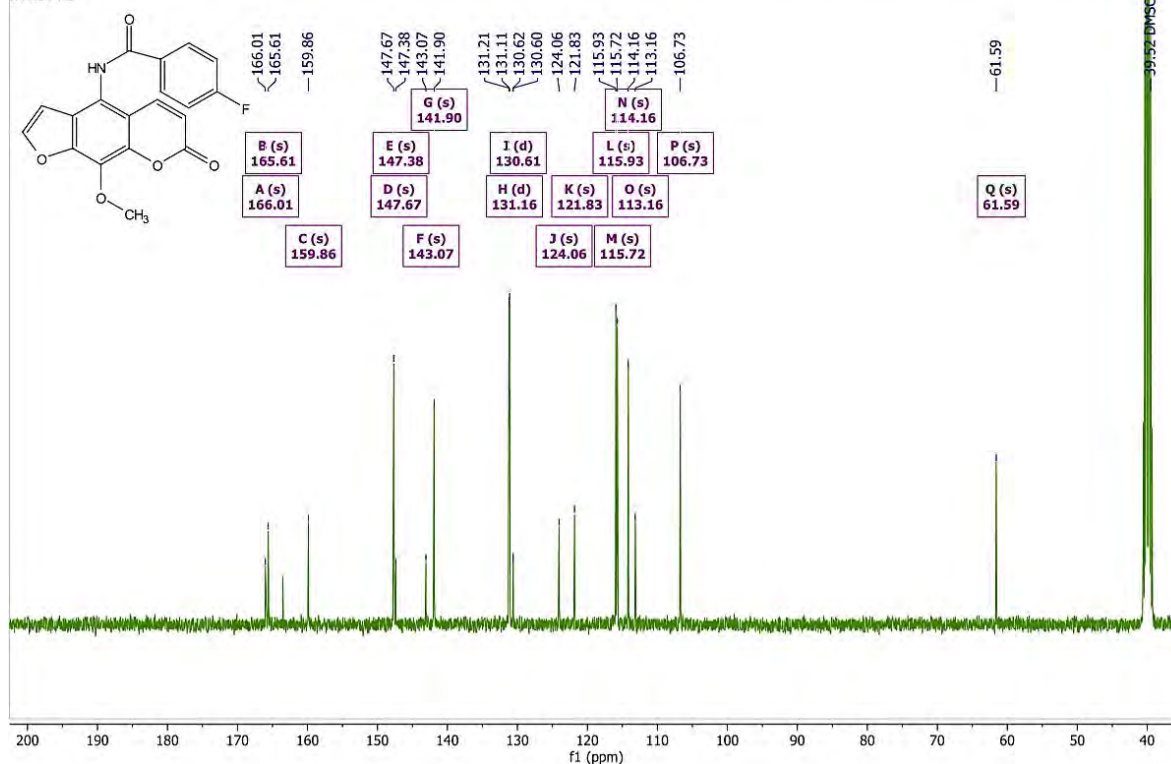
¹H NMR (400 MHz, DMSO) δ 10.60 (s, 1H), 8.11 (dd, *J* = 8.5, 5.4 Hz, 2H), 8.05 (d, *J* = 2.3 Hz, 1H), 8.02 (d, *J* = 9.8 Hz, 1H), 7.36 (t, *J* = 8.6 Hz, 2H), 6.90 (d, *J* = 2.3 Hz, 1H), 6.39 (d, *J* = 9.7 Hz, 1H), 4.14 (s, 3H).

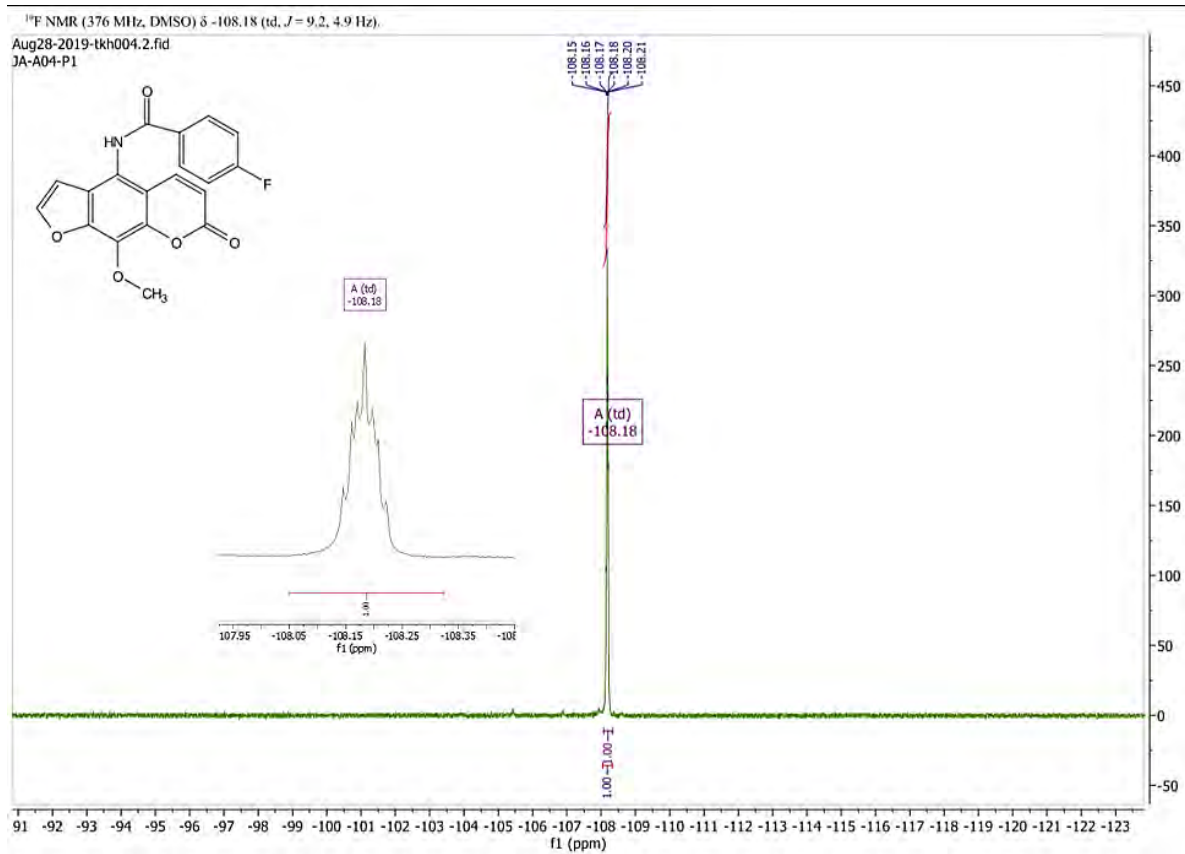
Aug28-2019-tkh004.1.fid
JA-A04-P1

Figure 44 ¹H NMR spectrum of 3b

¹³C NMR (101 MHz, DMSO) δ 166.01, 165.61, 159.86, 147.67, 147.38, 143.07, 141.90, 131.16 (d, *J* = 9.3 Hz), 130.61 (d, *J* = 2.9 Hz), 124.06, 121.83, 115.93, 115.72, 114.16, 113.16, 106.73, 61.59.

Aug28-2019-tkh004.3.fid
JA-A04-P1

Figure 45 ¹³C NMR spectrum of 3b

Figure 46 ¹⁹F NMR spectrum of 3b

Generic Display Report

Analysis Info

Analysis Name D:\Data\Data Service\200316\A04_RB6_01_3868.d
Method nv_pos_6min_profile_wguardcol_50-1500_191021.m
Sample Name A04
Comment

Acquisition Date 3/16/2020 4:34:49 PM

Operator CU
Instrument micrOTOF-Q II

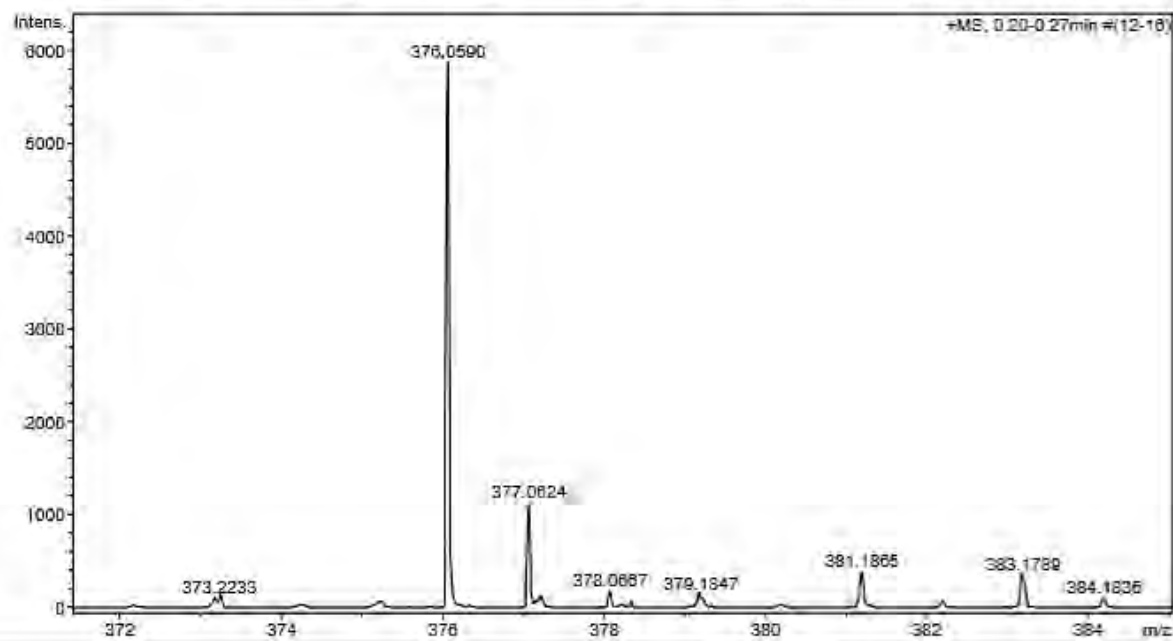
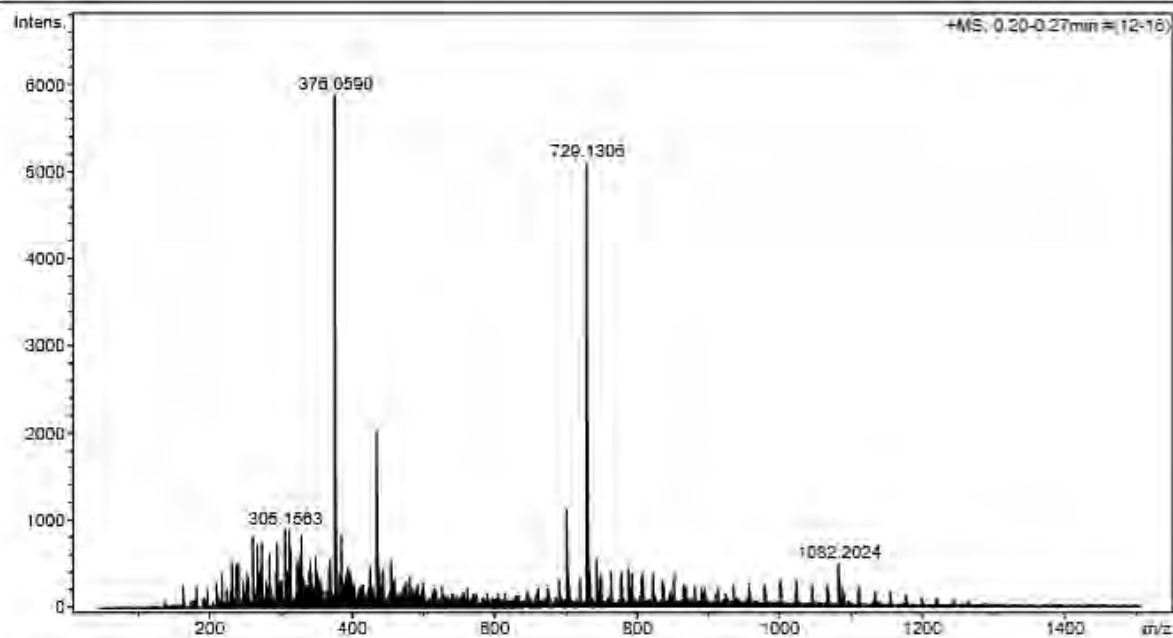
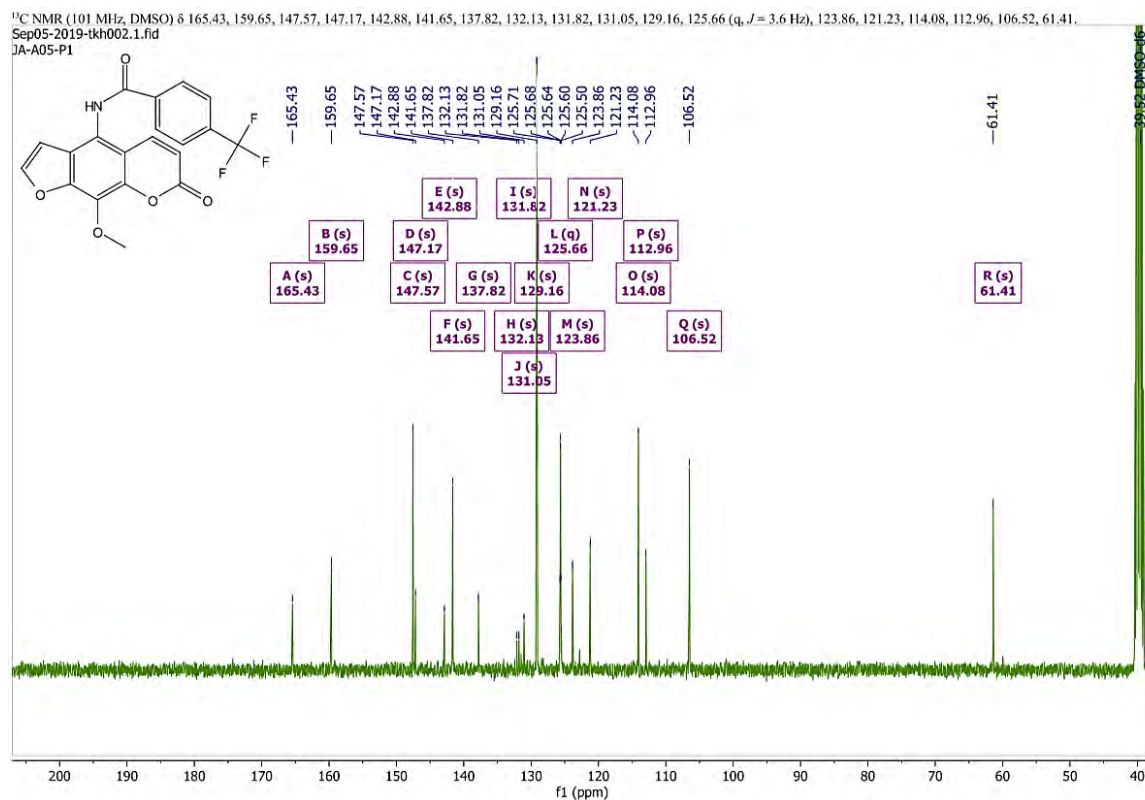
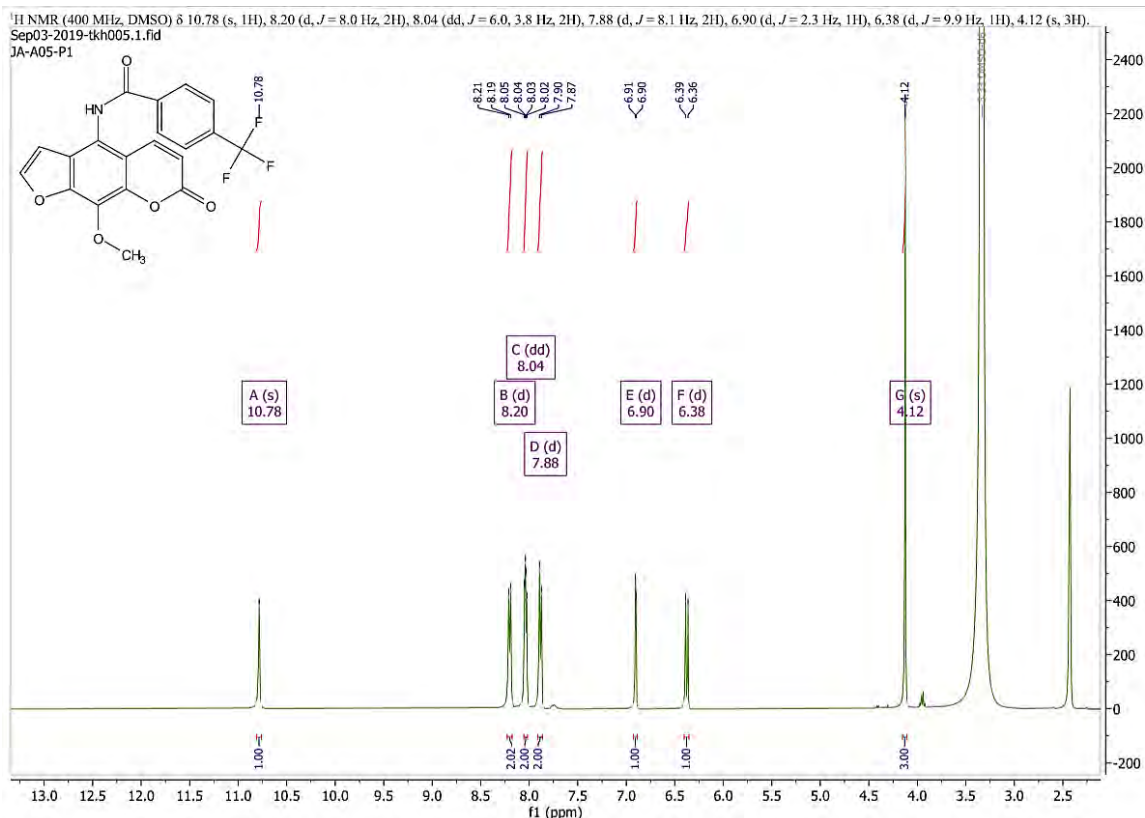
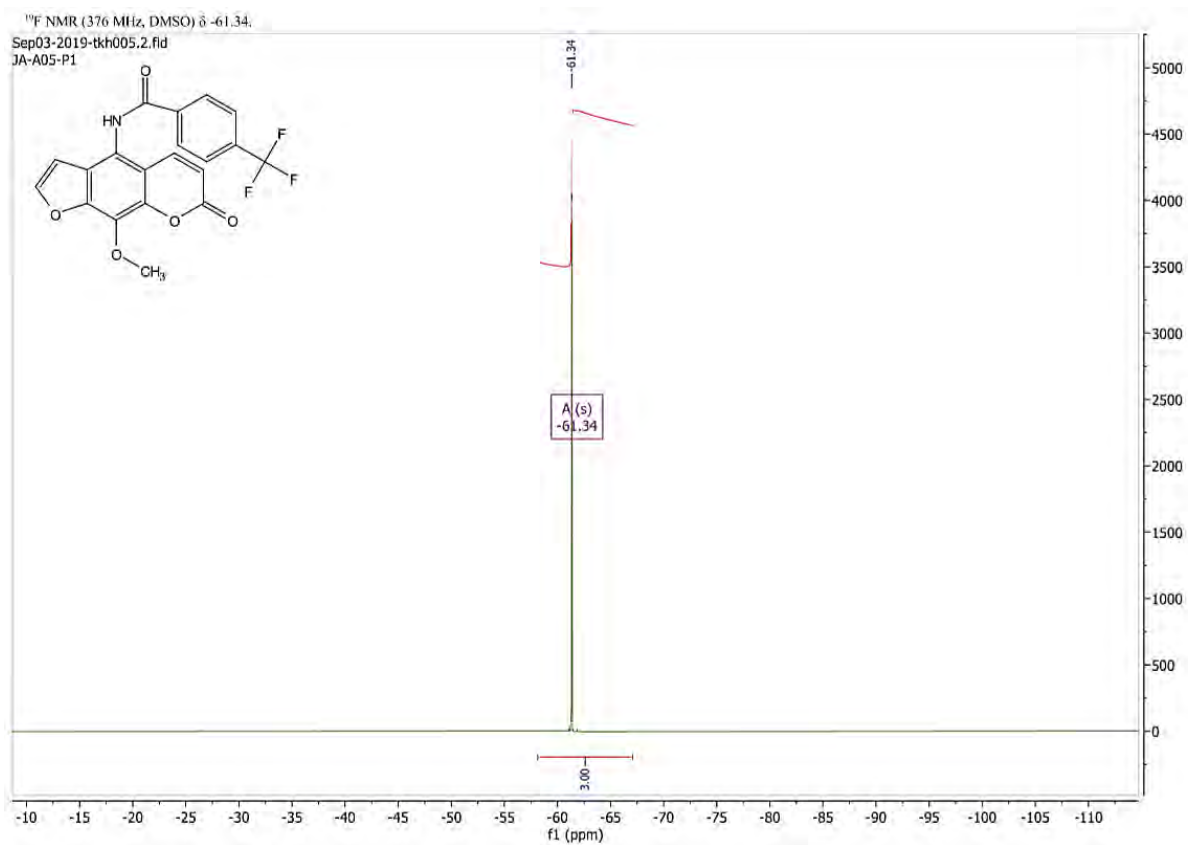


Figure 47 HRMS spectrum of 3b

N-(9-methoxy-7-oxo-7*H*-furo[3,2-*g*]chromen-4-yl)-4-(trifluoromethyl)benzamide (3c)



Figure 50 ¹⁹F NMR spectrum of 3c

Generic Display Report

Analysis Info

Analysis Name D:\Data\Data Service\200316\A05_RB7_01_3869.d
Method nv_pos_6min_profile_wguardcol_50-1500_191021.m
Sample Name A05
Comment

Acquisition Date 3/16/2020 4:41:25 PM
Operator CU
Instrument micrOTOF-Q II

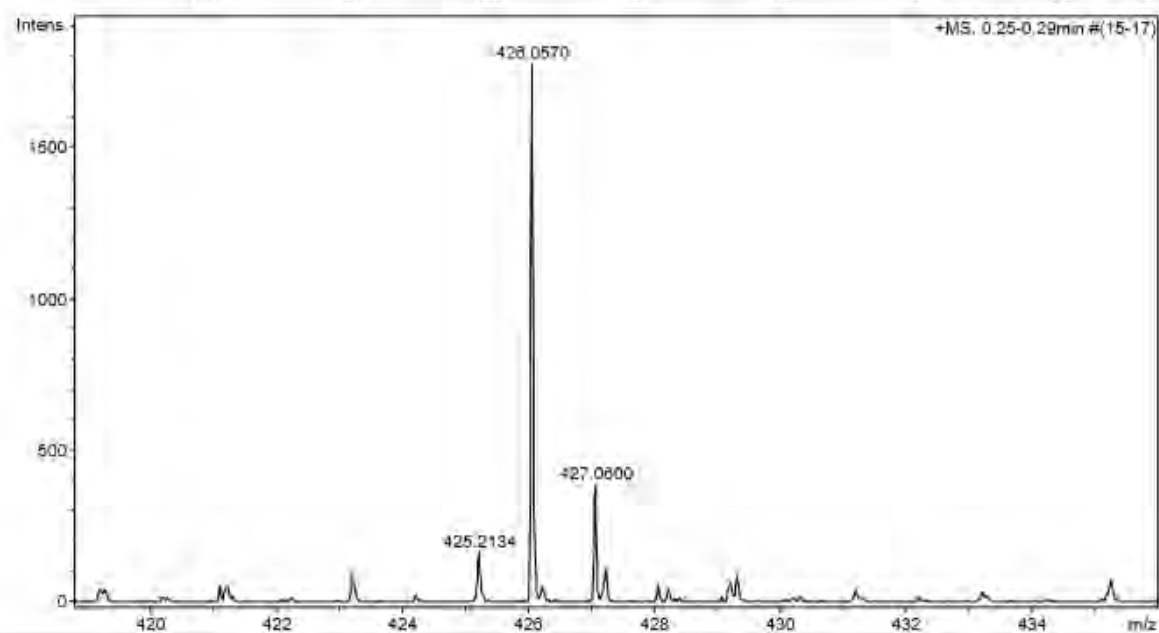
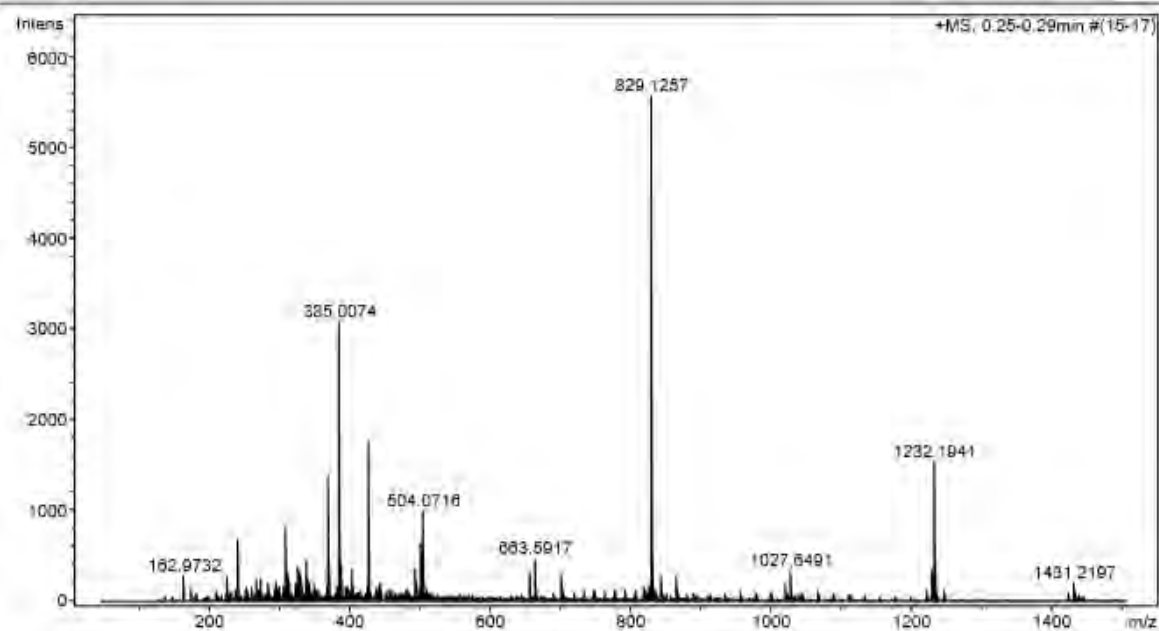
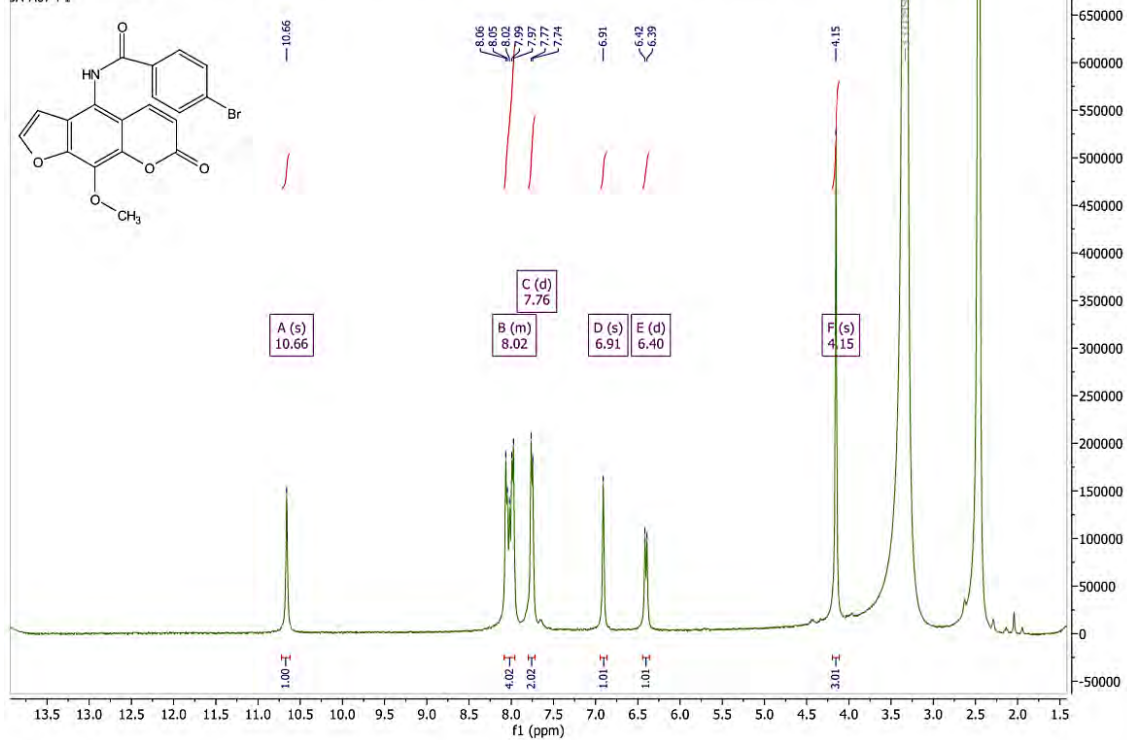


Figure 51 HRMS spectrum of 3c

4-bromo-*N*-(9-methoxy-7-oxo-7*H*-furo[3,2-*g*]chromen-4-yl)benzamide (3d)¹H NMR (400 MHz, DMSO) δ 10.66 (s, 1H), 8.07 – 7.95 (m, 4H), 7.76 (d, $J = 8.1$ Hz, 2H), 6.91 (s, 1H), 6.40 (d, $J = 9.8$ Hz, 1H), 4.15 (s, 3H).Sep20-2019-tkh007.1.1.1r
JA-A07-P1Figure 52 ¹H NMR spectrum of 3d

Generic Display Report

Analysis Info

Analysis Name D:\Data\Data Service\200316\A07_RB8_01_3871.d
Method nv_pos_6min_profile_vguardcol_50-1500_191021.m
Sample Name A07
Comment

Acquisition Date 3/16/2020 4:54:44 PM

Operator CU.
Instrument micrOTOF-Q II

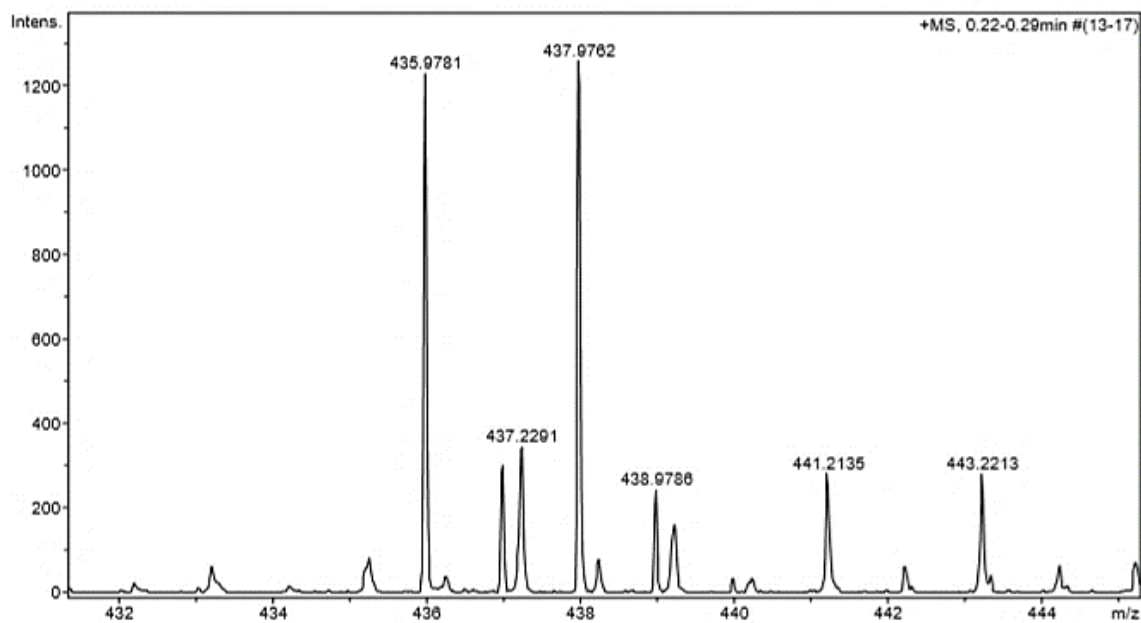
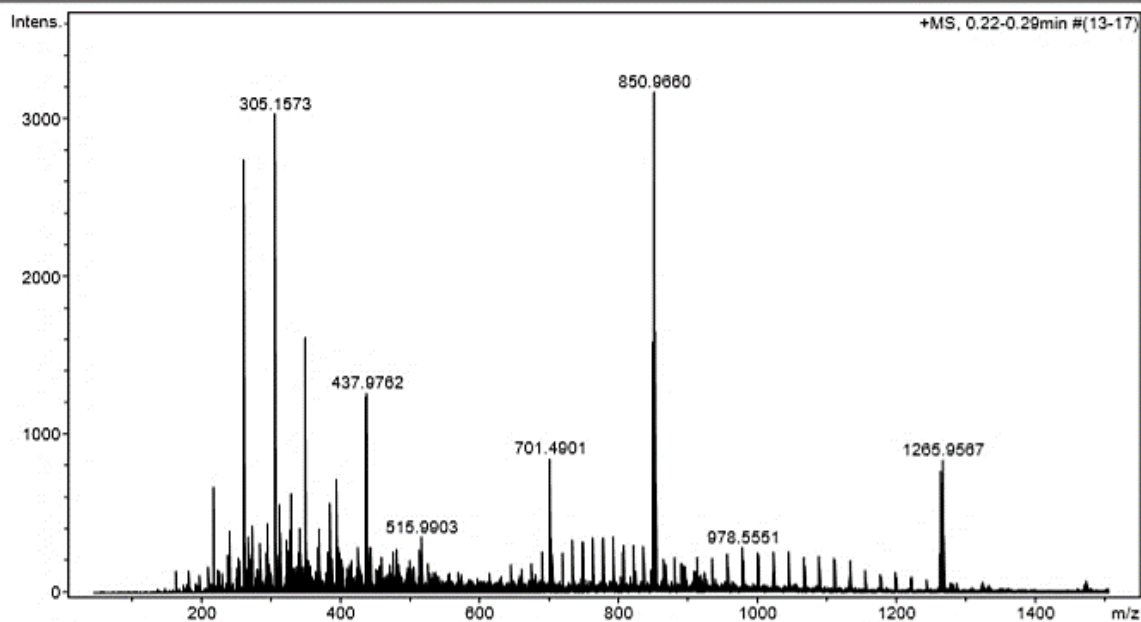


Figure 53 HRMS spectrum of 3d

N-(9-methoxy-7-oxo-7*H*-furo[3,2-*g*]chromen-4-yl)furan-2-carboxamide (3e)

¹H NMR (500 MHz, DMSO-*d*₆) δ 10.52 (s, 1H), 7.97 (d, *J* = 2.3 Hz, 1H), 7.93–7.85 (m, 2H), 7.28 (d, *J* = 3.4 Hz, 1H), 6.79 (d, *J* = 2.3 Hz, 1H), 6.63 (dd, *J* = 3.6, 1.8 Hz, 1H), 6.32 (d, *J* = 9.8 Hz, 1H), 4.06 (s, 1H).

2019-11-25-tkh003-JA-A15-P1

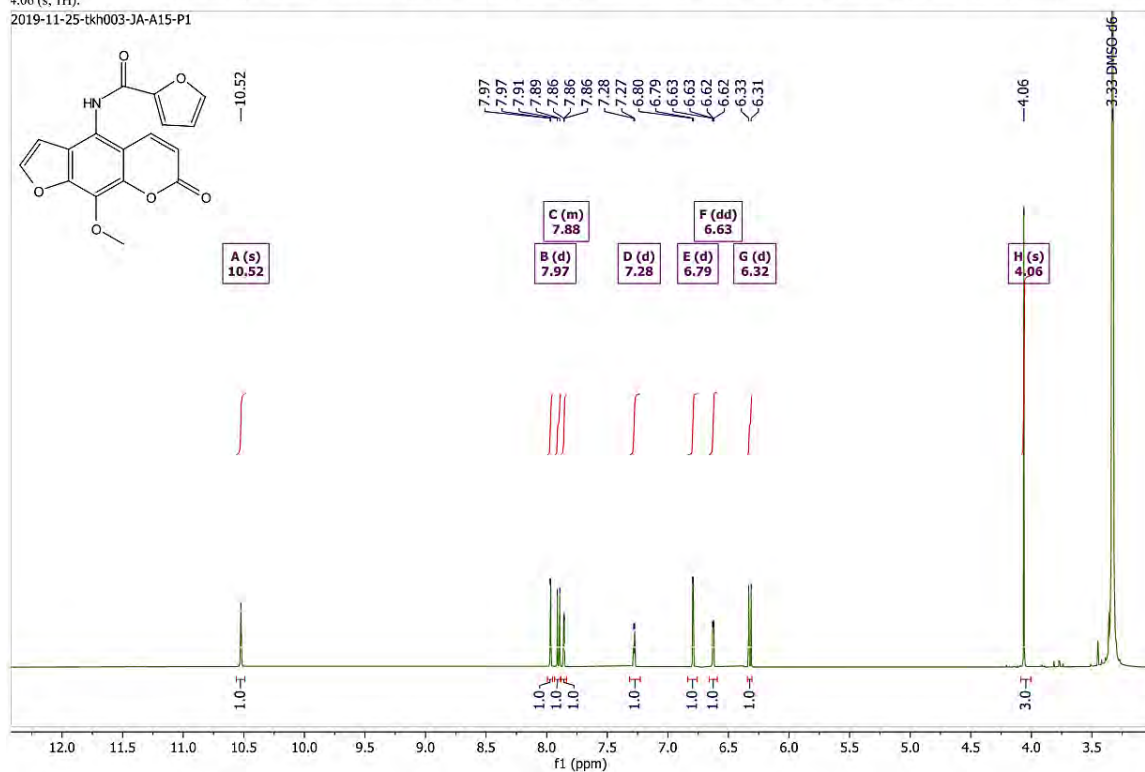


Figure 54 ¹H NMR spectrum of 3e

¹³C NMR (126 MHz, DMSO-*D*₆) δ 159.95, 157.54, 147.79, 147.40, 147.36, 146.49, 143.07, 141.90, 131.19, 124.17, 120.99, 115.86, 114.25, 113.26, 112.73, 106.77, 61.64.

2019-11-25-tkh003-JA-A15-P1

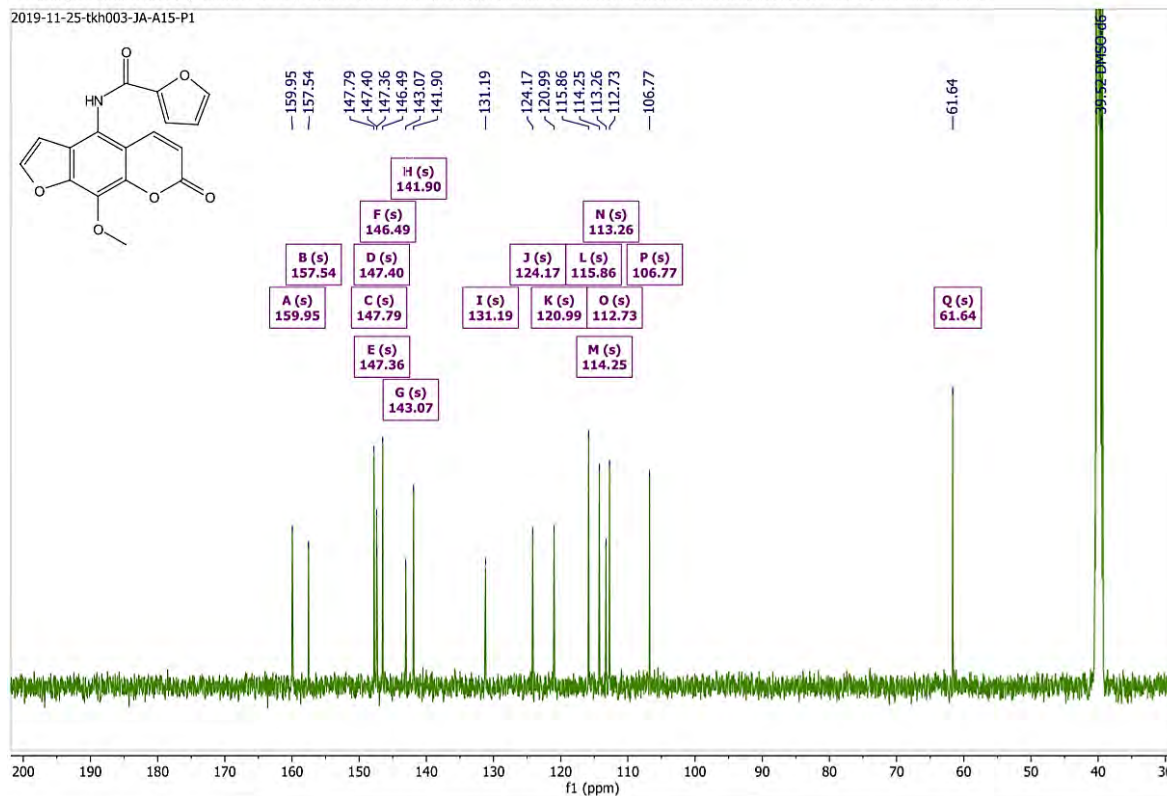


Figure 55 ¹³C NMR spectrum of 3e

Generic Display Report

Analysis Info

Analysis Name D:\Data\Data Service\200316\A15_RC2_01_3873.d
Method nv_pos_6min_profile_wguardcol_50-1500_191021.m
Sample Name A15
Comment

Acquisition Date 3/16/2020 5:08:17 PM

Operator CU
Instrument micrOTOF-Q II

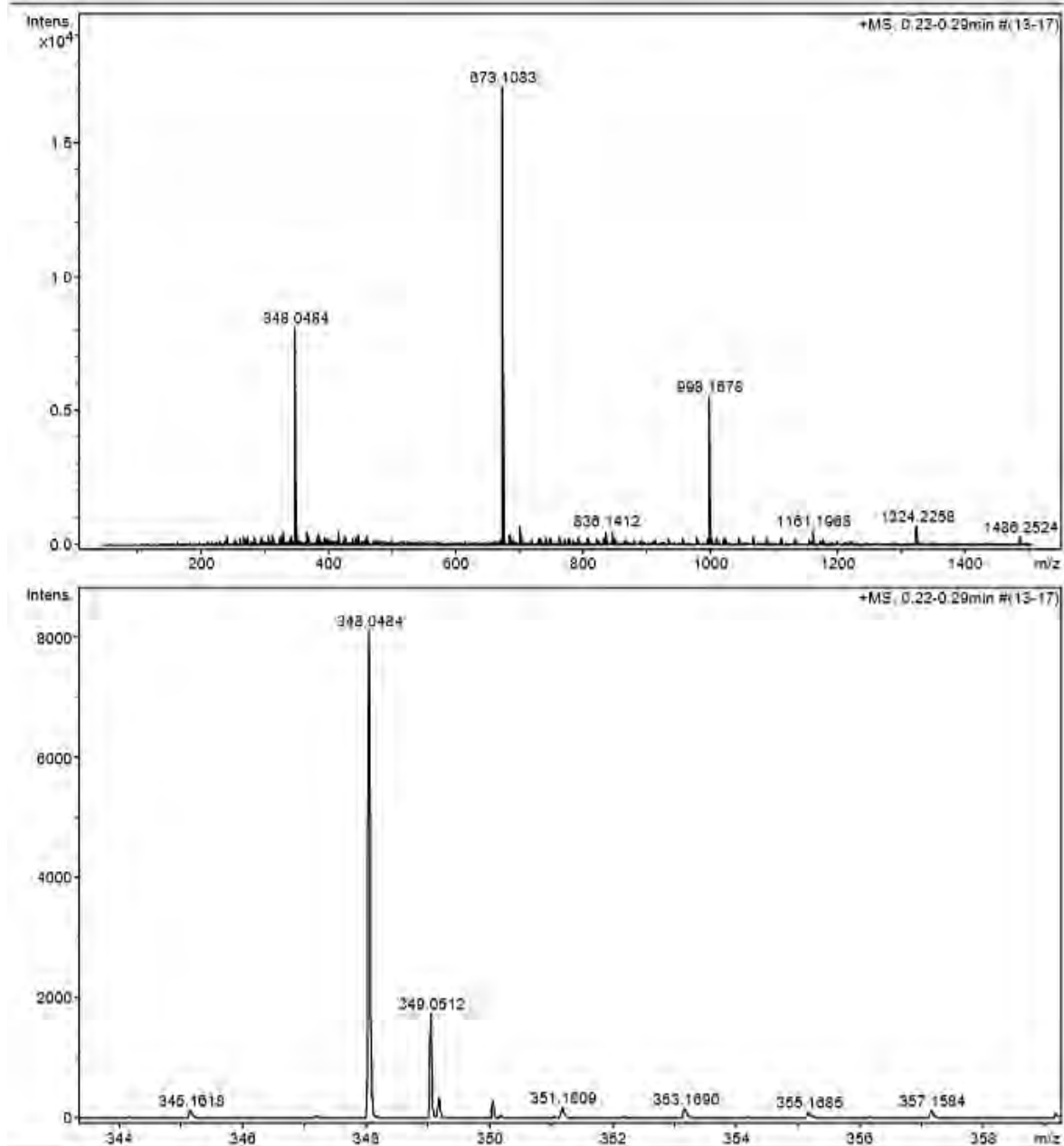


Figure 56 HRMS spectrum of 3e

N-(9-methoxy-7-oxo-7*H*-furo[3,2-*g*]chromen-4-yl) thiophene-2-carboxamide (**3f**)

¹H NMR (500 MHz, *DMSO-d*₆) δ 10.63 (s, 1H), 8.09 (d, *J* = 3.3 Hz, 1H), 8.08 (d, *J* = 2.2 Hz, 1H), 8.01 (d, *J* = 9.8 Hz, 1H), 7.88 (dd, *J* = 5.0, 0.9 Hz, 1H), 7.24 (dd, *J* = 4.9, 3.8 Hz, 1H), 6.90 (d, *J* = 2.2 Hz, 1H), 6.42 (d, *J* = 9.9 Hz, 1H), 4.16 (s, 3H).

2019-11-18-sja001-JA-A16-P1

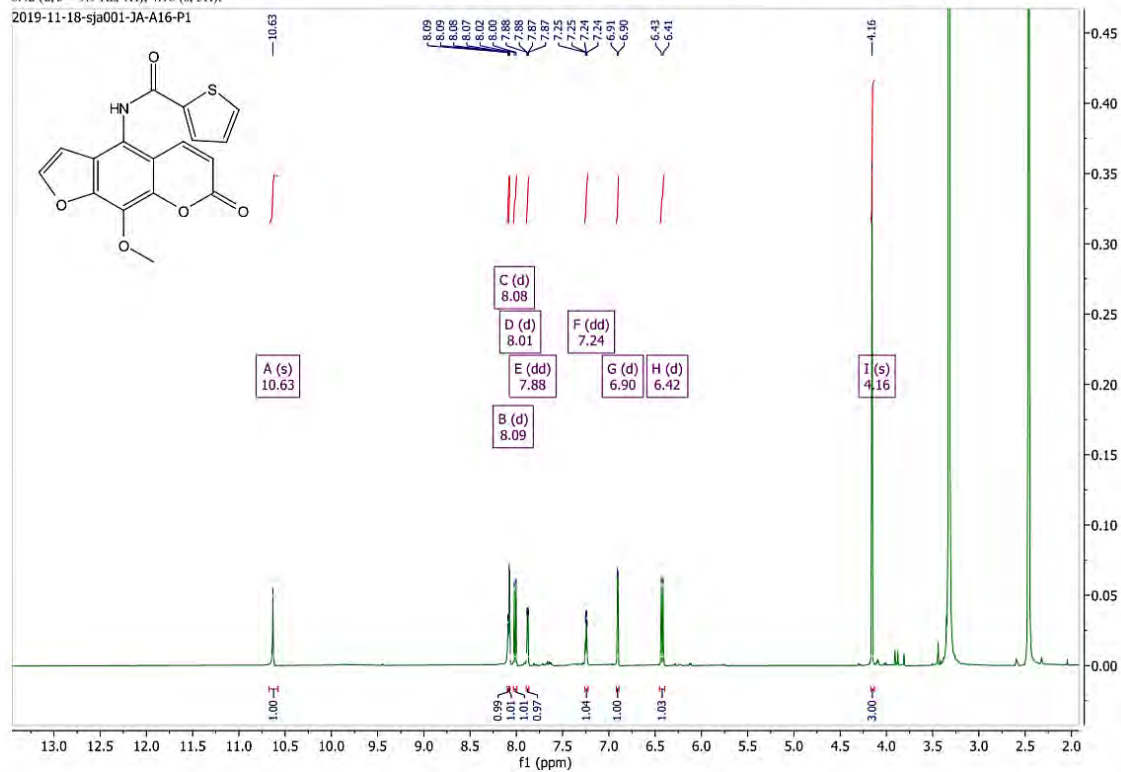


Figure 57 ¹H NMR spectrum of **3f**

¹³C NMR (126 MHz, *DMSO-d*₆) δ 161.08, 159.84, 147.77, 147.31, 143.01, 141.79, 139.07, 132.64, 131.12, 130.37, 128.63, 124.03, 121.24, 114.27, 113.13, 106.68, 61.56.

2019-11-25-tkh004-JA-A16-P1

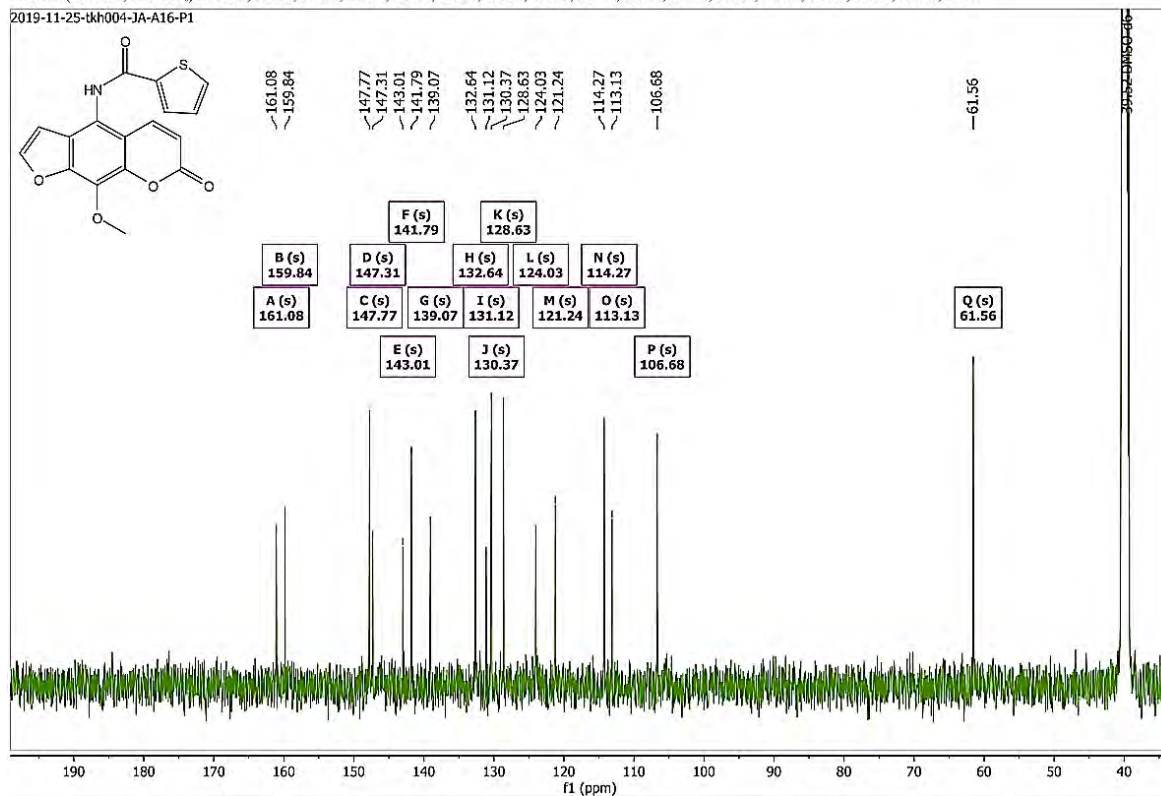


Figure 58 ¹³C NMR spectrum of **3f**

Generic Display Report

Analysis Info

Analysis Name D:\Data\Data Service\200316\A16_RC3_01_3874.d
Method nv_pos_6min_profile_wguardcol_50-1500_191021.m
Sample Name A16
Comment

Acquisition Date 3/16/2020 5:15:02 PM

Operator CU,
Instrument microTOF-Q II

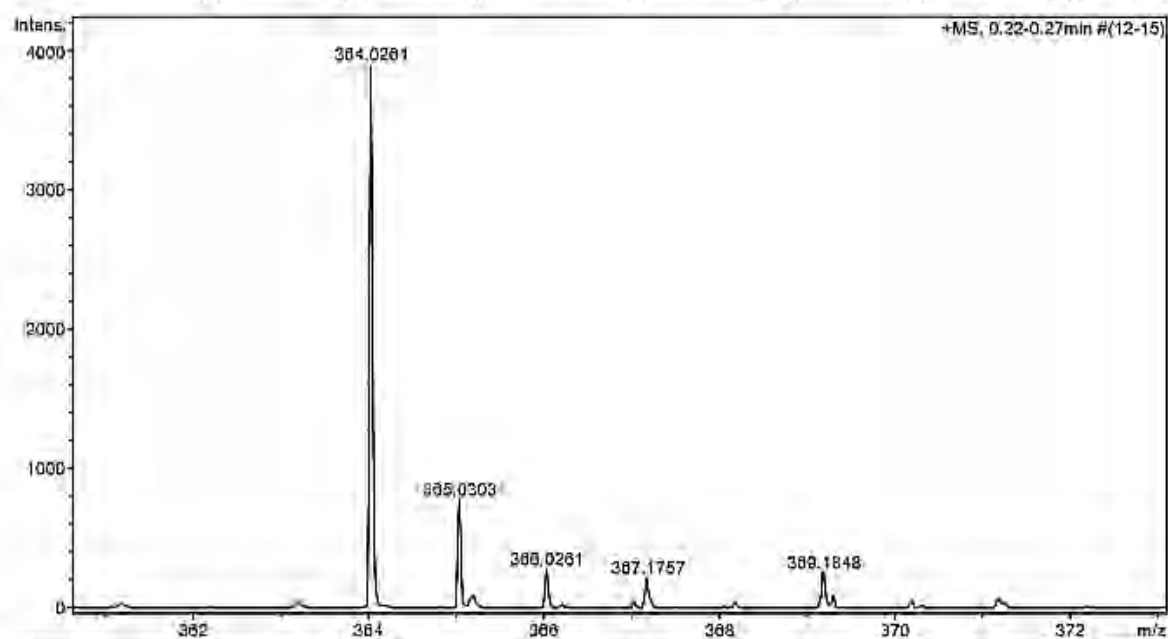
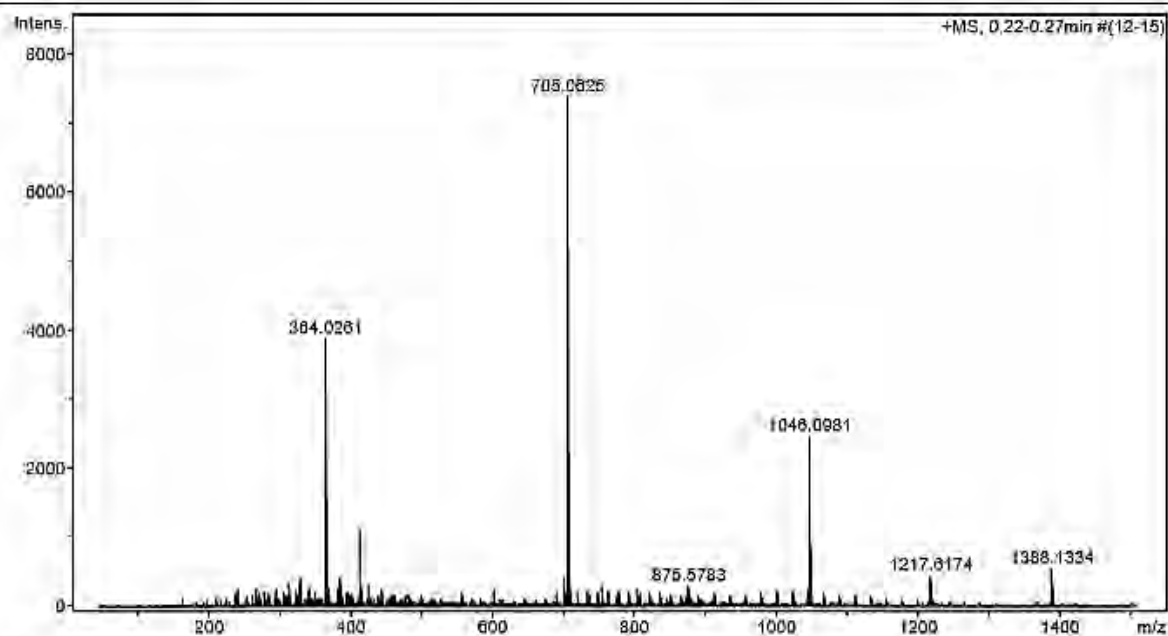
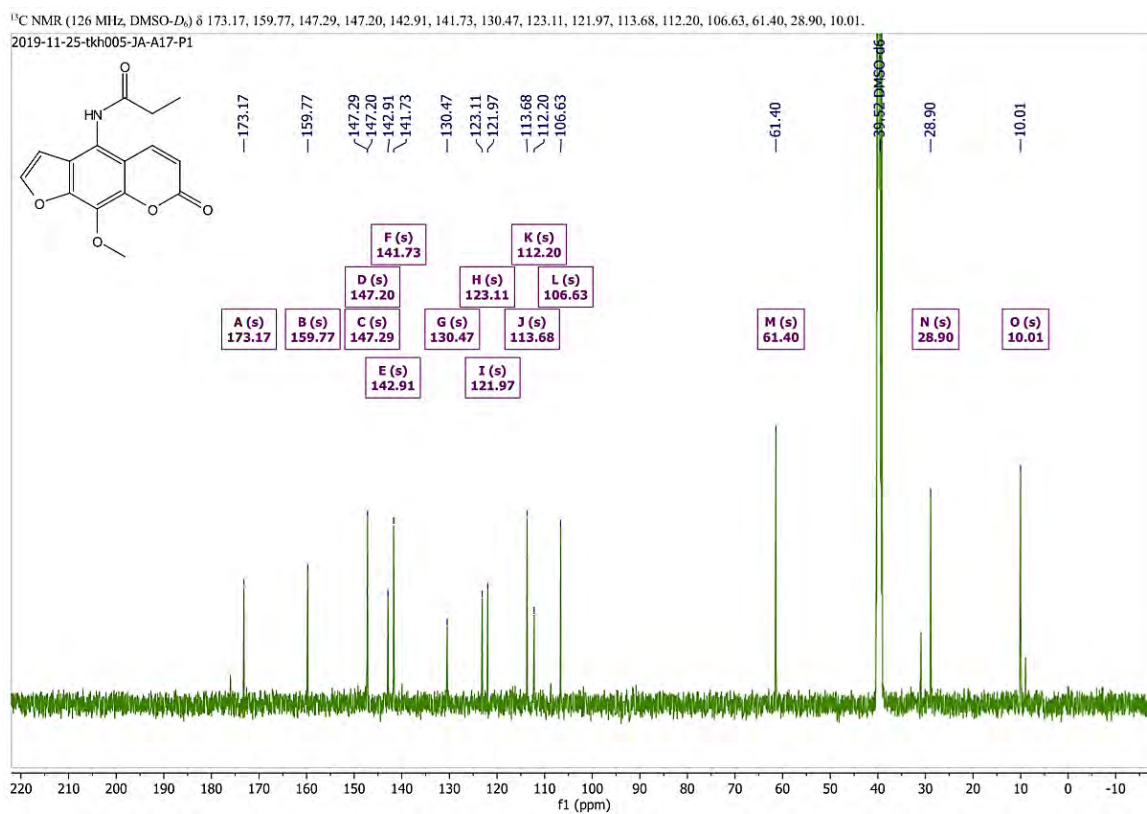
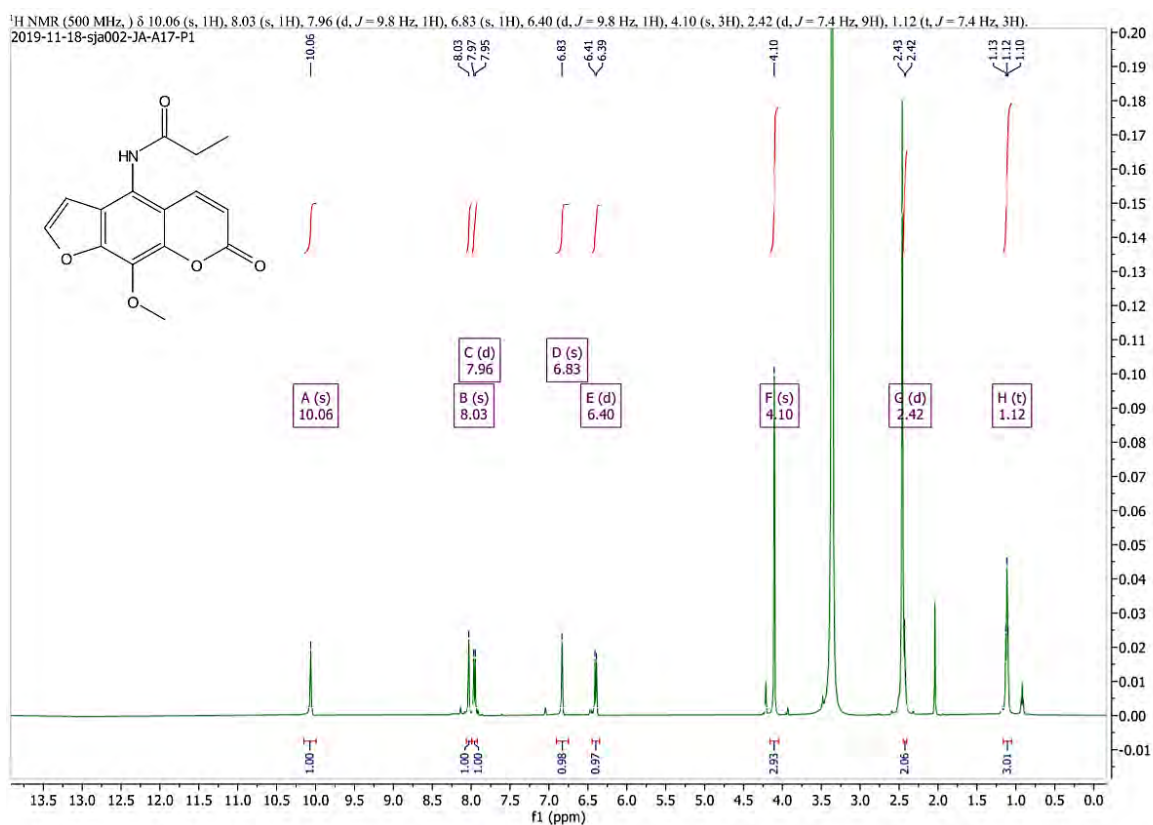


Figure 59 HRMS spectrum of 3f

N-(9-methoxy-7-oxo-7*H*-furo[3,2-*g*]chromen-4-yl)propionamide (3g)



Generic Display Report

Analysis Info

Analysis Name D:\Data\Data Service\200316\A17_RC4_01_3875.d
Method nv_pos_6min_profile_wguardcol_50-1500_191021.m
Sample Name A17
Comment

Acquisition Date 3/16/2020 5:21:46 PM
Operator CU
Instrument micrOTOF-Q II

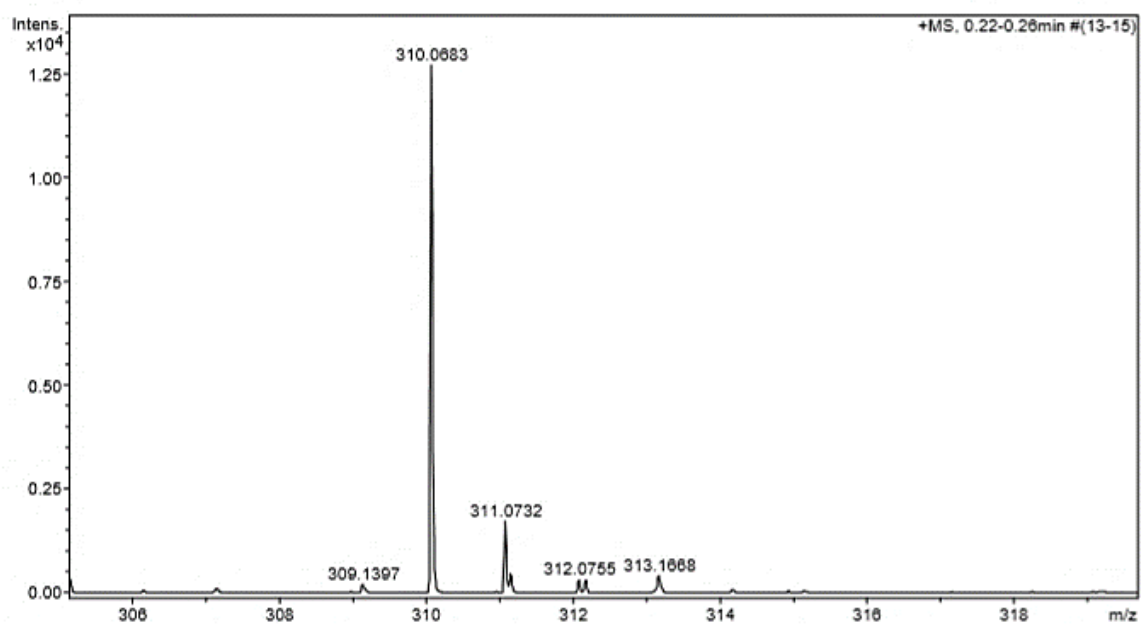
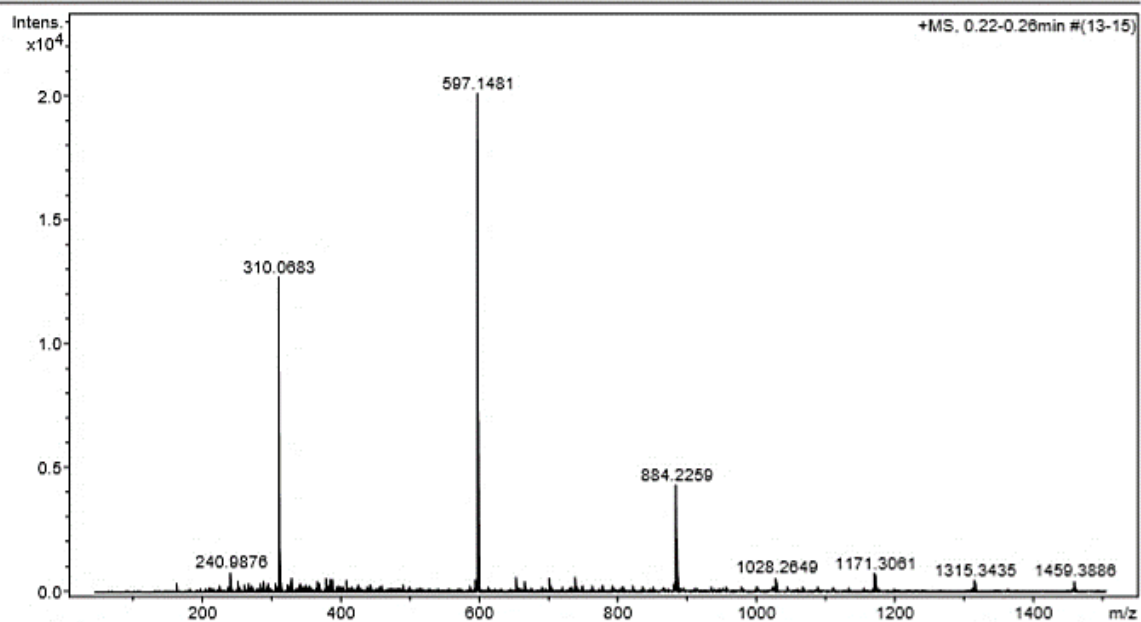


Figure 62 HRMS spectrum of 3g

N-(9-methoxy-7-oxo-7*H*-furo[3,2-*g*]chromen-4-yl)isobutyramide(3h)

¹H NMR (500 MHz, CHLOROFORM-*D*) δ 7.70 (d, *J* = 9.8 Hz, 1H), 7.62 (d, *J* = 2.2 Hz, 1H), 7.50 (s, 1H), 6.64 (d, *J* = 2.2 Hz, 1H), 6.31 (d, *J* = 9.7 Hz, 1H), 4.25 (s, 3H), 2.79 – 2.67 (m, 1H), 1.35 (d, *J* = 6.9 Hz, 6H).

2019-11-28-tjkh001-JA-A18-P3

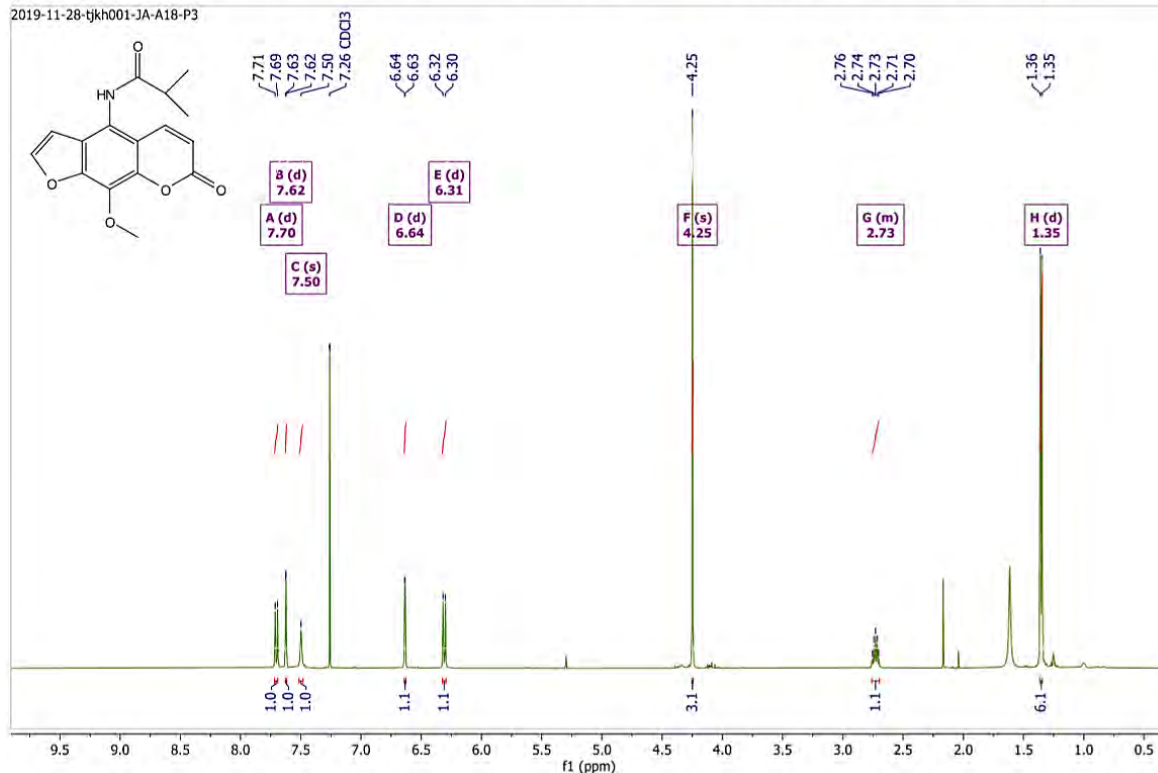


Figure 63 ¹H NMR spectrum of 3h

¹³C NMR (126 MHz, CHLOROFORM-*D*) δ 176.37, 159.89, 147.30, 146.27, 142.89, 139.48, 131.78, 123.53, 118.80, 114.46, 112.79, 104.94, 61.28, 35.77, 19.69.

2019-11-28-tjkh001-JA-A18-P3

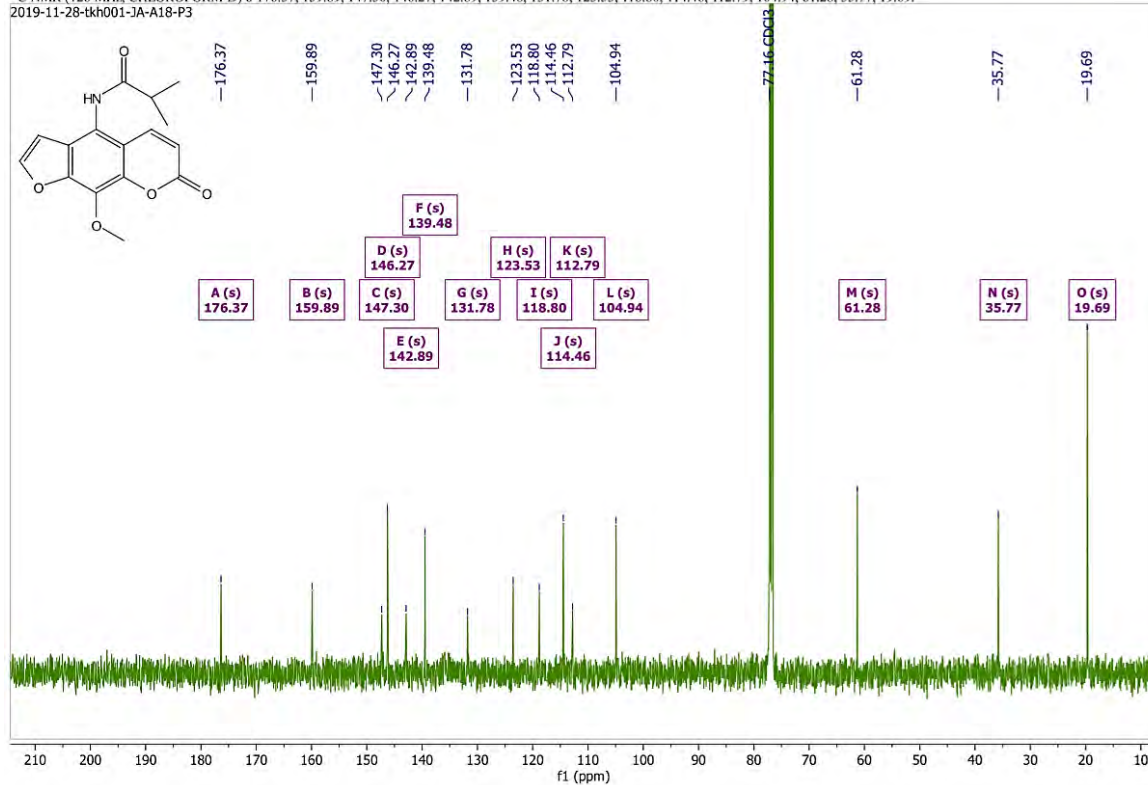


Figure 64 ¹³C NMR spectrum of 3h

Generic Display Report

Analysis Info

Analysis Name D:\Data\Data Service\200316\A18_RC5_01_3861.d
Method nv_pos_6min_profile_wguardcol_50-1500_191021.m
Sample Name A18
Comment

Acquisition Date 3/16/2020 3:37:32 PM

Operator CU.
Instrument micrOTOF-Q II

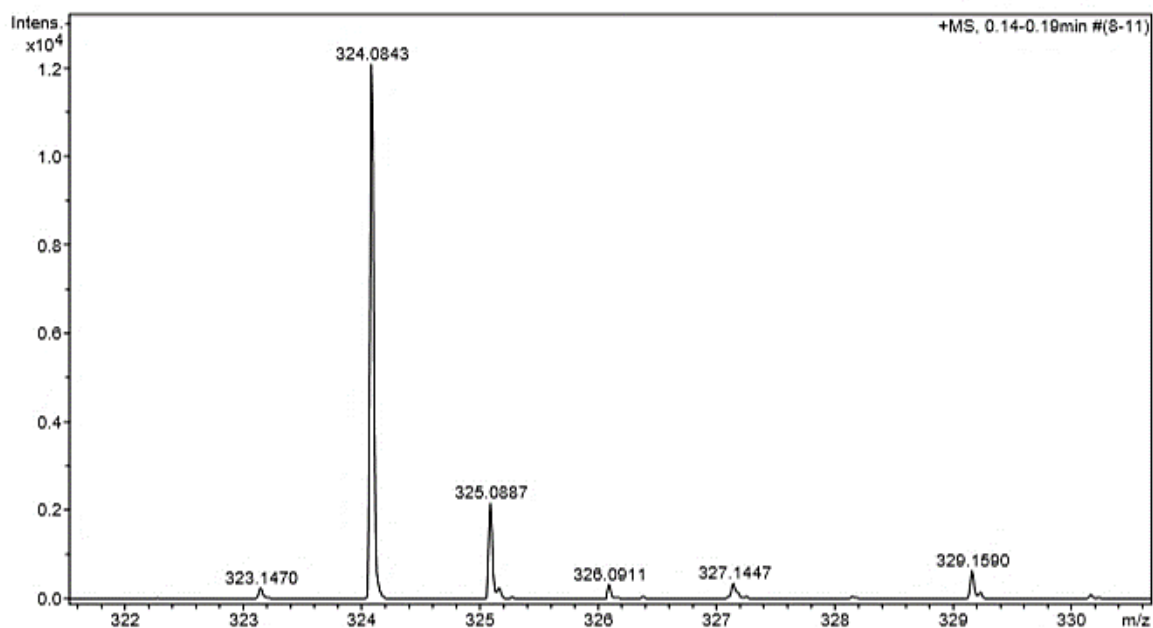
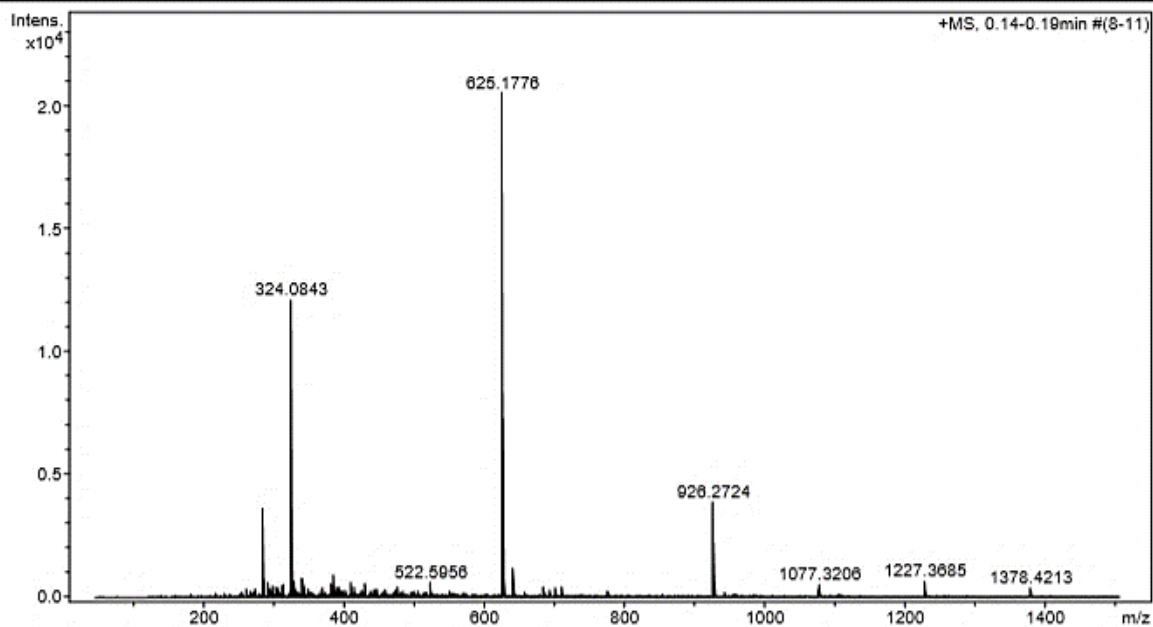
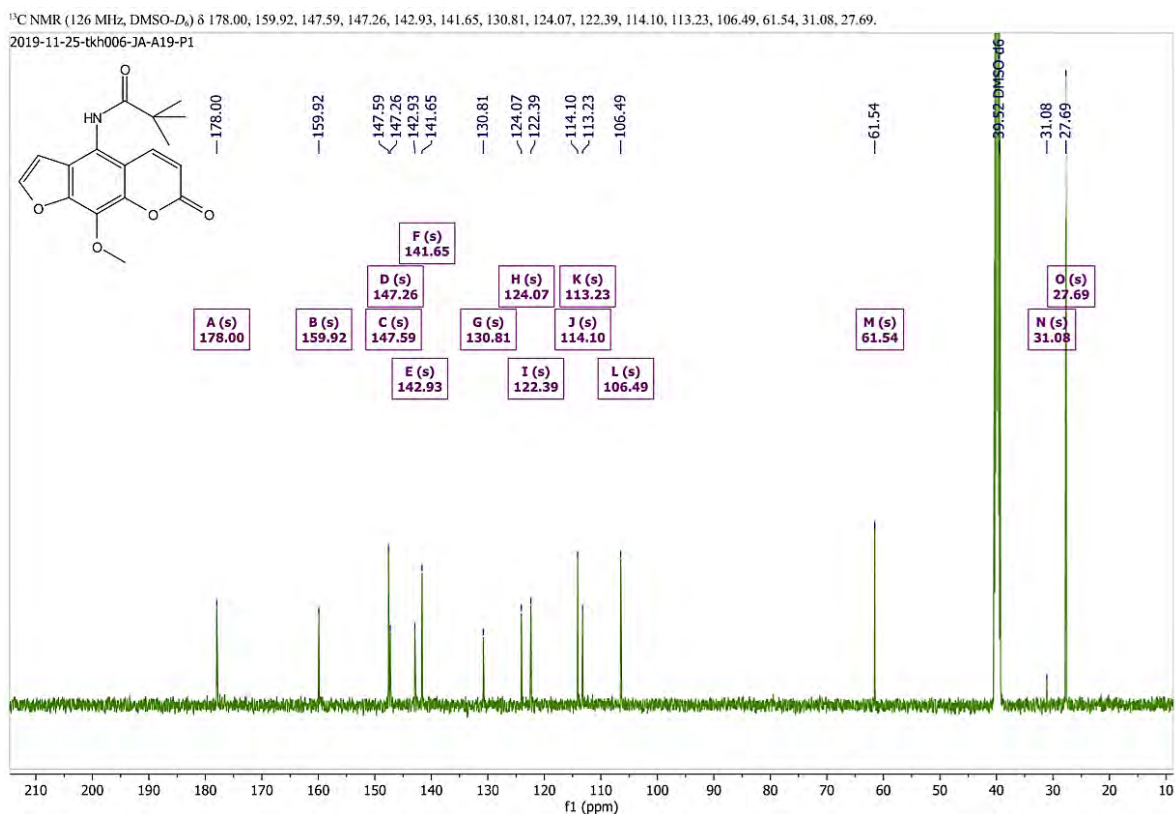
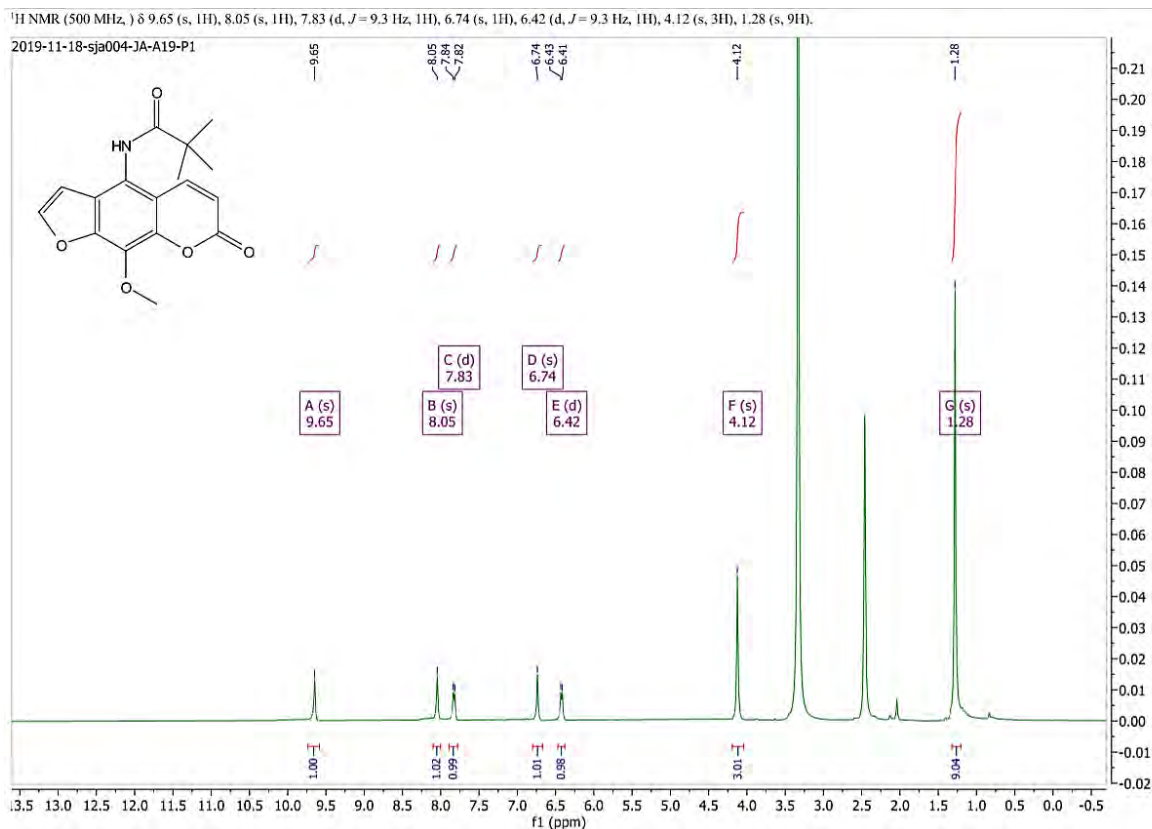


Figure 65 HRMS spectrum of 3h

N-(9-methoxy-7-oxo-7*H*-furo[3,2-*g*]chromen-4-yl)pivalamide (3i)



Generic Display Report

Analysis Info

Analysis Name D:\Data\Data Service\200316\A19_RC6_01_3876.d
Method nv_pos_6min_profile_wguardcol_50-1500_191021.m
Sample Name A19
Comment

Acquisition Date 3/16/2020 5:28:30 PM

Operator CU.
Instrument micrOTOF-Q II

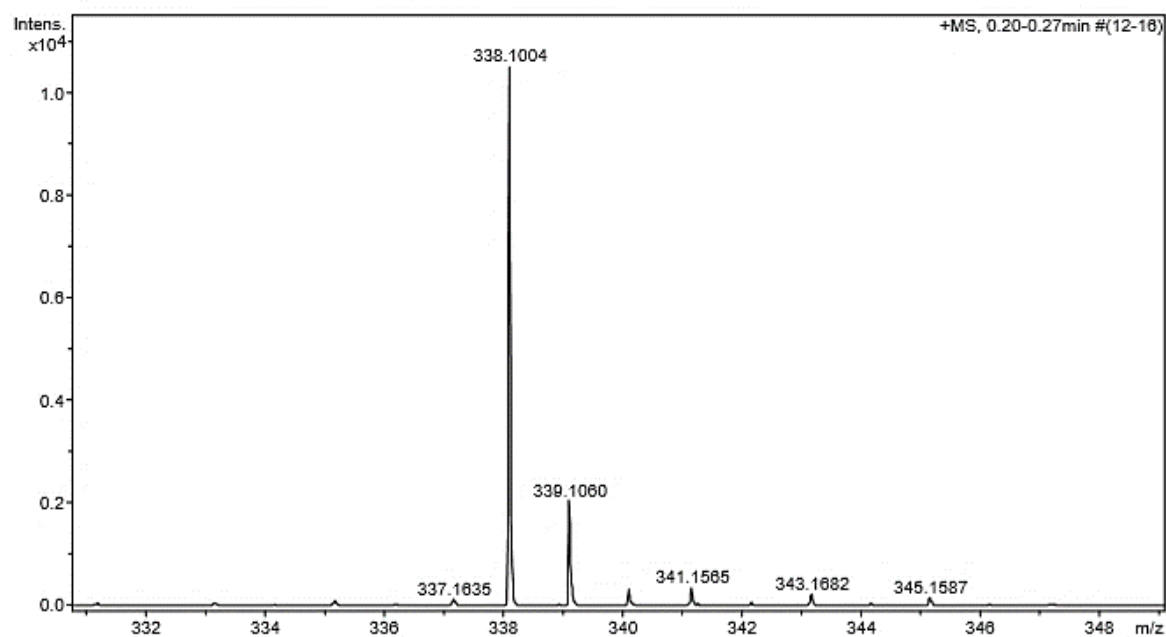
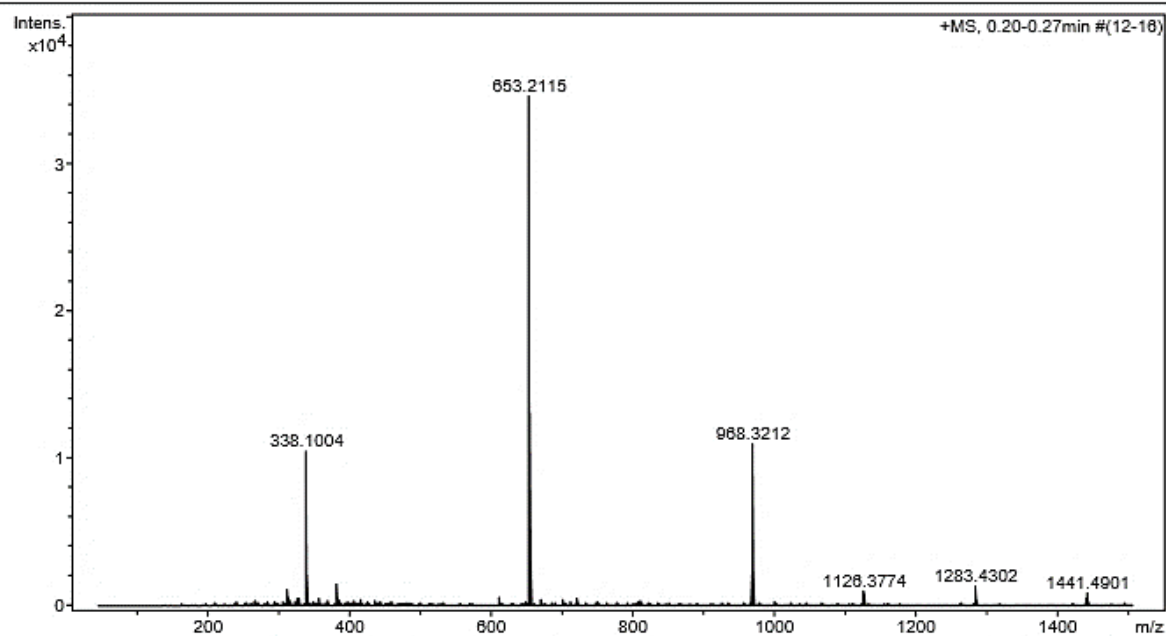


Figure 68 HRMS spectrum of 3i

4-methoxy-*N*-(9-methoxy-7-oxo-7*H*-furo[3,2-*g*]chromen-4-yl)benzamide (3j)

¹H NMR (500 MHz,) δ 10.44 (s, 1H), 8.05 (d, *J* = 2.3 Hz, 1H), 8.03 (d, *J* = 8.8 Hz, 2H), 7.99 (dd, *J* = 9.9 Hz, 1H), 7.06 (dd, *J* = 9.3, 2.3 Hz, 2H), 6.88 (d, *J* = 2.1 Hz, 1H), 6.40 (d, *J* = 9.8 Hz, 1H), 4.15 (s, 3H), 3.82 (s, 3H).

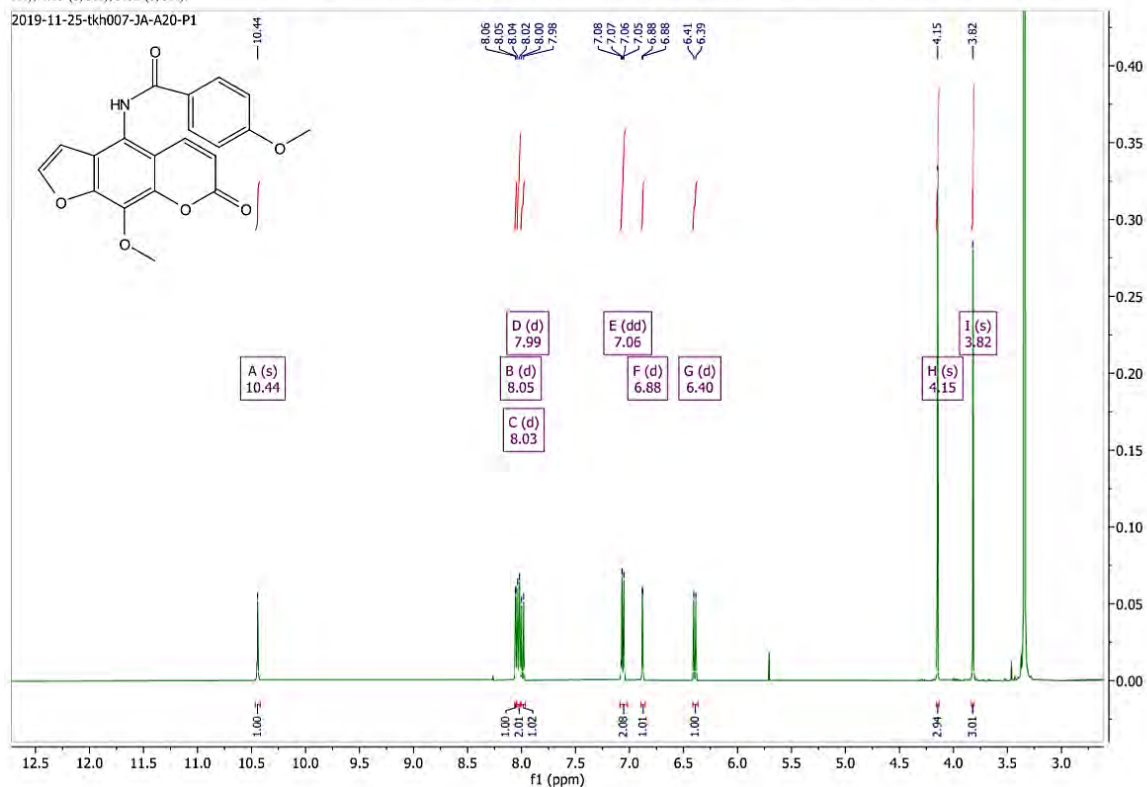


Figure 69 ¹H NMR spectrum of 3j

¹³C NMR (126 MHz, DMSO-*d*₆) δ 166.01, 162.66, 159.92, 147.60, 147.37, 143.06, 142.01, 130.91, 130.35, 126.12, 124.02, 122.27, 114.10, 114.02, 113.11, 106.78, 61.57, 55.90.

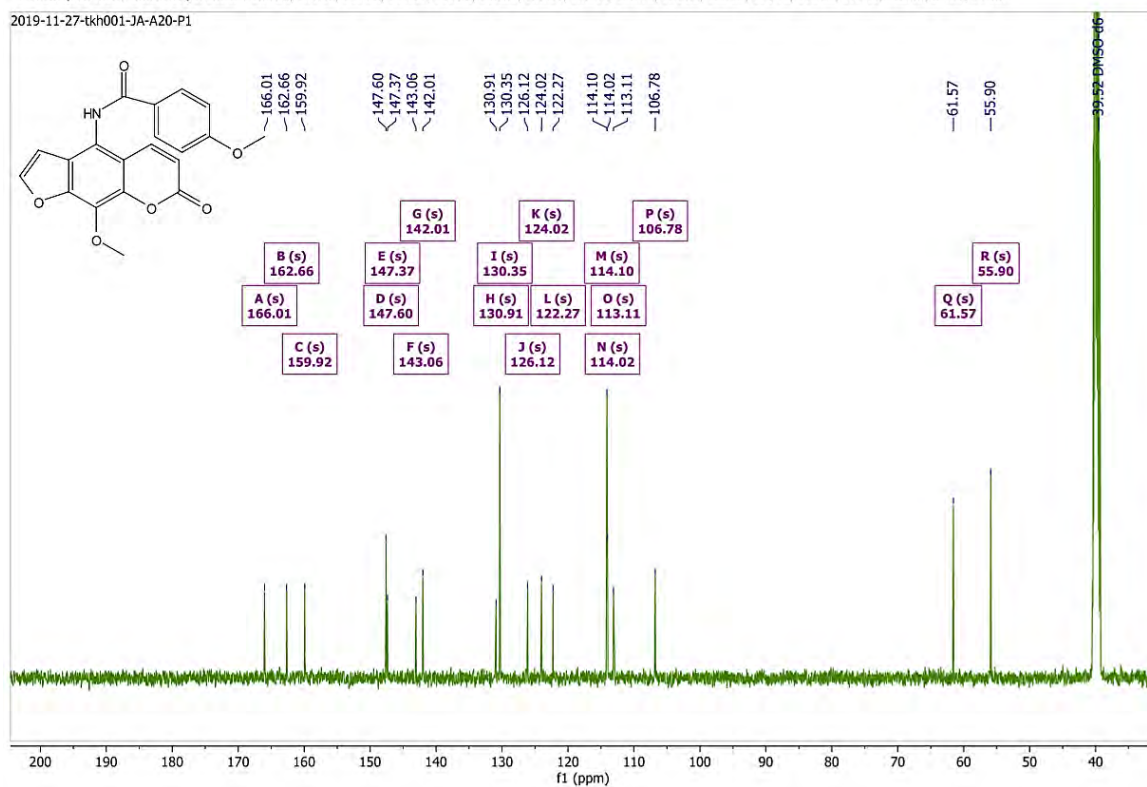


Figure 70 ¹³C NMR spectrum of 3j

Generic Display Report

Analysis Info

Analysis Name D:\Data\Data Service\200316\A20_RC7_01_3877.d
Method nv_pos_6min_profile_wguardcol_50-1500_191021.m
Sample Name A20
Comment

Acquisition Date 3/16/2020 5:35:17 PM

Operator CU.
Instrument micrOTOF-Q II

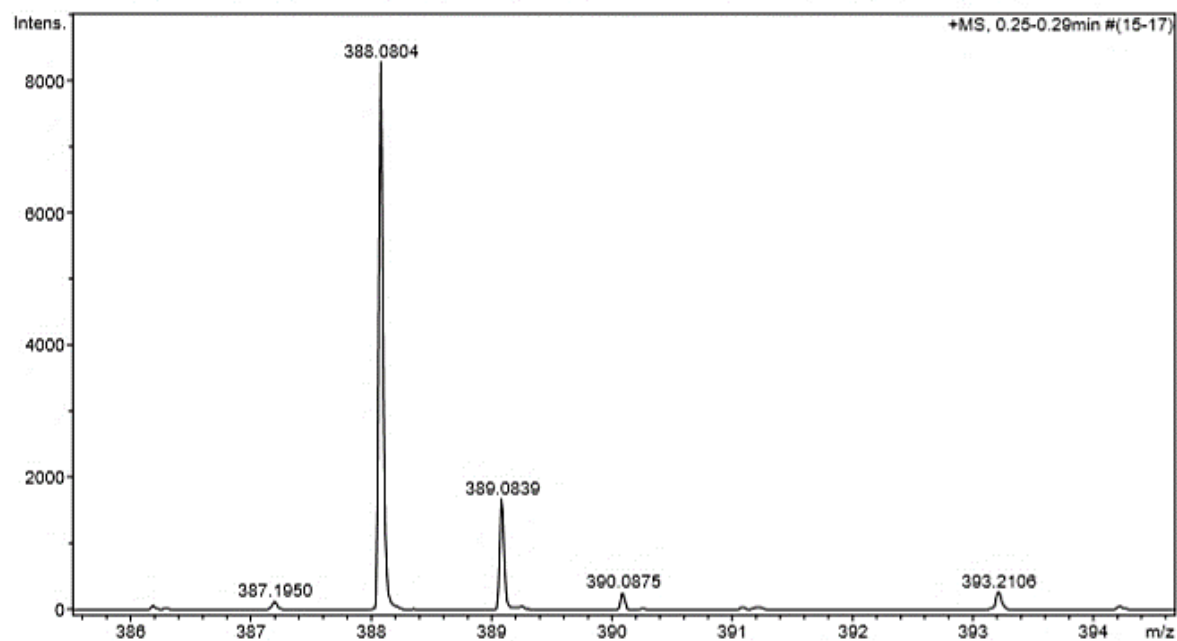
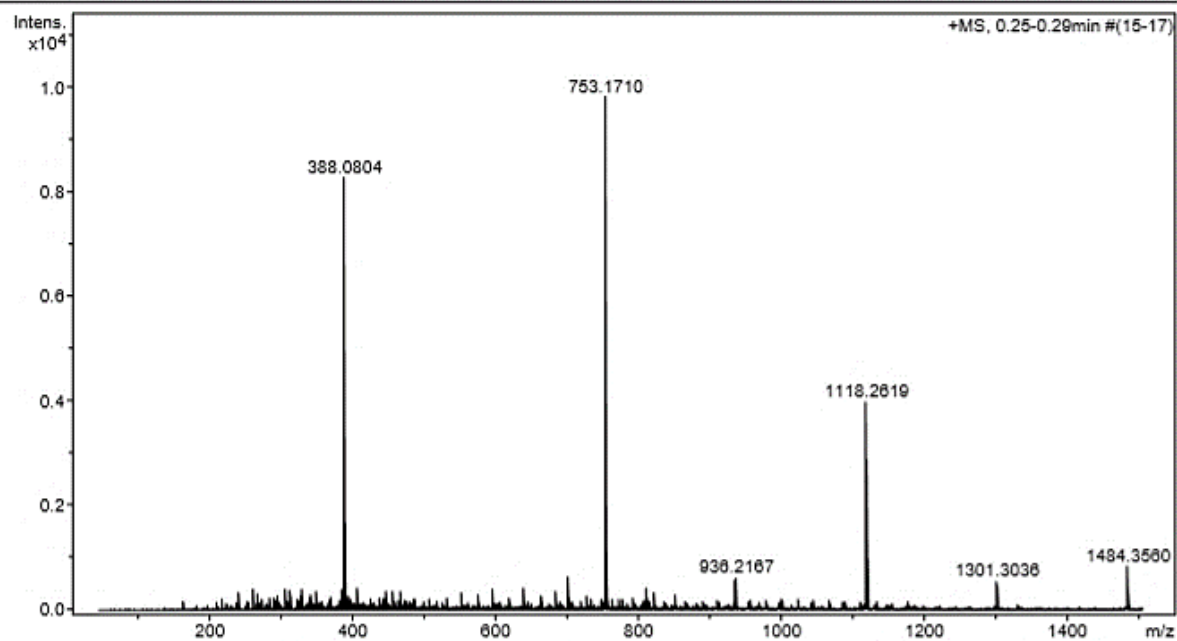


Figure 71 HRMS spectrum of 3j

N-hexanoyl-*N*-(9-methoxy-7-oxo-7*H*-furo[3,2-*g*]chromen-4-yl)hexanamide (3k)

¹H NMR (500 MHz,) δ 7.71 (d, *J* = 2.3 Hz, 1H), 7.54 (d, *J* = 9.8 Hz, 1H), 6.61 (d, *J* = 2.3 Hz, 1H), 6.44 (d, *J* = 9.9 Hz, 1H), 4.35 (s, 3H), 2.52 (t, 4H), 1.60 (p, *J* = 7.4 Hz, 4H), 1.31 – 1.16 (m, 8H), 0.84 (t, *J* = 7.0 Hz, 6H).

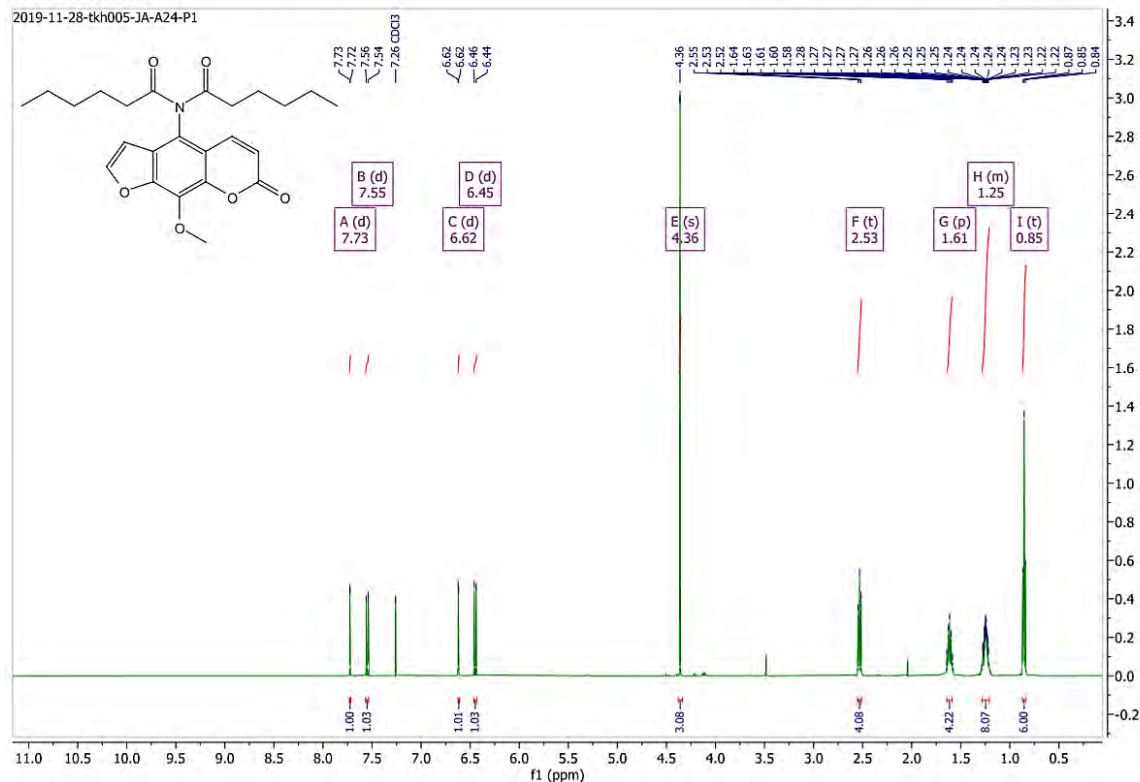


Figure 72 ¹H NMR spectrum of 3k

¹³C NMR (126 MHz, CHLOROFORM-*D*) δ 175.66, 159.31, 147.73, 147.04, 143.03, 137.87, 133.32, 125.49, 120.44, 116.62, 114.73, 103.82, 61.29, 37.99, 31.06, 24.22, 22.26, 13.74.

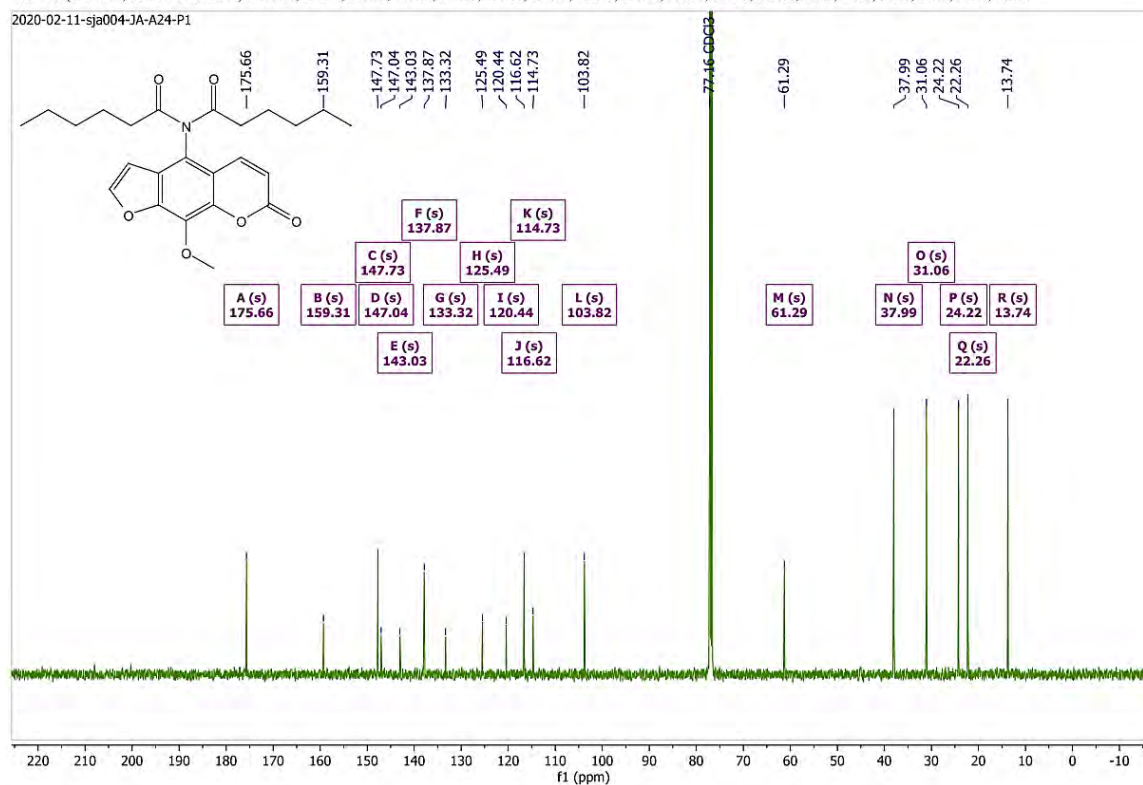


Figure 73 ¹³C NMR spectrum of 3k

Generic Display Report

Analysis Info

Analysis Name D:\Data\Data Service\200316\A24_RC8_01_3878.d
Method nv_pos_6min_profile_wguardcol_50-1500_191021.m
Sample Name A24
Comment

Acquisition Date 3/16/2020 5:42:02 PM

Operator CU.
Instrument micrOTOF-Q II

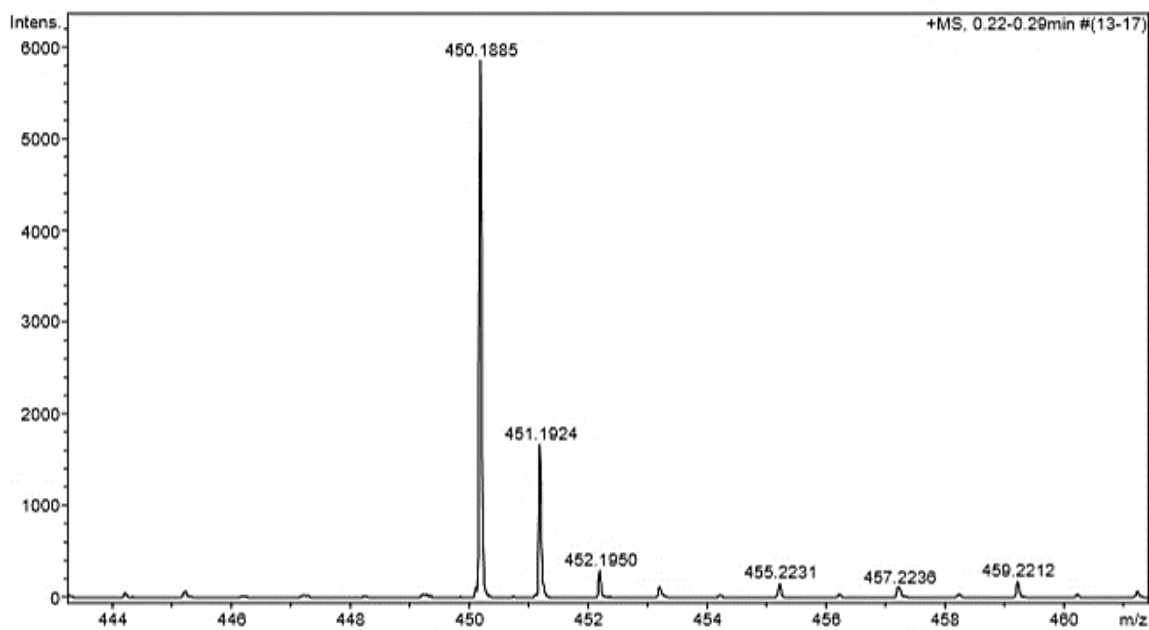
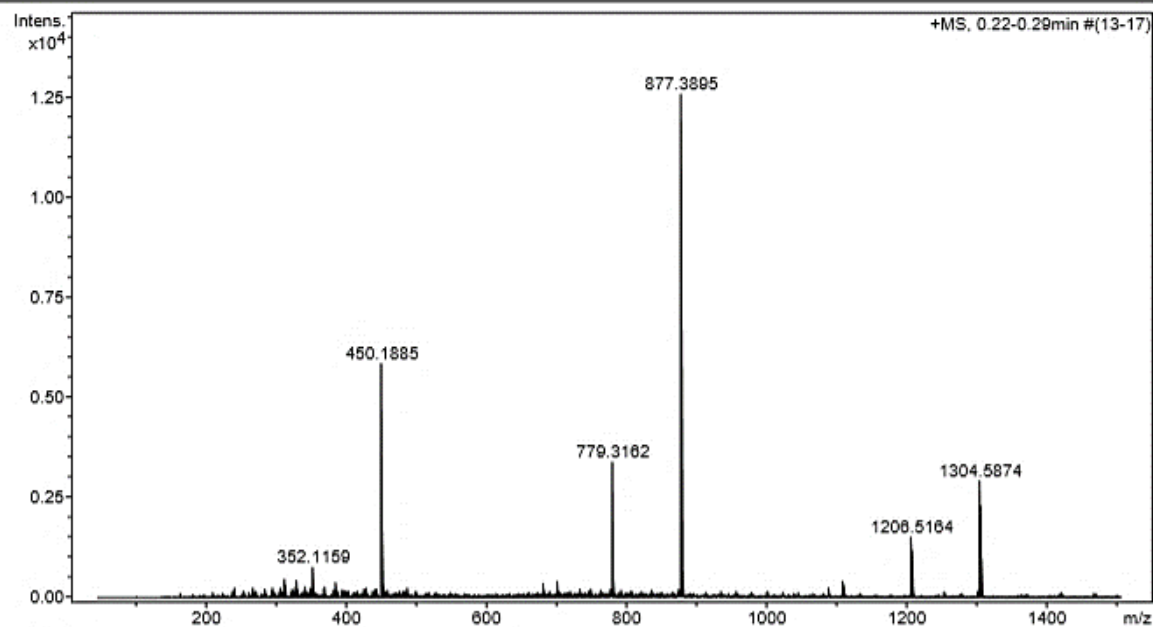


Figure 74 HRMS spectrum of 3k

(3*r*,5*r*,7*r*)-*N*-(9-methoxy-7-oxo-7*H*-furo[3,2-*g*]chromen-4-yl)adamantane-1-carboxamide
(3l)

¹H NMR (500 MHz,) δ 7.62 (s, 1H), 7.59 (d, *J* = 9.8 Hz, 1H), 7.58 (d, *J* = 2.2 Hz, 1H), 6.55 (d, *J* = 2.2 Hz, 1H), 6.23 (d, *J* = 9.8 Hz, 1H), 4.22 (s, 3H), 2.13 (s, 3H), 2.04 (d, *J* = 2.5 Hz, 6H), 1.79 (q, *J* = 12.5 Hz, 6H).

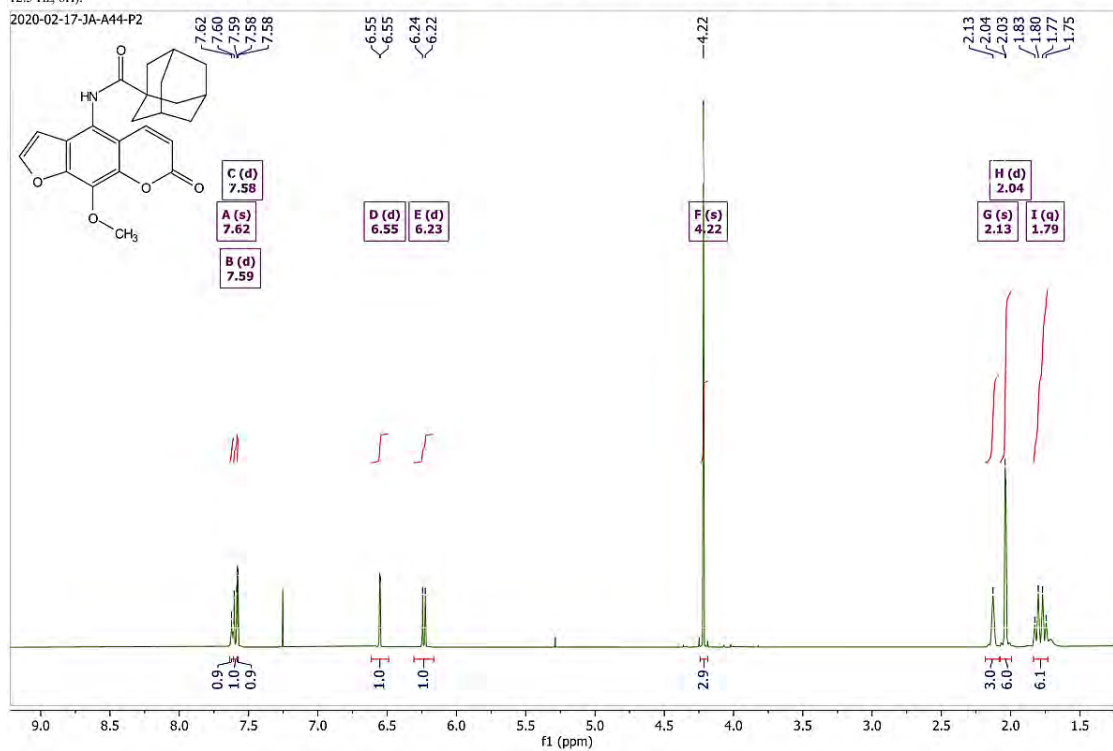


Figure 75 ¹H NMR spectrum of 3l

¹³C NMR (126 MHz, CHLOROFORM-*D*) δ 177.59, 160.13, 147.40, 146.35, 143.00, 139.76, 131.69, 123.79, 119.53, 114.38, 113.00, 105.18, 61.47, 41.62, 39.53, 36.47, 28.19.

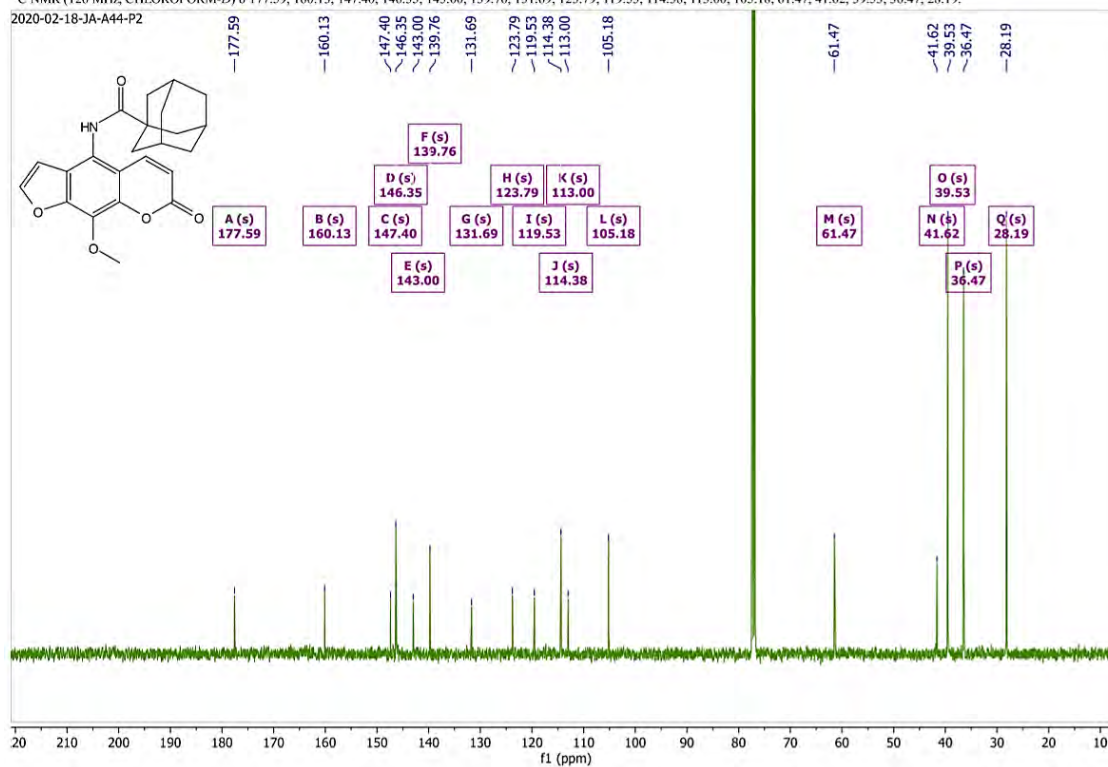


Figure 76 ¹³C NMR spectrum of 3l

Generic Display Report

Analysis Info

Analysis Name D:\Data\Data Service\200316\A44_RD1_01_3879.d
Method nv_pos_6min_profile_wguardcol_50-1500_191021.m
Sample Name A44
Comment

Acquisition Date 3/16/2020 5:48:47 PM

Operator CU,
Instrument micrOTOF-Q II

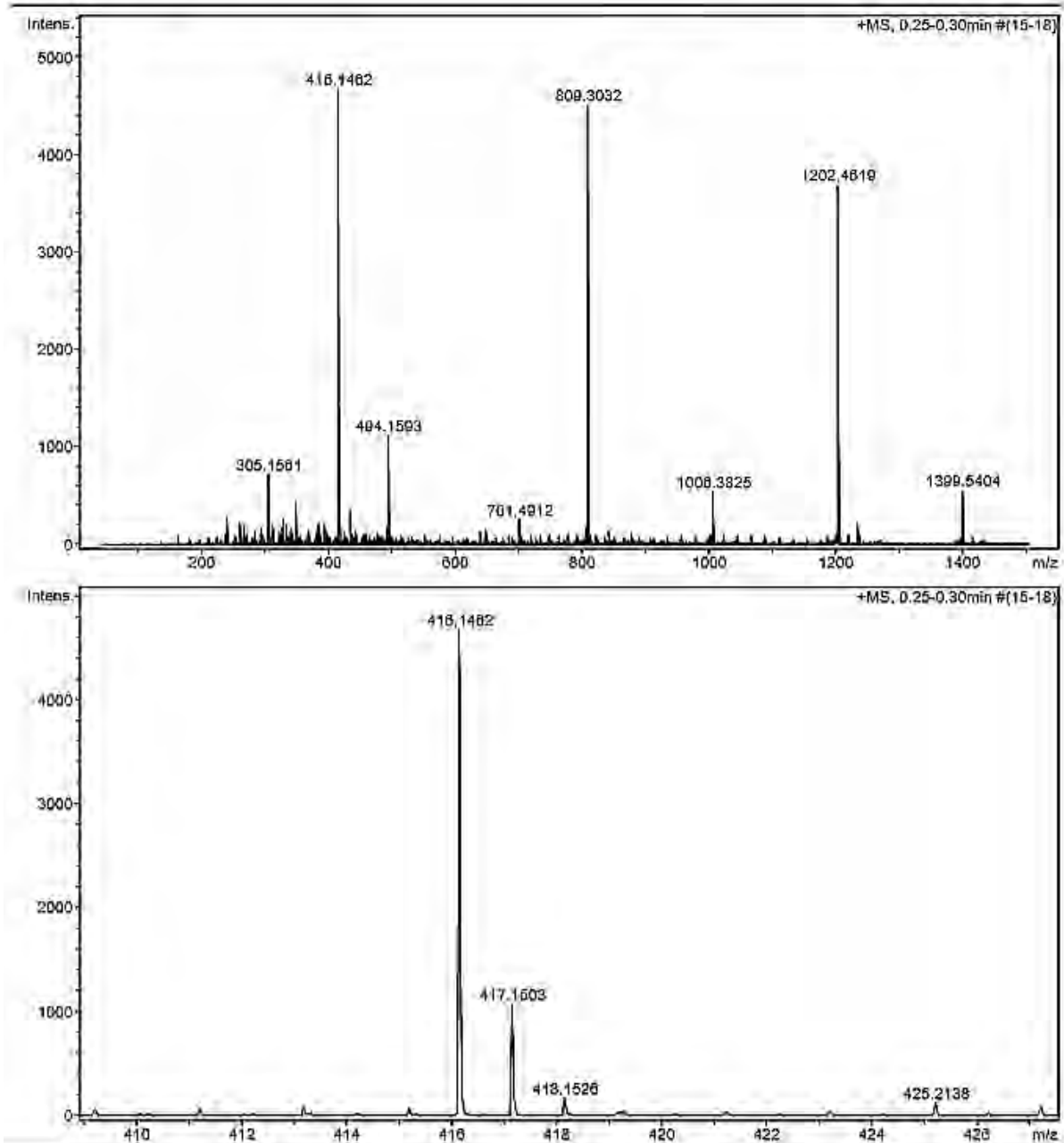


Figure 77 HRMS spectrum of 3l

N-(9-methoxy-7-oxo-7*H*-furo[3,2-*g*]chromen-4-yl)acetamide (3m)

¹H NMR (500 MHz, DMSO-*d*₆) δ 10.06 (s, 1H), 7.95 (d, *J* = 2.2 Hz, 1H), 7.91 (d, *J* = 9.9 Hz, 1H), 6.79 (d, *J* = 2.2 Hz, 1H), 6.32 (d, *J* = 9.8 Hz, 1H), 4.03 (s, 3H), 2.05 (s, 3H).
2019-11-21-sja003-JA-A12-P1

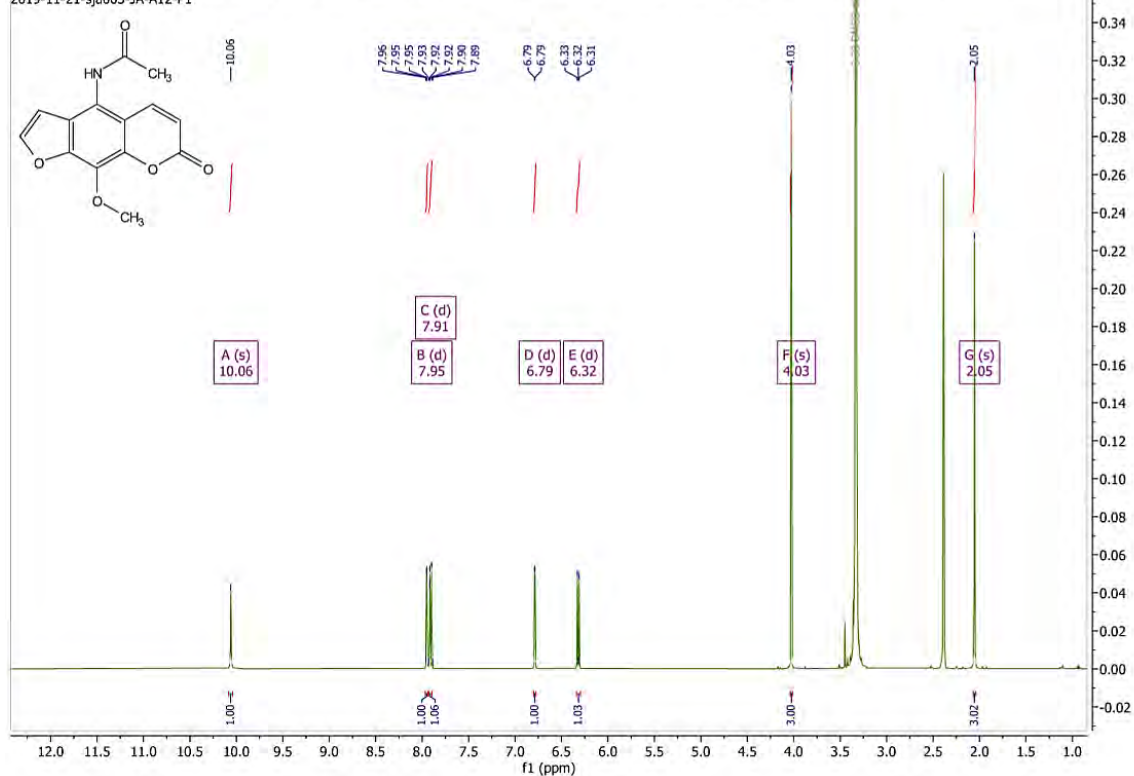


Figure 78 ¹H NMR spectrum of 3m

¹³C NMR (126 MHz, DMSO-*D*₆) δ 169.53, 159.81, 147.32, 147.27, 142.93, 141.80, 130.55, 123.16, 121.95, 113.73, 112.23, 106.67, 61.44, 23.20.

2019-11-21-sja004-JA-A12-P1

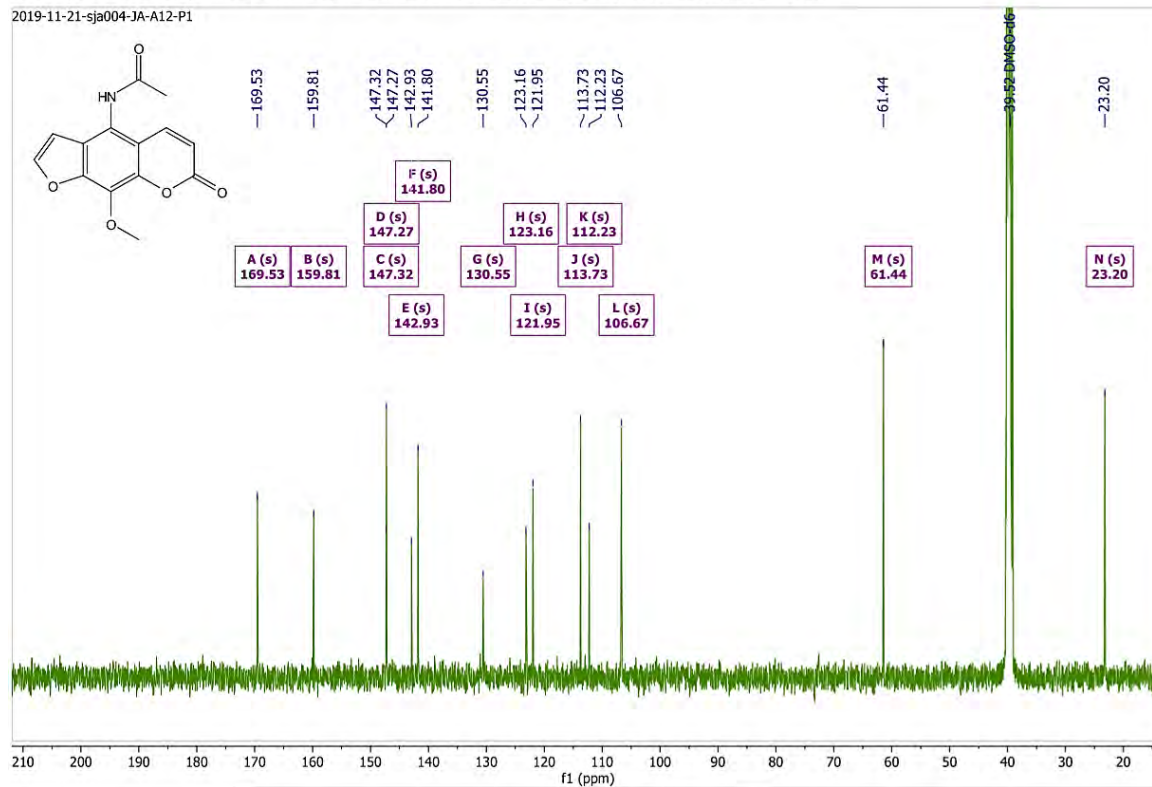


Figure 79 ¹³C NMR spectrum of 3m

Generic Display Report

Analysis Info

Analysis Name D:\Data\Data Service\200316\A12_RC1_01_3872.d
Method nv_pos_6min_profile_wguardcol_50-1500_191021.m
Sample Name A12
Comment

Acquisition Date 3/16/2020 5:01:31 PM

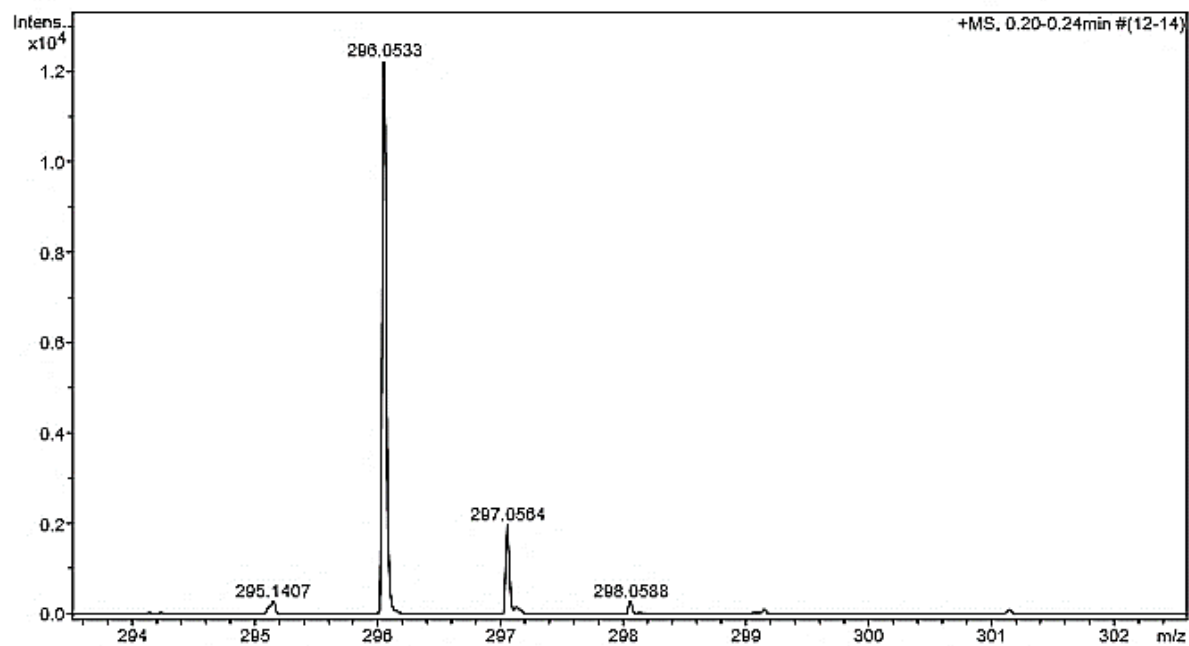
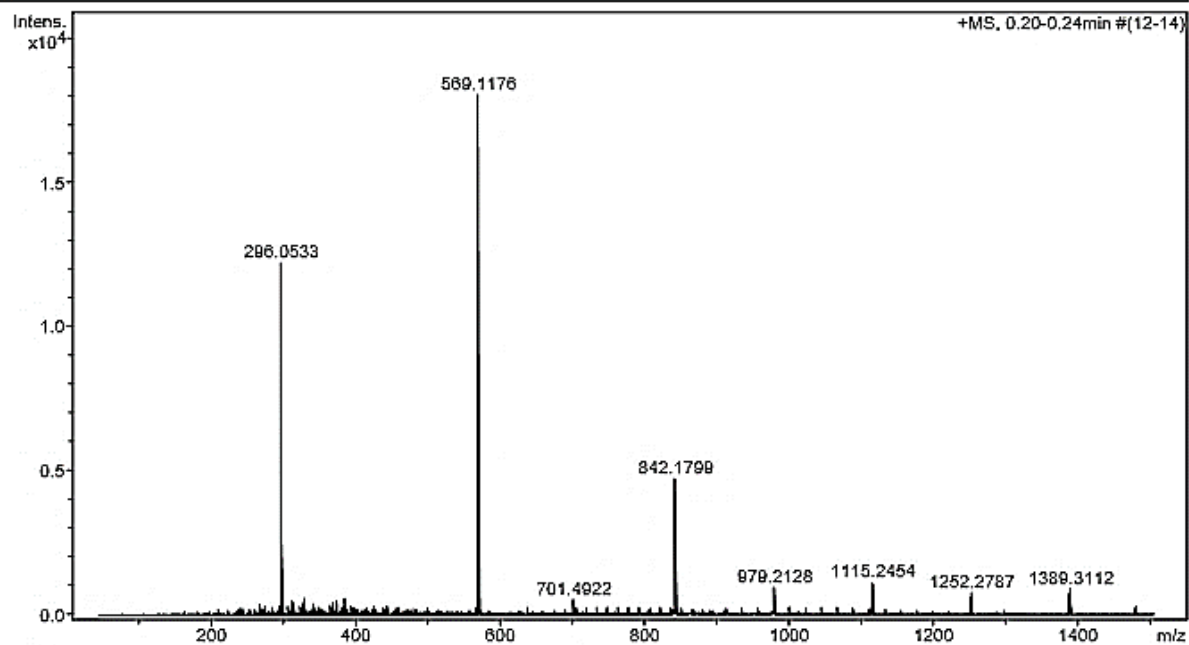
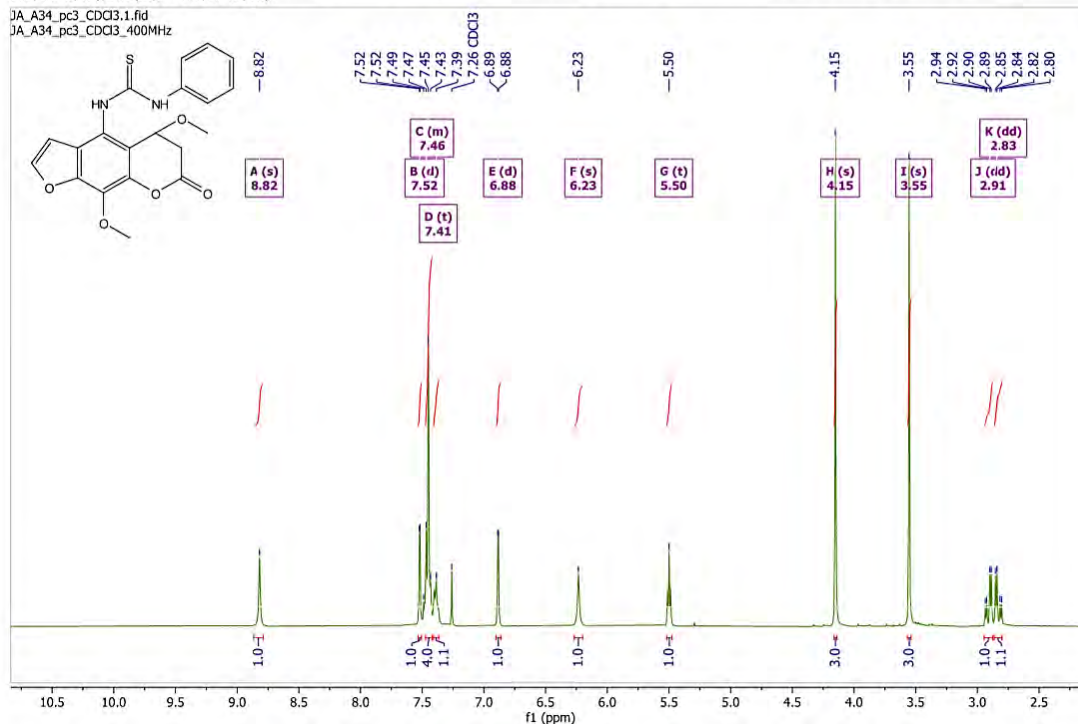
Operator CU.
Instrument microTOF-Q II

Figure 80 HRMS spectrum of 3m

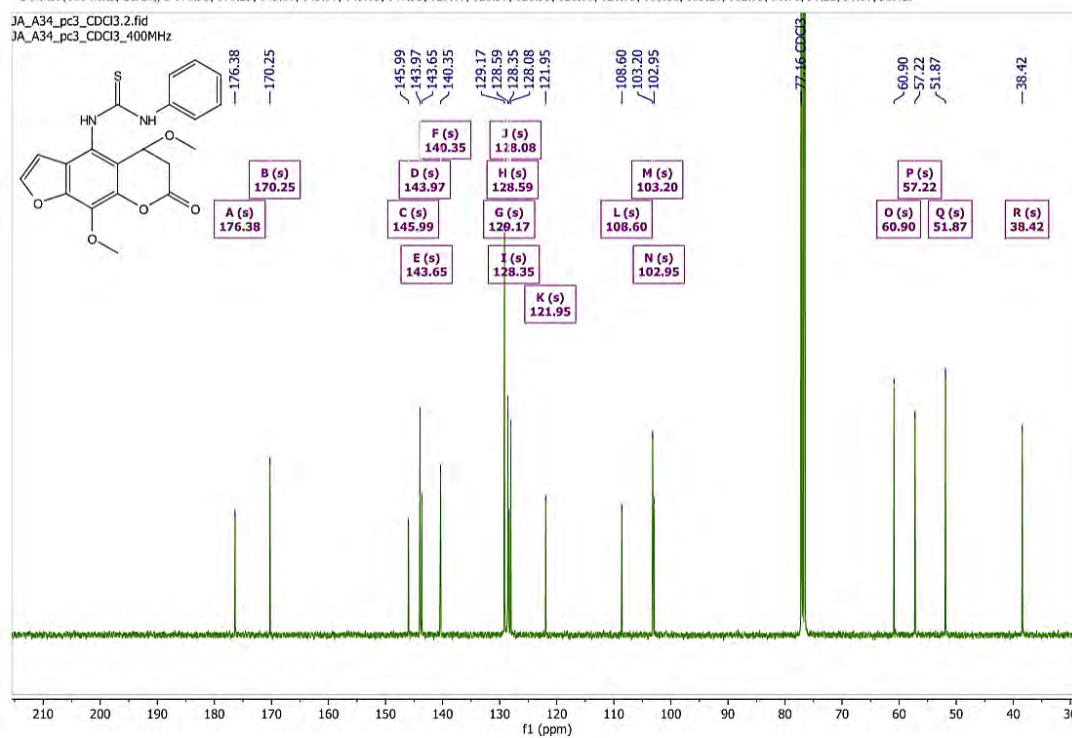
APPENDIX B
NMR and HRMS spectra of 4-5 and 7a-7b

1-(5,9-dimethoxy-7-oxo-6,7-dihydro-5H-furo[3,2-g]chromen-4-yl)-3-phenylthiourea (4)

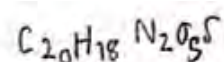
$^1\text{H NMR}$ (400 MHz, CDCl_3) δ 8.82 (s, 1H), 7.52 (d, 1H), 7.48 – 7.42 (m, 4H), 7.41 (t, $J = 18.7$ Hz, 1H), 6.88 (d, $J = 2.3$ Hz, 1H), 6.23 (s, 1H), 5.50 (t, 1H), 4.15 (s, 3H), 3.55 (s, 3H), 2.91 (dd, $J = 14.8, 4.9$ Hz, 1H), 2.83 (dd, $J = 14.8, 5.3$ Hz, 1H).

Figure 81 $^1\text{H NMR}$ spectrum of 4

$^{13}\text{C NMR}$ (101 MHz, CDCl_3) δ 176.38, 170.25, 145.99, 143.97, 143.65, 140.35, 129.17, 128.59, 128.35, 128.08, 121.95, 108.60, 103.20, 102.95, 60.90, 57.22, 51.87, 38.42.

Figure 82 $^{13}\text{C NMR}$ spectrum of 4

Mass Spectrum List Report



Analysis Info

Analysis Name TOFCRI25777 Julatip [AA34-PC3] E+.d
 Method Nitrat ESI pos 2019-1.m
 Sample Name ESipos

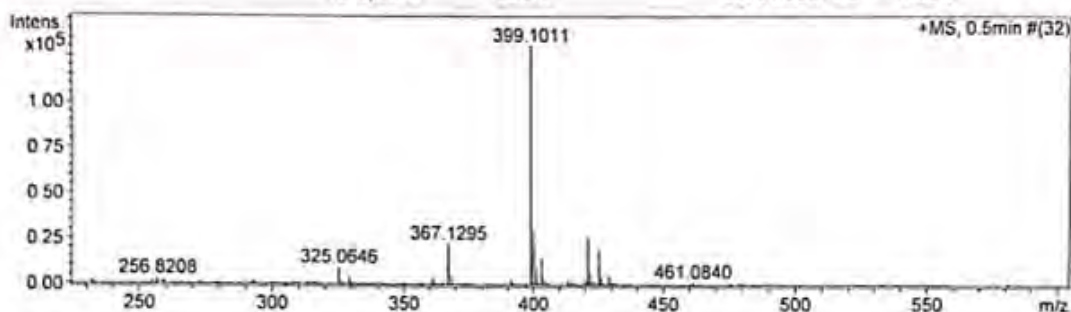
Acquisition Date 12/25/2019 12:46:05 AM
 Operator Administrator
 Instrument micrOTOF 74

Acquisition Parameter

Source Type ESI
 Scan Range n/a
 Scan Begin 100 m/z
 Scan End 850 m/z

Ion Polarity Positive
 Capillary Exit 110.0 V
 Hexapole RF 160.0 V
 Skimmer 1 33.0 V
 Hexapole 1 22.9 V

Set Corrector Fill 64 V
 Set Pulsar Pull 405 V
 Set Pulsar Push 405 V
 Set Reflector 1300 V
 Set Flight Tube 9000 V
 Set Detector TOF 1988 V



#	m/z	I	Res.
1	232.0600	1880	7165
2	254.8237	2278	7576
3	256.8208	3130	7683
4	259.1532	2277	7209
5	325.0646	9463	8141
6	329.1606	4124	7826
7	361.2217	3802	8301
8	367.1295	22695	8631
9	368.1321	5042	8910
10	391.2833	2940	8777
11	399.1011	131531	8670
12	400.1036	30431	8981
13	401.1007	10260	8683
14	403.2330	15070	8783
15	404.2359	3561	8873
16	413.2662	3307	8368
17	415.0980	2064	8360
18	420.2577	2673	8835
19	421.0827	25860	8945
20	422.0852	6187	8816
21	423.0806	2080	8622
22	425.2141	19629	8736
23	426.2181	4686	9195
24	429.1102	5082	8444
25	795.1760	7875	10640
26	796.1807	3697	10332
27	797.1833	3192	9872
28	819.1734	3869	10303
29	820.1769	1950	11413
30	827.4381	2524	10699

[M+4]⁺

Figure 83 HRMS spectrum of 4

N-(9-methoxy-7-oxo-7*H*-furo[3,2-*g*]chromen-4-yl)benzenesulfonamide (5)

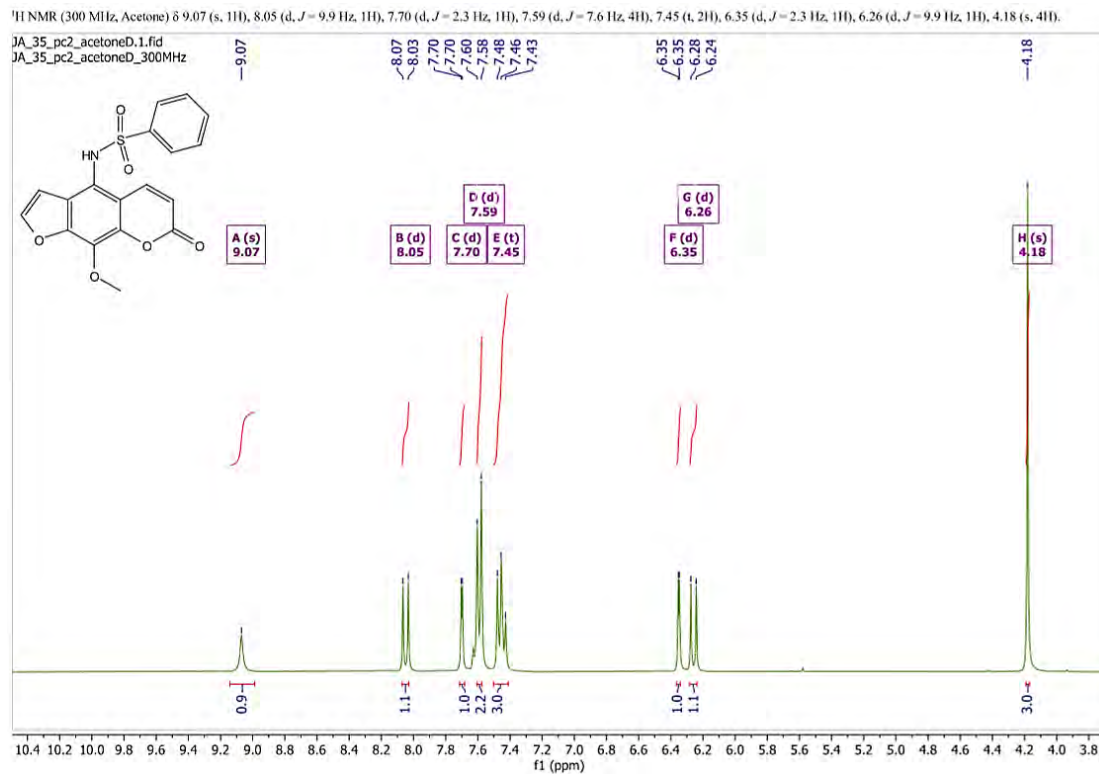


Figure 84 ¹H NMR spectrum of 5

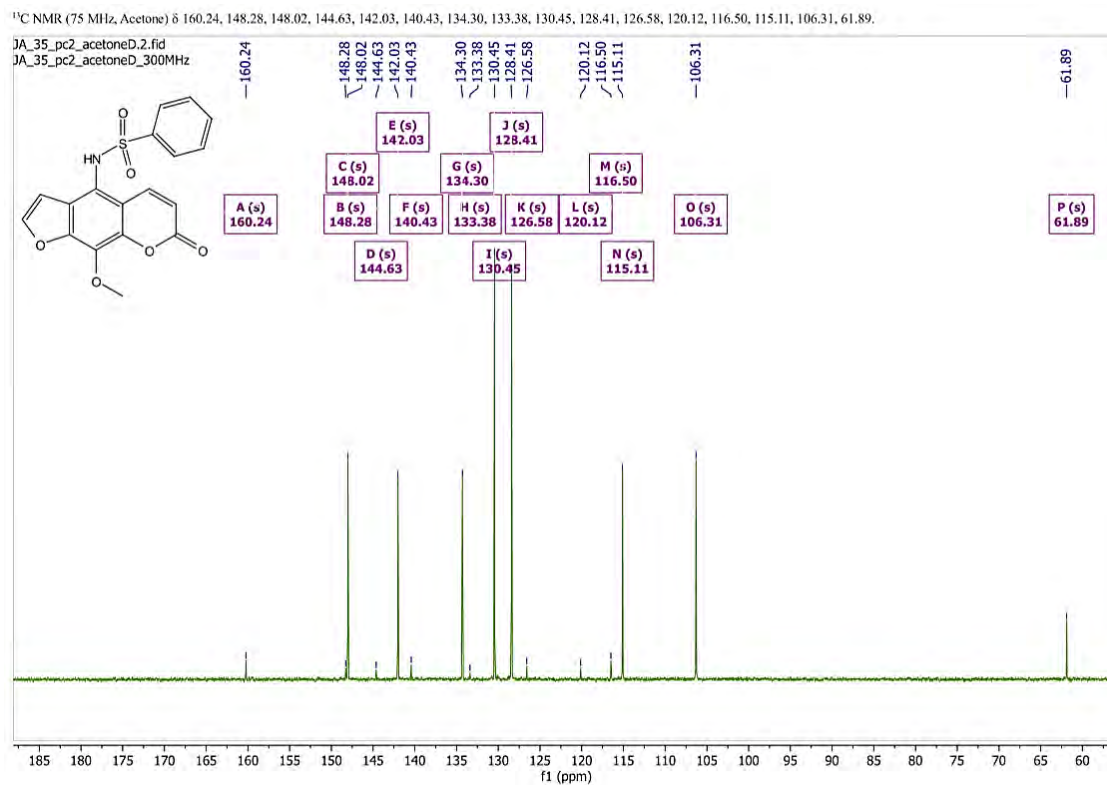


Figure 85 ¹³C NMR spectrum of 5

Mass Spectrum List Report

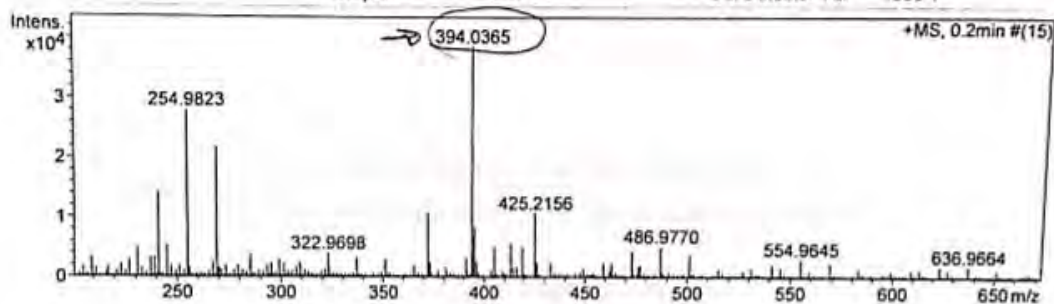
Analysis Info

Analysis Name TOFCRI25770 Jutatip JAA36-PC2 E+.d
 Method Nitirat ESI pos 2019-1.m
 Sample Name ESIpos

Acquisition Date 12/23/2019 1:34:51 AM
 Operator Administrator
 Instrument micOTOF 74

Acquisition Parameter

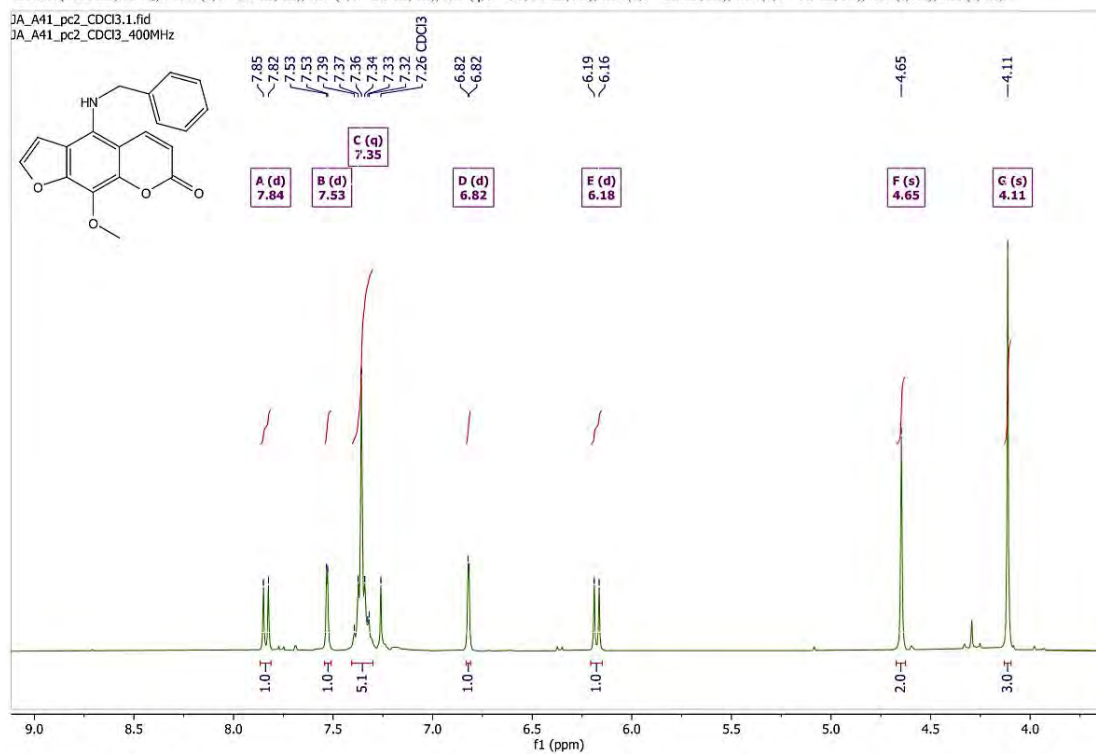
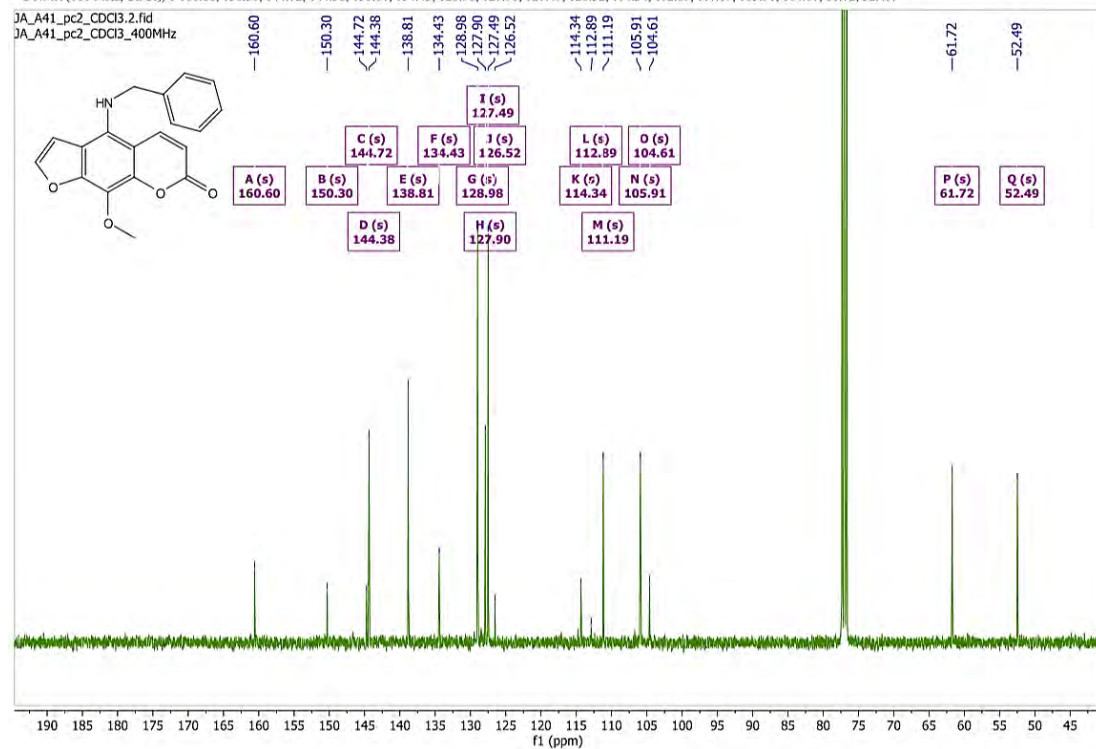
Source Type	ESI	Ion Polarity	Positive	Set Corrector Fill	64 V
Scan Range	n/a	Capillary Exit	110.0 V	Set Pulsar Pull	405 V
Scan Begin	100 m/z	Hexapole RF	160.0 V	Set Pulsar Push	405 V
Scan End	850 m/z	Skimmer 1	33.0 V	Set Reflector	1300 V
		Hexapole 1	22.9 V	Set Flight Tube	9000 V
				Set Detector TOF	1988 V



#	m/z	I	Res.
1	186.9982	5748	6456
2	209.0823	3324	6096
3	226.9534	2960	6917
4	230.9373	4893	7494
5	237.1121	3301	6750
6	239.0335	3367	6631
7	240.9669	14260	7240
8	244.9541	5295	7267
9	254.9823	28041	7421
10	268.9975	21872	7645
11	284.9894	2851	7183
12	285.1440	3834	7346
13	299.0077	2940	8055
14	322.9698	4034	8418
15	336.9854	3294	7743
16	350.9957	2970	7362
17	372.0536	10865	8357
18	390.9585	3288	8812
19	394.0365	38699	8519
20	395.0388	8496	8773
21	396.0363	2753	8225
22	404.9738	5157	8705
23	413.2655	5732	8633
24	418.9901	5154	9236
25	425.2156	10888	8982
26	472.9621	4376	8934
27	486.9770	5221	9017
28	500.9928	3743	9163
29	554.9645	3072	10022
30	765.0891	3552	10381

Figure 86 HRMS spectrum of 5

4-(benzylamino)-9-methoxy-7H-furo[3,2-g]chromen-7-one (7a)

¹H NMR (400 MHz, CDCl₃) δ 7.84 (d, *J* = 9.9 Hz, 1H), 7.53 (d, *J* = 2.3 Hz, 1H), 7.35 (q, *J* = 8.5, 7.5 Hz, 5H), 6.82 (d, *J* = 2.3 Hz, 1H), 6.18 (d, *J* = 9.9 Hz, 1H), 4.65 (s, 2H), 4.11 (s, 3H).Figure 87 ¹H NMR spectrum of 7a¹³C NMR (101 MHz, CDCl₃) δ 160.60, 150.30, 144.72, 144.38, 138.81, 134.43, 128.98, 127.90, 127.49, 126.52, 114.34, 112.89, 111.19, 105.91, 104.61, 61.72, 52.49.Figure 88 ¹³C NMR spectrum of 7a

Mass Spectrum List Report

Analysis Info

Analysis Name TOFCRI25780 Jutatip JA741-PC2 E+.d
 Method Nitral ESI pos 2019-1.m
 Sample Name ESIPos

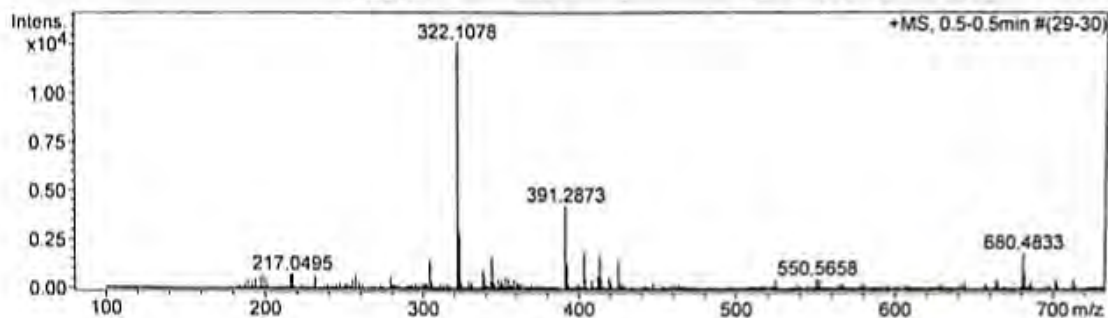
Acquisition Date 12/27/2019 1:54:37 AM
 Operator Administrator
 Instrument micrOTOF 74

Acquisition Parameter

Source Type ESI
 Scan Range n/a
 Scan Begin 100 m/z
 Scan End 850 m/z

Ion Polarity Positive
 Capillary Exit 110.0 V
 Hexapole RF 160.0 V
 Skimmer 1 33.0 V
 Hexapole 1 22.9 V

Set Corrector Fill 64 V
 Set Pulsar Pull 405 V
 Set Pulsar Push 405 V
 Set Reflector 1300 V
 Set Flight Tube 9000 V
 Set Detector TOF 1988 V



#	m/z	I	Res.
1	217.0495	760	5774
2	304.2986	1504	7793
3	322.1078	12612	8163
4	323.1117	2937	7952
5	338.3422	1001	7740
6	344.0881	1743	8236
7	391.2873	4333	8664
8	392.2912	1367	8934
9	403.2346	1926	9209
10	413.2687	1831	9227
11	425.2179	1520	8661
12	680.4833	1885	9834
13	681.4848	859	9332
14	780.7081	806	10282
15	794.7294	1424	10610
16	795.7380	754	10080
17	796.7462	894	10188
18	806.7311	766	10825
19	808.7494	1290	10007
20	820.7488	1483	10613
21	822.7593	1796	9831
22	823.7578	838	8637
23	824.7748	965	10088
24	834.7613	1019	9943
25	836.7761	1277	10875
26	848.7772	1469	10902
27	849.7856	866	11347
28	850.7955	1356	10554
29	851.7945	765	8837
30	876.8074	946	10400

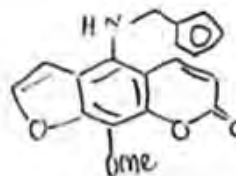
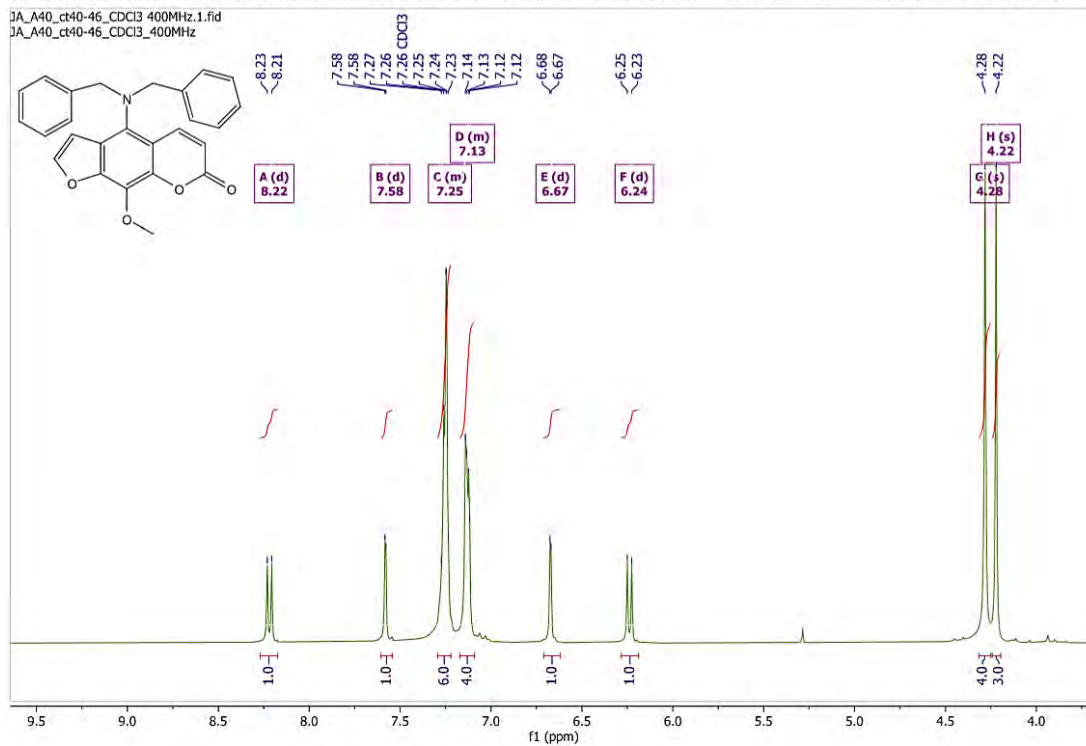


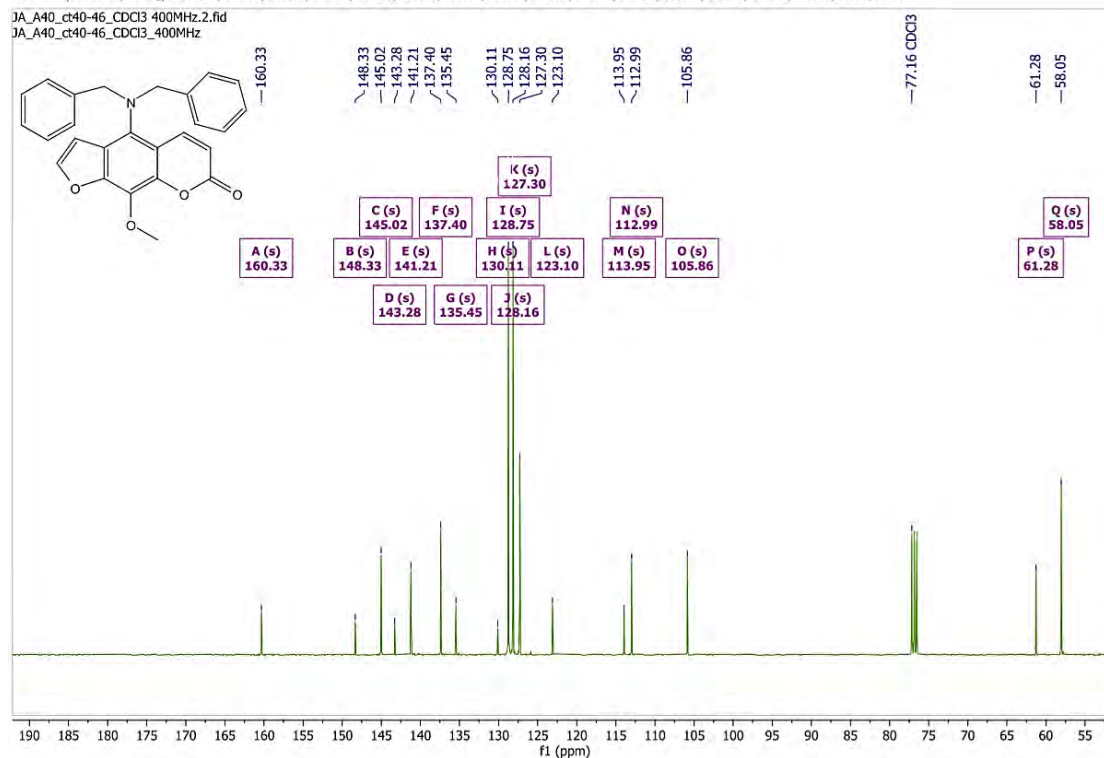
Figure 89 HRMS spectrum of 7a

4-(dibenzylamino)-9-methoxy-7H-furo[3,2-g]chromen-7-one (7b)

¹H NMR (400 MHz, CDCl₃) δ 8.22 (d, *J* = 9.7 Hz, 1H), 7.58 (d, *J* = 2.2 Hz, 1H), 7.33–7.19 (m, 6H), 7.19–7.09 (m, 4H), 6.67 (d, *J* = 2.3 Hz, 1H), 6.24 (d, *J* = 9.8 Hz, 1H), 4.28 (s, 4H), 4.22 (s, 3H).

Figure 90 ¹H NMR spectrum of 7b

¹³C NMR (101 MHz, CDCl₃) δ 160.33, 148.33, 145.02, 143.28, 141.21, 137.40, 135.45, 130.11, 128.75, 128.16, 127.30, 123.10, 113.95, 112.99, 105.86, 61.28, 58.05.

Figure 91 ¹³C NMR spectrum of 7b

Mass Spectrum List Report

Analysis Info

Analysis Name TOFCRI25781 Jutatip JAA40-Cl40-~~46~~ E+.d
 Method Nitrat ESI pos 2019-1.m
 Sample Name ESIPos

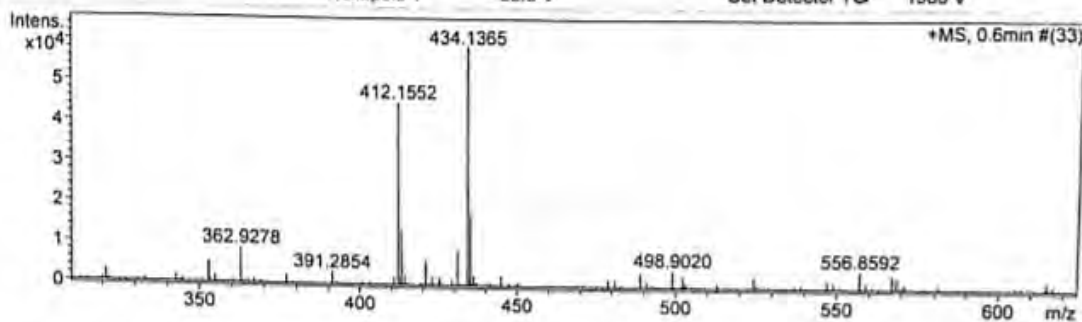
Acquisition Date 12/27/2019 1:56:55 AM
 Operator Administrator
 Instrument micrOTOF 74

Acquisition Parameter

Source Type ESI
 Scan Range n/a
 Scan Begin 100 m/z
 Scan End 850 m/z

Ion Polarity Positive
 Capillary Exit 110.0 V
 Hexapole RF 160.0 V
 Skimmer 1 33.0 V
 Hexapole 1 22.9 V

Set Corrector Fill 64 V
 Set Pulsar Pull 405 V
 Set Pulsar Push 405 V
 Set Reflector 1300 V
 Set Flight Tube 9000 V
 Set Detector TOF 1988 V



#	m/z	I	Res.
1	216.9237	16177	6889
2	218.9217	5203	7003
3	226.9524	54207	7103
4	240.9672	8456	7526
5	273.1669	7470	7314
6	294.9373	4049	7849
7	303.1776	9171	8227
8	321.1004	3081	7869
9	352.8979	5315	7958
10	362.9278	8747	8373
11	391.2854	3090	9116
12	412.1552	45213	8769
13	413.1601	13929	8875
14	413.2613	8397	8447
15	420.8839	6194	8856
16	430.9134	8828	9244
17	434.1365	59088	8623
18	435.1393	18157	9191
19	488.8736	3511	8210
20	498.9020	4440	9006
21	502.1344	2992	8648
22	556.8592	4461	9455
23	566.8892	3561	10153
24	624.8491	3596	9657
25	692.8371	3419	9998
26	760.8310	3052	11142
27	824.4204	4035	11315
28	840.3452	3160	10933
29	845.2974	16020	10597
30	846.3018	9687	11384

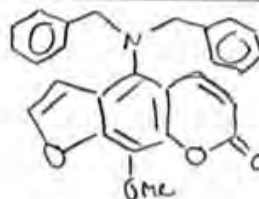


Figure 92 HRMS spectrum of 7b

Autobiography

Miss Chiphada Aekrungrueangkit was born in 1998, April 28 at Nakhon Ratchasima province. She graduated high school from Suranaree Wittaya School, Nakhon Ratchasima, Thailand in the academic year 2015. In the academic year 2016, she began to study chemistry at the Department of Chemistry, Chulalongkorn University. Her present address is 358, Moo 2 Mittraphap Road, Tambon Bankao Amphoe Mueang, Nakhon Ratchasima, 30000. Her E-mail address is Chiphada.a@student.chula.ac.th.